



PPG
ECB

PROGRAMA DE
PÓS GRADUAÇÃO
EM ECOLOGIA E CONSERVAÇÃO
DA BIODIVERSIDADE

UNIVERSIDADE FEDERAL DE MATO GROSSO
INSTITUTO DE BIOCÊNCIAS
CURSO DE DOUTORADO EM ECOLOGIA E CONSERVAÇÃO DA
BIODIVERSIDADE

RELAÇÕES FILOGENÉTICAS EM *Oecomys* THOMAS, 1906, COM ÊNFASE EM
SISTEMÁTICA E DIVERSIFICAÇÃO DO COMPLEXO *Oecomys catherinae*
THOMAS, 1909 (RODENTIA, SIGMODONTINAE)

JULIANE SALDANHA DA SILVA

CUIABÁ - MT

2020

UNIVERSIDADE FEDERAL DE MATO GROSSO
INSTITUTO DE BIOCÊNCIAS
CURSO DE DOUTORADO EM ECOLOGIA E CONSERVAÇÃO DA
BIODIVERSIDADE

Relações filogenéticas em *Oecomys* Thomas, 1906, com ênfase em sistemática e diversificação do complexo *Oecomys catherinae* Thomas, 1909 (Rodentia, Sigmodontinae)

JULIANE SALDANHA DA SILVA

Tese apresentada ao Curso de Pós-Graduação,
do Instituto de Biociências, para obtenção do
título de Doutor em Ecologia e Conservação
da Biodiversidade.

CUIABÁ - MT

2020

Dados Internacionais de Catalogação na Fonte.

S162r Saldanha da Silva, Juliane.

Relações filogenéticas em *Oecomys* Thomas, 1906, com ênfase em sistemática e diversificação do complexo *Oecomys catherinae* Thomas, 1909 (Rodentia, Sigmodontinae) / Juliane Saldanha da Silva. – 2020

xi, 135 f. : il. color. ; 30 cm.

Orientador: Rogério Vieira Rossi.

Co-orientadora: Izeni Pires Farias.

Tese (doutorado) - Universidade Federal de Mato Grosso, Instituto de Biociências, Programa de Pós-Graduação em Ecologia e Conservação da Biodiversidade, Cuiabá 2020.

Inclui bibliografia.

1. Taxonomia. 2. Diversidade críptica. 3. Fluxo gênico. 4.

Ficha catalográfica elaborada automaticamente de acordo com os dados fornecidos pelo(a) autor(a).

Permitida a reprodução parcial ou total, desde que citada a fonte

ORIENTADOR:

Prof. Dr. Rogério Vieira Rossi
Universidade Federal de Mato Grosso

CO-ORIENTADORA:

Prof^a. Dr^a. Izeni Pires Farias
Universidade Federal do Amazonas

BANCA EXAMINADORA

Examinador Titular: Dr. Rafael do Nascimento Leite
Instituto Nacional de Pesquisas da Amazônia

Examinadora Titular: Dr^a. Lena Geise
Universidade do Estado do Rio de Janeiro

Examinador Titular: Dr^a. Ana Carolina Loss
Instituto Nacional da Mata Atlântica

Examinadora Titular: Dr^a. Sandra Mariotto
Instituto Federal de Mato Grosso

Examinadora Titular: Dr. Vítor de Queiroz Piacentini
Universidade Federal de Mato Grosso - Departamento de Biologia e Zoologia

Examinador Suplente: Dr. Felipe Franco Curcio
Universidade Federal de Mato Grosso - Departamento de Biologia e Zoologia

Examinadora Suplente: Dr^a. Paulo César Venere
Universidade Federal de Mato Grosso - Departamento de Biologia e Zoologia

AGRADECIMENTOS

Ao Programa de Capacitação em Taxonomia – PROTAX, e Coordenação de Aperfeiçoamento de Pessoal de Nível Superior – CAPES, pela concessão da bolsa de Doutorado.

Ao Programa de Pós-Graduação em Ecologia e Conservação da Biodiversidade (PPG-ECB) da Universidade Federal de Mato Grosso em especial à Nilce, secretária do PPG-ECB, pela disponibilidade e paciência em esclarecer as dúvidas sobre formulários e processos, desde a matrícula até o ofício de defesa.

Ao meu orientador Dr. Rogério Vieira Rossi, que me acompanha desde o mestrado, com todos os ensinamentos que têm sido essenciais na minha formação profissional e pessoal.

À professora Dr^a Izeni Pires Farias e ao professor Dr. Tomas Hrbek, pela oportunidade de trabalhar com dados genômicos e pela paciência, orientação e ensinamentos durante o tempo na UFAM em Manaus.

Ao Fabricio Bertuol pelos ensinamentos de procedimentos e técnicas de bancada para obtenção de RADseq e ao Érico Polo pelo auxílio nas primeiras análises dos dados genômicos.

À Professora Dr. Daniela Cristina Ferreira que me acompanha desde o mestrado, pelo suporte, todo apoio e pela parceria no laboratório de genética da UFMT.

Aos curadores e técnicos das coleções zoológicas, que permitiram o acesso aos exemplares analisados: Juliana Gualda e Ismael de Jesus (MZUSP), Manoel Santos-Filho (UNEMAT), João Alves de Oliveira (MNRJ), Ana Cristina Mendes-Oliveira (UFPA), Alexandra Maria Ramos Bezerra (MPEG), Maria Nazareth (INPA), Hugo Vieira (UnB) e Monique Nascimento (UFES).

Aos colegas e amigos que gentilmente me receberam e hospedaram durante as visitas as coleções: José Delmondes e Jéssica, São Paulo – SP; Gerlane Medeiros, Tatiane e Aldair, Cáceres - MT; Junior Andrade Albedi, Juliano Santana e Thaynara Pacheco, Rio de Janeiro - RJ; Victor Fonseca e sua mãe Maria das Graças, Belém - PA; Jussara Dayrell e Ariane Silva, Manaus - AM; Elisandra Chiquito e Mariana, Vitória - ES. Alguns destes não me conheciam anteriormente, mas mesmo assim me receberam com muito carinho.

Às amigas que conheci no laboratório da UFMT, mas que vou levar pra minha vida, pois são muito especiais: Ravena Mendonça e Jhennifer Ribeiro, obrigada por estarem comigo em todos os momentos e por toda a amizade além da vida acadêmica; Claudilívia Ferreira obrigada pelo companheirismo e apoio no laboratório e durante as viagens as coleções; Maria Nazaré obrigada pelo apoio e pelos inúmeros almoços que me salvaram do miojo de cada dia.

Aos amigos Luan Gabriel Lima, sempre disposto a discutir sobre a morfologia e análises morfométricas, e Thiago Semedo pelas contribuições no desenvolvimento do projeto inicial do doutorado, auxílio nas análises morfológicas, morfométricas e pelas oportunidades e ensinamentos nos trabalhos em campo. Ao amigo Victor Fonseca, por todos ensinamentos no laboratório de genética e que mesmo distante sempre contribuiu e muito com todas as análises genéticas.

Às amigas Thais Teixeira e sua mãe Isamaela pelo acolhimento durante o início do doutorado e por toda amizade durante todos estes anos.

Ao meu primo, amigo e “roommate” Douglas, pelo companheirismo, sempre me ouvindo, me fazendo rir, e por estar presente em todos os momentos.

Ao Sergio Gabriel Rossi, pelo companheirismo e apoio durante estes anos!

Agradeço principalmente a minha família, minha mãe Ana Maria Saldanha, meu pai João Evandir, minha irmã Tatiane Saldanha, meus sobrinhos Beatriz e Henrique e meu cunhado Gustavo. Mesmo distante, sempre recebi muito apoio, incentivo, amor e carinho! Vocês são a razão da minha existência, não existem palavras que possam expressar meu amor e minha gratidão a vocês!

Agradeço a Deus por ter me dado força, paz e perseverança para seguir este longo caminho e chegar até aqui.

A todos que participaram desta etapa, meu muito obrigada!

SUMÁRIO

LISTA DE FIGURAS	ix
Capítulo I	ix
Capítulo II	ix
Capítulo III	x
LISTA DE TABELAS	xii
Capítulo I	xii
Capítulo II	xii
Capítulo III	xii
RESUMO	1
ABSTRACT	2
1. INTRODUÇÃO GERAL	3
2. REFERÊNCIAS BIBLIOGRÁFICAS	5
CAPÍTULO I - Genetic diversity of <i>Oecomys</i> (Rodentia, Sigmodontinae) from the Tapajós River basin and the role of rivers as barriers for the genus in the region	7
Abstract	8
Introduction	9
Materials and Methods	10
Sampling	10
DNA extraction, amplification and sequencing	10
Phylogenetic analysis and diversity	12
Populational analyses and structure	13
Results	14
Diversity of <i>Oecomys</i> in the Tapajós River basin	14
Population structure of <i>O. bicolor</i> , <i>O. cleberi</i> and <i>O. paricola</i> from the Tapajós	15
Discussion	16
Diversity of <i>Oecomys</i> in the Tapajós River basin	16
Population structure of <i>Oecomys</i> from the Tapajós River basin	19
Acknowledgements	21
References	21
Figures	25
Tables	29
Supplementary Material	30
CAPÍTULO II - Integrative analysis supports a new species of the <i>Oecomys catherinae</i> complex (Rodentia, Cricetidae) from Amazonia	39
Materials and Methods	44
Results	49
Taxonomy	52
Discussion	61
Acknowledgments	64
Supplementary Data	64

Literature Cited	65
Figures	71
Tables.....	80
Appendix I: Specimens examined	88
CAPÍTULO III - Diversificação do complexo <i>Oecomys catherinae</i> Thomas, 1909 (Rodentia, Sigmodontinae): quantas espécies existem?	101
RESUMO.....	102
ABSTRACT.....	102
1. INTRODUÇÃO	103
2. MATERIAL E MÉTODOS	105
Dados moleculares	105
Obtenção de dados mitocondriais	105
Análise de dados mitocondriais	106
Obtenção de dados genômicos	106
Análise de dados genômicos	108
Dados morfométricos	110
3. RESULTADOS	111
Dados mitocondriais.....	111
Dados genômicos	114
Dados morfométricos	118
4. DISCUSSÃO	121
5. REFERÊNCIAS BIBLIOGRÁFICAS	125
ANEXO 01	128
ANEXO 02	133
3. CONCLUSÃO FINAL.....	135

LISTA DE FIGURAS

Capítulo I

Fig. 1. Map indicating the main rivers in the Tapajós River basin and sampled localities. Numbers indicate the collection points and the symbols indicate the species collected at these points. Coordinates and number of locations are listed in Supplementary Material, Table 1. 25

Fig. 2. Bayesian Inference topology based on *Oecomys* cytochrome b gene data. Rigid circles indicate posterior probability greater than 0.95 and maximum likelihood bootstrap of more than 80%. Half black circles indicate posterior probability above 0.95. Numbers in parentheses refer to the localities from the Tapajós River basin indicated in Fig. 1. Boldfaced samples indicate sequences obtained in this study. Identification of samples and their locations are listed in Supplementary Material, Table 1. 27

Fig. 3. Bayesian Inference topology based on concatenated data from cytochrome b gene and nuclear marker intron 7 β -fibrinogen gene of *Oecomys*. Circles indicate posterior probability greater than 0.95 and maximum likelihood bootstrap greater than 80%. Half black circles indicate posterior probability above 0.95. Numbers in parentheses refer to the localities from the Tapajós River basin indicated in Fig. 1. Boldfaced samples indicate sequences obtained in this study. Identification of samples and their locations are listed in Supplementary Material, Table 1. 28

Fig. 4. Median-joining haplotype network based on cytochrome b gene data, representing the relationships in the *Oecomys bicolor/Oecomys cleberi* species complex. The size of the circle is proportional to the frequency of the haplotypes and the colors correspond to the localities. The mutational steps are indicated on the branches. 28

Fig. 5. Median-joining haplotype network based on data from the cytochrome b gene of *Oecomys paricola*. The size of the circle is proportional to the frequency of the haplotypes and the colors correspond to the localities. The mutational steps are indicated on the branches. 28

Fig. 6. Mismatch distribution graphs based on cytochrome b data from *Oecomys bicolor* (A), *Oecomys cleberi* (B) and *Oecomys paricola* (C). Dotted gray line indicates the expected distribution and solid black line indicates the frequency of distribution observed. 29

Capítulo II

Fig. 1.—Map of samples of the *Oecomys catherinae* complex *s. l.* included in this study, with discrimination of the lineages recognized for the complex. Stars indicate the type localities of *Oecomys* sp. nov. (1; western lineage), *Oecomys catherinae* (51), and *Oryzomys concolor bahiensis* (39). 71

Fig. 2.—Bayesian Inference topology based on mitochondrial Cytochrome b gene. Numbers above the branches indicate bayesian posterior probabilities and below the branches indicate maximum likelihood bootstrap values. Side bars indicate evolutionary lineages recognized in bPTP (black) and GMYC (medium gray) analyses. The light gray side bars indicate *Oecomys* sp. nov. and the *Oecomys catherinae* complex *s.s.* recognized in this study. The sample data are presented in Supplementary Data S1. 72

Fig. 3.—Bayesian Inference topology based on the mitochondrial Cytochrome b gene and nuclear intron 7 β -fibrinogen concatenated. Numbers above the branches indicate bayesian posterior probabilities and below the branches indicate maximum likelihood bootstrap values. The black side bars indicate evolutionary lineages recognized in the analysis of bPTP and the light gray bars indicate *Oecomys* sp. nov. and the *Oecomys catherinae* complex recognized in this study. Sample data is provided in Supplementary Data S1. 73

Fig. 4.—Scatterplot of principal components 1 and 2 of Principal Component Analysis (top) and of canonical variate 1 and 2 of Discriminant Analysis (bottom) of 31 craniodental measurements of the *Oecomys catherinae* complex *s. l.* The western lineage corresponds to *Oecomys* sp. nov. described in this study. 74

Fig. 5.—Dorsal view (above) and ventral view (below) of: A) the holotype of *Oecomys* sp. nov. (UFMT 4118), and specimens of the *Oecomys catherinae* complex lineages: B) eastern (MN 10748), C) central (PCH 4077), D) westernmost (APC 292), and E) northern (MZUSP 35535 above, and MZUSP 29532 below). 75

Fig. 6.—Dorsal, ventral and lateral views of skull and lateral view of mandible of the holotype (UFMT 4118) of *Oecomys* sp. nov. from Estância Santa Clara, Alta Floresta, Mato Grosso state, Brazil. Scale: 5 mm. 76

Fig. 7.—Anatomical traits that differentiate *Oecomys* sp. nov. (UFMT 4118) from the *O. catherinae* complex lineages: A) posterior nasal terminus (shorter dashed line) surpassing the maxillary-frontal suture (longer dashed line) and the premaxillaries terminating anterior to the nasal in *Oecomys* sp. nov. ; B) posterior nasal terminus (shorter dashed line) anterior to the maxillary-frontal suture (longer dashed line) and the premaxillaries aligned to the posterior margin of the nasals in *O. catherinae* (BNMH 9.11.19.24); C) supraorbital and temporal crests poorly developed in *Oecomys* sp. nov. ; D) supraorbital crest dorsolaterally expanded in *O. catherinae* northern lineage (MPEG 39899), being more developed than temporal crest; E) subsquamosal fenestra present, always smaller than postglenoid foramen, and parietal slightly expanded below the lateral edges of the dorsum of the braincase (white arrow) in *Oecomys* sp. nov. ; F) subsquamosal fenestra ossified and parietal deeply expanded onto the lateral surface of the braincase (white arrow) in *O. catherinae* northern lineage (MPEG 39899).. 78

Fig. 8.—Paratype of *Oecomys* sp. nov. from Teles Pires Hydroelectric Power Plant, Paranaíta municipality, Mato Grosso state, Brazil (UFMT 1680): upper molar series (left) and lower molar series (right). Abbreviation: ac, anterior cingulum. 79

Capítulo III

- Figura 1. Topologia de inferência Bayesiana com o marcador mitocondrial Citocromo b de *Oecomys* sp. nov. e do complexo *O. catherinae* (senso Saldanha & Rossi, no prelo). Números próximos aos ramos indicam a probabilidade posterior (PP). Os dados das amostras e grupo externo utilizados são apresentados no Anexo 01: tabela 1. 112
- Figura 2. Mapa com as localidades das amostras de *Oecomys* sp. nov. e do complexo *O. catherinae* (senso Saldanha & Rossi, no prelo). As cores representam as espécies e linhagens obtidas nas análises filogenéticas. Triângulos representam exemplares com dados morfológicos, quadrados com dados moleculares, e círculos com ambos os dados. As estrelas pretas representam a localidade tipo de *O. catherinae* (1), *O. bahiensis* (2) e *Oecomys* sp. nov. (3). 113
- Figura 3. Rede haplotípica com o marcador mitocondrial Citocromo b de *Oecomys* sp. nov. e do complexo *O. catherinae* (senso Saldanha & Rossi, no prelo). As cores representam as espécies e linhagens obtidas nas análises filogenéticas, e o tamanho das amostras (círculos) representa o número de haplótipos. Círculos pretos representam haplótipos não amostrados e as barras representam eventos de passos mutacionais. 113
- Figura 4. Topologia de inferência Bayesiana com matriz de dados de ddRADseq de *Oecomys* sp. nov. e do complexo *O. catherinae* (senso Saldanha & Rossi, no prelo). Valores acima dos ramos indicam a probabilidade posterior (PP) e, abaixo dos ramos, o valor de bootstrap. Os dados das amostras são apresentados no Anexo 01: tabela 1. 115
- Figura 5. Árvore datada de *Oecomys* sp. nov. e do complexo *O. catherinae* (senso Saldanha & Rossi, no prelo). Os valores acima dos nós se referem às datas de divergência estimadas em milhões de anos pelo BEAST, e as barras correspondem aos intervalos de confiança de 95% das datas estimadas. Os dados das amostras são apresentados no Anexo 01: tabela 1. 116
- Figura 6. Árvore de espécie obtida no programa SNAPP para o modelo com *Oecomys* sp. nov. mais seis linhagens/subclados de *O. catherinae* (extremo oeste, norte, central, nordeste, leste A e leste B). 117
- Figura 7. Grupos biológicos apontados pelo FastSTRUCTURE com K=4 para *Oecomys* sp. nov., e as linhagens do complexo *O. catherinae*. As cores aplicadas aos exemplares indicam as espécies e linhagens reconhecidas nas análises filogenéticas. 118
- Figura 8. Gráfico de dispersão dos componentes principais 1 e 2 (A) e funções discriminantes 1 e 2 (B), de espécimes de *Oecomys* sp. nov. e linhagens do complexo *Oecomys catherinae* com base em 17 medidas crânio-dentárias. 120

LISTA DE TABELAS

Capítulo I

Table 1. Percentage of variation and fixation index of Analysis of Molecular Variance (AMOVA) based on cytochrome b data of the *Oecomys bicolor/Oecomys cleberi* complex (2 groups) and *O. paricola*. *Significant values ($p < 0.05$)..... 29

Table 2. Genetic diversity indices and demographic expansion of *Oecomys bicolor*, *O. cleberi* and *O. paricola* based on cytochrome b data. N: Sample number; H: number of haplotypes; h: haplotype diversity, π : nucleotide diversity. *Significant values ($p < 0.05$). 29

Capítulo II

Table 1.—Uncorrected p-distances of the Cytochrome b within and among *Oecomys* species. Eastern, central, northern, western, and westernmost, correspond to lineages in the *Oecomys catherinae* complex *sensu lato*. Values above diagonal correspond to standard deviation and bold numbers to genetic distance within clades. Values in percentage..... 80

Table 2.—External, cranial and dental measurements (in mm) and weight (in grams) of adult specimens of *Oecomys* sp. nov. and lineages of the *Oecomys catherinae* complex *stricto sensu*. See “Material and Methods” section for abbreviations. 81

Table 3.—External and craniodental character comparisons among *Oecomys* sp. nov. and lineages of the *Oecomys catherinae* complex *stricto sensu* (central, eastern, northern, and westernmost). HBL, head and body length; M1, upper first molar; TL, tail length. See the “Comparisons” section for comparisons of *Oecomys* sp. nov. with other congeneric species. 85

Capítulo III

Tabela 1. Modelos de linhagens testadas pela *Bayes Factor Delimitation* (BFD*) para os dados de SNPs. ML: marginal likelihood, BF= Bayes Factor. 117

Tabela 2. Resultado da Análise de Componentes Principais de espécimes de *Oecomys* sp. nov. e linhagens do complexo *Oecomys catherinae* com base em 17 medidas crânio-dentárias. As descrições das medidas são apresentadas na seção Material e Métodos. 119

Tabela 3. Resultado da análise de Função Discriminante de espécimes de *Oecomys* sp. nov. e linhagens do complexo *Oecomys catherinae* com base em 17 medidas crânio-dentárias. As descrições das medidas são apresentadas na seção Material e Métodos. 120

RESUMO

Roedores do gênero *Oecomys* Thomas, 1906, possuem ampla distribuição em biomas brasileiros, com a maior diversidade relatada para a região Amazônica. Entretanto, a identificação da diversidade e os limites de espécies no gênero ainda são confusos. Atualmente, são reconhecidas 18 espécies, cujas relações interespecíficas ainda não são amplamente conhecidas. A grande diversidade de *Oecomys* é relatada em estudos sobre a existência de complexos de espécies, com linhagens que podem representar novas espécies. Com isso, o objetivo deste estudo é avaliar e descrever a diversidade taxonômica e as relações filogenéticas de espécies de *Oecomys*, com ênfase no mais diverso complexo de espécies – *Oecomys catherinae* – com ampla distribuição em três biomas brasileiros. Para isso, inicialmente realizamos análises filogenéticas com base em marcador molecular mitocondrial e nuclear para elucidar a diversidade e as relações entre as espécies do gênero da bacia do Tapajós e o papel dos rios na distribuição das espécies. Posteriormente, para o complexo *O. catherinae* apresentamos análises moleculares de delimitação de espécies, assim como análises morfológicas e morfométricas. Além disso, apresentamos uma abordagem genômica sobre as relações filogenéticas e diversificação das linhagens que compõem o complexo com base representação genômica de ddRADseq. Nossas hipóteses filogenéticas sobre o gênero *Oecomys* revelam grande diversidade de espécies para a região da bacia do Tapajós, com a distribuição de algumas espécies moldada pelo rio Tapajós. Além disso, nossos dados indicam que o rio Teles Pires não atua como barreira para o fluxo gênico. As análises de delimitação de espécies, morfologia e morfometria indicam a existência de uma nova espécie do complexo *O. catherinae* para esta região, descrita neste estudo. Além disso, com a abordagem genômica, apontamos as divergências e diversidade entre as demais linhagens do complexo de espécies *O. catherinae*, com indícios da existência de duas espécies distintas e a comprovação de linhagens crípticas com ocorrência na Mata Atlântica e Cerrado. As diversificações entre linhagens do complexo foram estimadas para o Pleistoceno, em grande parte moldada pelos refúgios e glaciações deste período.

Palavras-chave: Fluxo gênico, diversidade críptica, Taxonomia, ddRADseq.

ABSTRACT

The arboreal rat *Oecomys* Thomas, 1906 are widely distributed in Brazilian biomes, with the greatest diversity reported for the Amazonia region. Currently, 18 species are recognized. However, the real diversity and species boundaries in the genus remains uncertain., and the interspecific relationships still poorly known. The great diversity of *Oecomys* is reported in studies about species complex, with lineages that may represent new species. The aim of this study is to evaluate the taxonomic diversity and phylogenetic relationships of *Oecomys* species, with emphasis on the most diverse species complex – *Oecomys catherinae* – which is widely distributed in Brazilian biomes. We performed phylogenetic analyses based on mitochondrial and nuclear marker to elucidate the diversity and relationships between *Oecomys* species of Tapajós basin and the role of Amazonian rivers in the species distribution. For the *O. catherinae* complex, we performed molecular analyses of species delimitation, and morphological and morphometric analyses. In addition, we used a genomic representation of ddRADseq to evaluate the phylogenetic relationships and diversification of the lineages of the complex. Our phylogenetic hypotheses for *Oecomys* genus reveal great species diversity for the Tapajós basin, with the distribution of some species shaped by the Tapajós river, but the Teles Pires river does not act as a barrier to gene flow for other species. The species delimitation, morphology and morphometric analyses indicate the existence of a new species of the *O. catherinae* complex for this region, described in this study. The genomic approach reveals the divergences and diversity between the other lineages of the *O. catherinae* complex, with evidence of two distinct species in Amazonia, and cryptic species occurring in the Atlantic Forest and Cerrado biomes. The diversifications between lineages of the complex were estimated for the Pleistocene, largely shaped by the refuges and glaciations of this period.

Keywords: Gene flow, Cryptic diversity, Taxonomy, ddRADseq.

1. INTRODUÇÃO GERAL

A subfamília Sigmodontinae é a representante da maior diversidade de roedores cricetídeos, dividida em sete tribos. Entre elas está a tribo Oryzomyini, na qual a maioria das espécies possui hábito terrícola, porém algumas são arborícolas, como as do gênero *Oecomys* Thomas, 1906 (Oliveira & Bonvicino 2011; Hershkovitz 1960). Representantes deste gênero possuem comprimento da cabeça e corpo entre 71 e 176 mm, comprimento da cauda entre 80 e 192 mm, pelagem macia variando de castanha-escura a castanha-avermelhada no dorso, e ventre esbranquiçado/amarelado com ou sem pelos de base cinza; possuem vibrissas longas, patas traseiras curtas e largas com dedos relativamente longos, cauda moderadamente mais longa que a cabeça e corpo, com a porção terminal pilosa em algumas espécies, e quatro pares de mamas: peitoral, pós-axial, abdominal e inguinal. (Carleton & Musser 2015; Oliveira & Bonvicino 2011; Bonvicino et al. 2008).

Na taxonomia, os nomes mais antigos ligados ao gênero *Oecomys* são *Hesperomys concolor* Wagner, 1845 e *Hesperomys bicolor* Tomes, 1860. Estas espécies foram listadas por Trouessart (1898) como membro do gênero *Rhipidomys*. No entanto, em 1906, Thomas determinou os caracteres para a definição do gênero *Rhipidomys* e alocou as espécies arborícolas com palato longo em *Oecomys* como um subgênero de *Oryzomys*, designando como espécie tipo *Rhipidomys benevolens* (= *Hesperomys bicolor*) (Musser & Carleton 2005; Hershkovitz 1960; Tate 1932). Em seguida, Thomas (1909) percebeu que, diferentemente de *Oryzomys*, o gênero *Oecomys* possui placa externa da raiz anterior do zigomático mal projetada anteriormente, e elevou *Oecomys* à categoria de gênero.

Ellerman (1941) discordou do arranjo de Thomas (1909) afirmando que este não poderia ser considerado mais do que um subgênero, pois a única característica do grupo era a cauda ligeiramente provida de tufo (Hershkovitz 1960). Com a revisão de Hershkovitz (1960), *Oecomys* foi consolidado como um subgênero de *Oryzomys* incluindo as vinte e cinco espécies associadas ao gênero em apenas duas espécies politípicas, sendo *O. bicolor* considerada a espécie “com porte menor”, com quatro subespécies, e *O. concolor* a espécie “com porte maior”, com cinco subespécies.

Somente com a revisão publicada por Musser & Carleton (1993) o status genérico de *Oecomys* foi reconhecido e posteriormente corroborado por análises moleculares, sendo a primeira destas realizadas por Patton & Da Silva (1995). Estes autores avaliaram as relações filogenéticas dentro da tribo Oryzomyini, incluindo o gênero *Oecomys*, apontando que este constitui um grupo monofilético, tal como outros autores posteriormente.

Embora o monofiletismo do gênero esteja comprovado, as informações sobre as relações filogenéticas entre as espécies de *Oecomys* e a distribuição geográfica das mesmas são pouco conhecidas (Rocha et al. 2011; Musser & Carleton, 2005; Patton et al. 2000). Mesmo nos estudos com uma filogenia mais completa para o gênero, existem evidências de complexos de espécies dentro de *Oecomys* (Suárez-Villota et al. 2018; Rocha et al. 2018; Malcher et al. 2017; Rosa et al. 2012).

Atualmente, o gênero possui 18 espécies válidas, das quais uma recentemente descrita e outra revalidada (Rocha et al. 2018; Pardiñas et al. 2016; Carleton & Musser 2015). A distribuição do gênero geralmente é associada à floresta tropical de baixa altitude, e a maior diversidade de espécies está concentrada na Bacia Amazônica (Carleton & Musser 2015; Oliveira & Bonvicino 2011; Bonvicino et al. 2008). Em um dos recentes estudos sobre a sistemática de *Oecomys*, Suárez-Villota et al. (2018) reúnem representantes de 14 espécies de localidades da Amazônia, Cerrado, Pantanal e Mata Atlântica. Os autores confirmam sete espécies válidas, sendo elas *O. auyantepui*, *O. concolor*, *O. rex*, *O. rutilus*, *O. superans*, *O. sydandersoni* e *O. trinitatis*; três não descritas (*Oecomys* sp.1– 3); e cinco complexos de espécies, com linhagens que podem corresponder a 15 espécies: duas do grupo *O. bicolor* / *O. cleberi*, duas de *O. franciscorum* / *O. mamorae*, três de *O. paricola*, três de *O. roberti* e cinco em *O. catherinae*.

Entre os complexos de espécies mencionados, *O. catherinae* é o mais diverso em número de linhagens que podem representar novas espécies. As linhagens deste complexo apresentam ampla distribuição que inclui os biomas florestais Mata Atlântica e Amazônia, além de florestas de galeria no bioma Cerrado. Descrita por Thomas (1909) para Joinville, estado de Santa Catarina, *O. catherinae* teve sua distribuição ampliada para regiões amazônicas e florestas de galeria do Cerrado no Brasil Central (Saldanha et al. 2019; Asfora et al. 2011). No entanto, Malcher et al. (2017) levantaram a possibilidade de *O. catherinae* se tratar de um complexo de espécies, dada a existência de variações cromossômicas significativas entre as populações da Amazônia e da Mata Atlântica. Estas variações indicam a ausência de fluxo gênico entre as referidas populações, porém a divergência genética de Citocromo b entre elas é de 1,7%, valor considerado baixo quando comparado às divergências entre as demais espécies do gênero.

Comparações morfológicas e moleculares dos trabalhos de Suárez-Villota et al. (2018) são exemplos de como a diversidade específica deste gênero foi subestimada em estudos anteriores. Estes são indicativos da necessidade de estudos mais amplos no gênero *Oecomys*. Além de indicarem maior diversidade dentro do gênero, outros trabalhos que

envolvem análises moleculares e cariotípicas ainda refletem na distribuição geográfica mais ampla de algumas espécies (Malcher et al. 2017; Rosa et al. 2012; Rocha et al. 2011; Asfora et al. 2011).

Com isso, este estudo visa ampliar o conhecimento sobre a diversidade de *Oecomys*, com ênfase no complexo *O. catherinae*. No capítulo 1 são apresentadas as relações filogenéticas entre as espécies e a diversidade deste gênero na região da bacia do Tapajós, assim como o papel de rios como barreira para o fluxo gênico nesta região. No capítulo 2 é apresentada uma análise integrativa de dados moleculares e morfológicos com a descrição de uma das linhagens do complexo *Oecomys catherinae* como uma nova espécie. Já no capítulo 3 são investigadas as relações filogenéticas e diversificação das linhagens do complexo *Oecomys catherinae*, com uma abordagem genômica.

2. REFERÊNCIAS BIBLIOGRÁFICAS

Asfora, P. H., Palma, A. R. T., Astúa, D. & Geise, L. (2011). Distribution of *Oecomys catherinae* Thomas, 1909 (Rodentia: Cricetidae) in northeastern Brazil with karyotypical and morphometrical notes. *Biota Neotropical*, 11(2), 415–424.

Bonvicino, C. R., Oliveira, J. A. & D'Andrea, P. S. (2008). *Guia dos roedores do Brasil, com chaves para gêneros baseadas em caracteres externos*. Rio de Janeiro: Centro Pan-Americano de Febre Aftosa - OPAS/OMS.

Carleton, M. D. & Musser, G. G. (2015). *Genus Oecomys Thomas, 1906*, in: Patton, J., Pardiñas, U. F. J., D'Elia, G. (Eds.), *Mammals of South America*, vol.2, rodents. University of Chicago Press, Chicago, Illinois, pp. 393–417.

Ellerman, J. R. (1941). *The families and genera of living rodents*. 1941. Vol 2. British Museum (Natural History), London, 690 p.

Hershkovitz, P. (1960). Mammals of Northern Colombia, preliminary report N°. 8: Arboreal rice rats, a systematic revision of the subgenus *Oecomys*, genus *Oryzomys*. *Proceedings of the United States National Museum*, 110 (3420), 513–568.

Malcher, M. S., Pieczarka, J. C., Geise, L., Rossi, R. V., Pereira, A. L., O'Brien, P. C. M., Asfora, P. H., Silva, V. F., Sampaio, M. I., Ferguson-Smith, M. A. & Nagamachi, C. Y. (2017). *Oecomys catherinae* (Sigmodontinae, Cricetidae): Evidence for chromosomal speciation? *PLoS ONE*, 12(7), e0181434.

Musser, G. G. & Carleton, M. D. (1993). *Superfamily Muroidea*, in: Wilson, D.E., Reeder D.A., (Eds.), *Mammal Species of the World: a taxonomic and geographic reference*, second ed. John Smithsonian Institution Press, Washington D.C., pp. 501–755.

Musser, G. G. & Carleton, M. D. (2005). *Superfamily Muroidea*, in: Wilson, D.E., Reeder, D.A., (Eds.), *Mammal Species of the World: a taxonomic and geographic reference*, third ed. Vol.2, pp. 894–1531.

Oliveira, J. A. & Bonvicino, C. R. (2011). *Ordem Rodentia*, in: Reis, N. R., Peracchi, A. L., Pedro, W. A., Lima, I. P. (Eds.), *Mamíferos do Brasil*. 2ª ed. Londrina (PR), Universidade Estadual de Londrina, pp. 358–415.

Pardiñas, U. F. J., Teta, P., Salazar-Bravo, J., Myers, P. & Galliari, C. A. (2016). A new species of arboreal rat, genus *Oecomys* (Rodentia, Cricetidae) from Chaco. *Journal of Mammalogy*, 97(4), 1177–1196.

Patton, J. L. & Da Silva, M. N. F. (1995). A review of the spiny mouse genus *Scolomys* (Rodentia: Muridae: Sigmodontinae) with the description of a new species from the western Amazon of Brazil. *Proceedings of the Biological Society of Washington*, 108, 319–337.

Patton, J. L., Da Silva, M. N. F. & Malcom, J. R. (2000). Mammals of the rio Juruá and the evolutionary and ecological diversification of Amazonia. *Bulletin of the American Museum of Natural History*, 244, 1–306.

Rocha, R. G., Duda, R., Flores, T., Rossi, R., Sampaio, I., Mendes-Oliveira, A. C., Leite, Y. L. R. & Costa, L. P. (2018). Cryptic diversity in the *Oecomys roberti* complex: revalidation of *Oecomys tapajinus* (Rodentia, Cricetidae). *Journal of Mammalogy*, 99, 174–186.

Rocha, R. G., Ferreira, E., Costa, B. M. A., Martins, I. C. M., Leite, Y. L. R., Costa, L. P. e Fonseca, C. (2011). Small mammals of the mid-Araguaia River in central Brazil, with the description of a new species of climbing rat. *Zootaxa*, 2789, 1–34.

Rosa, C. C., Flores, T., Pieczarka, J. C., Rossi, R. V., Sampaio, M. I. C., Rissino, J. D., Amaral, P. J. S. & Nagamachi, C. Y. (2012). Genetic and morphological variability in South American rodent *Oecomys* (Sigmodontinae, Rodentia): evidence for a complex of species. *Journal of Genetics*, 91(3), 265–277.

Saldanha, J., Ferreira, D. C., da Silva, V. F., Santos-Filho, M., Mendes-Oliveira, A. C. & Rossi, R. V. (2019). Genetic diversity of *Oecomys* (Rodentia, Sigmodontinae) from the Tapajós River basin and the role of rivers as barriers for the genus in the region. *Mammalian Biology*, 97, 41–49.

Suárez-Villota, E. Y., Carmignotto, A. P., Brandão, M. V., Percequillo, A. R. & Silva, M. J. J. (2018). Systematics of the genus *Oecomys* (Sigmodontinae: Oryzomyini): molecular phylogenetic, cytogenetic and morphological approaches reveal cryptic species. *Zoological Journal of the Linnean Society*, 184, 182–210.

Tate, G. H. H. (1932). The taxonomic history of the South and Central American Oryzomine genera of rodents (excluding *Oryzomys*): *Nesoryzomys*, *Zygodontomys*, *Chilomys*, *Delomys*, *Phaenomys*, *Rhagomys*, *Rhipidomys*, *Nyctomys*, *Oecomys*, *Thomasomys*, *Inomys*, *Aepeomys*, *Neacomys* and *Scolomys*. *American Museum novitates*, 581 p.

Thomas, O. (1909). New species of *Oecomys* and *Marmosa* of Amazonia. *Annals and Magazine of Natural History*, 8(3), 378-380.

Trouessart, E.L. (1898). *Fasciculos II: Rodentia II*. In: Berolini, R., Friedländer e Sohn. *Catalogus mammalium tam viventium quam fossilium*, pp. 519–520.

CAPÍTULO I

Genetic diversity of *Oecomys* (Rodentia, Sigmodontinae) from the Tapajós River basin and the role of rivers as barriers for the genus in the region

Artigo publicado pela revista *Mammalian Biology*, 97, 41–49

ISSN: 1616-5047; classificação CAPES: A2

<https://doi.org/10.1016/j.mambio.2019.04.009>

Saldanha, J., Ferreira, D.C., Silva, V. F., Santos–Filho, M., Mendes–Oliveira, A. C. & Rossi, R. V. (2019). Genetic diversity of *Oecomys* (Rodentia, Sigmodontinae) from the Tapajós River basin and the role of rivers as barriers for the genus in the region. *Mammalian Biology*, 97, 41–49.

1 **Genetic diversity of *Oecomys* (Rodentia, Sigmodontinae) from the Tapajós**
2 **River basin and the role of rivers as barriers for the genus in the region**

3 Juliane Saldanha^{a,b}, Daniela Cristina Ferreira^b, Victor Fonsêca da Silva^a, Manoel
4 Santos-Filho^c, Ana Cristina Mendes-Oliveira^d, Rogério Vieira Rossi^a

5 ^a Laboratório de Mastozoologia, Instituto de Biociências, Universidade Federal do
6 Mato Grosso, Cuiabá, Mato Grosso, Brasil,

7 ^b Laboratório de Citogenética e Genética Animal, Instituto de Biociências,
8 Universidade Federal do Mato Grosso, Cuiabá, Mato Grosso, Brasil,

9 ^c Laboratório de Mastozoologia, Universidade do Estado de Mato Grosso, Cáceres,
10 Mato Grosso, Brasil,

11 ^d Laboratório de Zoologia e Ecologia de Vertebrados, ICB, Universidade Federal do
12 Pará, Pará, Brasil.

13 **Abstract**

14 The genus *Oecomys* is one of the most speciose within the subfamily
15 Sigmodontinae, with most species found in the Amazon region. Recent studies have
16 shown that the diversity, recognition of specific boundaries and geographical
17 distribution is still imprecise for the genus. Herein, we investigate the genetic diversity
18 of *Oecomys* in the Tapajós River basin and determine whether its rivers (Tapajós,
19 Teles Pires, and Juruena) act as barriers for some species or populations in this
20 genus based on phylogenetic analyzes with the mitochondrial marker cytochrome b
21 (cytb) and the nuclear marker intron 7 β -fibrinogen, and on populational analysis with
22 cytb. The phylogenetic relationships showed the presence of seven species in the
23 region, namely *O. bicolor*, *Oecomys* aff. *catherinae*, *O. catherinae*, *O. cleberi*, *O.*
24 *paricola*, *O. roberti*, and *O. tapajinus*. The geographic distributions of *O. bicolor* and
25 *O. cleberi* seem to be shaped by the Tapajós and Teles Pires Rivers, with the former
26 species occurring on the right bank and the latter species on the left bank of both
27 rivers. Moreover, *O. cleberi* was the only *Oecomys* species to be recorded on the left
28 bank of the Tapajós River. Our results also indicate that gene flow occurs between
29 *O. cleberi* populations from the west Juruena and Tapajós Rivers and is absent
30 between opposite banks of the Juruena River. The isolation by distance was
31 discarded for this species. No evidence of gene flow was found for *O. bicolor*
32 populations, and the isolation by distance was positive for this species. The spatial
33 distribution of specimens and haplotypes of *O. paricola* indicates that the Teles Pires
34 River does not act as a barrier for this species. Finally, F_s test significant results for

35 *O. cleberi* and *O. paricola* showed that species population expansion cannot be
36 discarded for these species.

37 **Key-words:** Phylogeny, Geographic distribution, Gene flow, Teles Pires River,
38 Juruena River.

39 **Introduction**

40 Knowledge about species richness of genus *Oecomys*, has increased
41 considerably in recent years through the use of chromosomal and molecular
42 analyses, revealing new species and greater geographic distribution for the genus
43 (Asfora et al., 2011; Malcher et al., 2017; Rocha et al., 2011, 2018; Rosa et al., 2012;
44 Suárez-Villota et al., 2018). Currently, the genus comprises eighteen species, one of
45 which was recently described and another recently revalidated (Pardiñas et al., 2017;
46 Rocha et al., 2018).

47 Richness estimates of *Oecomys* in any region are still unreliable due to the
48 difficulty in defining the morphological limits and geographical distribution of the
49 species. The majority of *Oecomys* species occur in the Amazon basin (Bonvicino et
50 al., 2008; Carleton and Musser, 2015; Oliveira and Bonvicino, 2011; Paglia et al.,
51 2012), which is considered one of the most biodiverse regions on the planet. Among
52 the various hypotheses that try to explain the origin of the high mammal diversity in
53 the Amazonia, the presence of rivers as barriers (Wallace, 1852) is one of the most
54 studied (Antonelli et al., 2010). According to Patton et al. (2000), Wallace's
55 hypothesis was based on distribution patterns, but also implies that rivers from the
56 Amazonia not only separate distinct faunas but may strongly reduce gene flow
57 between populations of opposite banks, and thus have promoted speciation.

58 Evidences that river dynamics contribute to the Amazonian diversification have
59 been pointed out by Ribas et al. (2012), who linked the development of rivers to the
60 isolation and delimitation of endemic areas for birds of the genera *Psophia*.
61 Conversely, Oliveira et al. (2017) claimed that Amazonian rivers do not demarcate
62 areas of endemism, but act as dispersal barriers for some species, resulting in areas
63 with different species compositions.

64 The Tapajós River has been recognized as a biogeographical barrier that
65 separates two Amazonian centers of endemism (Silva et al., 2005). The Tapajós
66 River basin covers about 492,200 km² in the south-central part of the Amazon and

67 includes the Teles Pires and Juruena Rivers as tributaries (PERH-MDA, 2011).
68 According to and Carleton and Musser (2015) and Pardiñas et al. (2017), four
69 species of *Oecomys* are expected to occur in the Tapajós River basin, namely *O.*
70 *bicolor*, *O. paricola*, *O. roberti*, and *O. trinitatis*. More recently, Suárez-Villota et al.
71 (2018) pointed out the occurrence of seven evolutionary lineages for the region,
72 probably representing different species associated to the complexes *O. bicolor/O.*
73 *cleberi*, *O. catherinae*, *O. paricola*, and *O. roberti*. Finally, the recently revalidated
74 species *O. tapajinus* was recognized for the region by Rocha et al. (2018).

75 These recent findings confirm the difficulty in determining species limits and
76 geographical distributions of *Oecomys* species in the Tapajós River basin. A great
77 sample of *Oecomys* sequences obtained by us provided the chance to investigate
78 the genetic diversity of this genus in the region and evaluate if the Tapajós River and
79 two major tributaries – the Teles Pires and the Juruena Rivers – act as barriers for
80 some species or populations of *Oecomys*, based on phylogenetic and population
81 analyses using the mitochondrial marker cytochrome b and the nuclear marker intron
82 7 β -fibrinogen.

83 **Materials and Methods**

84 **Sampling**

85 In this study, sequences were generated from 101 specimens of *Oecomys*
86 from 21 localities on the banks of the Tapajós, Juruena, and Teles Pires Rivers (Fig.
87 1), as well as two *Oecomys rex* specimens and one *Euryoryzomys macconnelli*
88 specimen from the State of Pará (Supplementary Material, Table 1). The muscle
89 tissue aliquots were extracted from samples preserved in 100% alcohol and stored at
90 -20° C in the Zoological Collection at the Universidade Federal de Mato Grosso
91 (UFMT), Universidade Federal do Pará (UFPA), and Universidade do Estado de
92 Mato Grosso (Unemat). The sampling of the genus was complemented with
93 sequences of 67 *Oecomys* specimens from the GenBank, 21 of which come from five
94 localities in the Tapajós River basin (Fig. 1 and Supplementary Material, Table1).

95 **DNA extraction, amplification and sequencing**

96 The total DNA was obtained using the saline extraction protocol with
97 modifications by Aljanabi and Martinez (1997) and was visualized in 1% agarose gel
98 stained with red gel to verify its integrity. For molecular analyses, we used the

99 mitochondrial cytochrome gene b (cytb) and the nuclear marker intron 7 β -fibrinogen
100 (i7-fgb).

101 The cytb mitochondrial gene was amplified using the Polymerization Chain
102 Reaction (PCR) technique, using the MVZ05
103 (CGAAGCTTGATATGAAAACCATCGTTG) and MVZ16
104 (AAATAGGAARTATCAYTCTGGTTTRAT) initiators (Smith and Patton, 1993). The
105 PCRs were carried out with a final volume of 13.5 μ l, containing 1.5 μ l de dNTP (1.25
106 mM), 1.25 μ l 10x buffer, 1 μ l of the initiator MVZ05 (2 mM), 1 μ l of the initiator MVZ16
107 (2 mM), 0.4 to 0.65 μ l de $MgCl_2$ (50 mM), 0.2 μ l of Taq DNA Polimerase (Ludwig,
108 5U/ μ l), 1 μ l of DNA, and autoclaved Milli-Q filtered H_2O until the final volume. The
109 reactions were processed in a thermocycler (Applied Biosystems, Veriti), with initial
110 denaturation at 94°C for 5 minutes, followed by 30 cycles of denaturation at 94°C for
111 30 seconds, annealing at 45°C to 52°C for 45 seconds, extension at 72°C for 45
112 seconds, and final extension at 72°C for 5 minutes.

113 The nuclear marker i7-fgb was amplified with the initiators β I7-mammL
114 (ACCCAGTAGTATCTGCCGTTTGGATT) and β fib-mammU
115 (CACAACGGCATGTTCTTCAGCAC) (Matocq et al., 2007). The PCR's were carried
116 out with a final volume of 35 μ l, containing 4 μ l of dNTP (1.25 mM), 3.5 μ l 10x buffer,
117 2 μ l of the initiator β I7-mammL (2 mM), 2 μ l of the initiator β fib-mammU (2 mM), 2 μ l
118 of $MgCl_2$ (50 mM), 0.3 μ l of Taq DNA Polimerase (Ludwig, 5 U/ μ l), 1 μ l of DNA, and
119 autoclaved Milli-Q filtered H_2O until the final volume. The reactions were processed in
120 a thermocycler (Applied Biosystems, Veriti), with initial denaturation at 93°C for 5
121 minutes, followed by 35 cycles of denaturation at 93°C for 1 minute, annealing 55°C
122 for 1 minute, extension at 72°C for 2 minutes and 45 seconds, and final extension at
123 72°C for 2 minutes.

124 PCR products were purified using the enzyme method with EXO-SAP
125 (Affymetrix). The two tapes (forward and reverse) were sequenced for the two genes,
126 cytb and i7-fgb, with the same initiators used in the PCR and BigDye® Terminator v
127 3.1 Cycle Sequencing kit, following the manufactures' protocol for the Sequencer ABI
128 3500 (Applied Biosystems®).

129 The sequences obtained were displayed and aligned to assemble the
130 consensus sequence in the Geneious® program. Subsequently, the sequences
131 were edited and aligned by the ClustalW tool in the BioEdit 7.0.5.2 program (Hall,

132 1999). These sequences were also subjected to a saturation test implemented in the
133 DAMBE5 program (Xia, 2013).

134 **Phylogenetic analysis and diversity**

135 In order to assess the relationships of *Oecomys* specimens from the Tapajós
136 River basin with other congeners, phylogenetic analyses were carried out using
137 partial sequences of the cytb gene (801 base pairs) from 170 individuals
138 (Supplementary Material, Table 1), including representatives of all currently
139 recognized species, except for *O. flavicans*, *O. phaeotis*, and *O. speciosus*, which
140 had no available sequences. *Euryoryzomys macconnelli* (this study), *Handleyomy*
141 *intectus*, "*Handleyomys*" *melanotis* (species provisionally allocated under
142 *Handleyomys*; see Pardiñas et al., 2017), and *Oligoryzomys utiaritensis* (GenBank
143 sequences) were employed as external group. Phylogenetic analyses were also
144 performed using the concatenated sequences of cytb and i7-fgb (736 base pairs)
145 from 77 specimens of *Oecomys* and sequences of *Handleyomys melanotis* and
146 *Oligoryzomys utiaritensis* as external group (Supplementary Material, Table 1).
147 Lineage names were defined according to Suárez-Villota et al. (2018) and Rocha et
148 al. (2018).

149 The evolutionary models that best represented the data matrix were generated
150 in the JModeltest program (Posada, 2008). The model that best represented the cytb
151 data matrix was the GTR+I+G. The matrix of concatenated data was best
152 represented by the GTR+I+G model for the partition of cytb and TIM2+I+G for the
153 partition of the i7-fgb marker. The data matrix for analysis based on the cytb and the
154 i7-fgb presented 311 and 93 nucleotide substitutions, respectively. The data did not
155 show saturation (cytb: transition $R^2= 0.9629$ transversion $R^2= 0.9348$; i7-fgb:
156 transition $R^2= 0.9387$ transversion $R^2= 0.8956$).

157 The Bayesian Inference (BI) analyses were carried out in the MrBayes 3.1.2
158 program (Ronquist and Huelsenbeck, 2003), with four chains, 20 million generations,
159 a sampling tree every 100 generations and 25% burn-in. Maximum Likelihood (MV)
160 analyses were carried out in the Garli 2.0 program (Zwickl, 2006), with bootstrap
161 support of 1000 replicas. The trees obtained in the Garli program were summarized
162 by majority consensus in the SumTrees program. The trees obtained from MV and BI
163 were viewed and edited in the program Figtree version 1.4.3 (Rambaut, 2016). The

164 genetic distances between and within the clades were calculated in the MEGA7
165 (Kumar et al., 2016) using the Kimura 2 parameters (K2p) method.

166 **Populational analyses and structure**

167 Population analyses were carried out using *O. bicolor* and *O. cleberi* samples
168 together to investigate genetic variability and geographical structuring in the *O.*
169 *bicolor/O. cleberi* species complex. Population analyses were also carried out with
170 the samples of *O. paricola*, whose species served as a model to investigate if the
171 rivers acted as barriers to gene flow, given its geographical distribution in the Tapajós
172 River basin region. For these analyses, the number of haplotypes (H) was generated
173 in the DnaSP V6 program (Rozas et al., 2017) and the relationships between
174 haplotypes were evaluated through the networks with *cytb* data by the Median-
175 Joining method (Bandelt et al., 1999) in the PopArt program
176 (<http://popart.otago.ac.nz>). The differentiation of populations into hierarchical levels
177 was calculated by the Molecular Variance Analysis (AMOVA) (Excoffier et al., 1992)
178 and, for the *O. bicolor/O. cleberi* species complex, these levels were considered two
179 distinct groups. The population structure was verified based on the genetic
180 differences between populations by comparing the F_{ST} (Weir and Cockerham, 1984).
181 Both analyses were calculated in the Arlequin 3.5 program (Excoffier and Lischer,
182 2010). To test the isolation by distance, the Mantel test was carried out in the Alleles
183 in Space program (Miller, 2005).

184 The mismatch distribution analysis in the DnaSP v6 program was used to test
185 population expansion (Rozas et al., 2017), which compared the observed and
186 expected distribution in an expansion model. In this model, the statistical test for
187 deviations was the raggedness index (Harpending, 1994), in which an expanding
188 population generates distributions of regular and unimodal mismatch. For
189 demographic pattern description, we verified haplotype (h) and nucleotide (π)
190 diversity values. The deviations of neutrality were verified by D (Tajima, 1989) and F_s
191 (Fu, 1997) tests, which were carried out in the Arlequin 3.5 program (Excoffier and
192 Lischer, 2010).

193 Results

194 Diversity of *Oecomys* in the Tapajós River basin

195 From the 101 samples analyzed in the present study, it was verified that there
196 are either six or seven species with occurrence for the Tapajós River basin (Figs. 2
197 and 3). BI analysis with *cytb* recognized six highly supported lineages, namely *O.*
198 *bicolor*/*O. cleberi*, *Oecomys* aff. *catherinae*, *O. catherinae*, *O. paricola*, *O. roberti*,
199 and *O. tapajinus* (Fig. 2) with genetic mean distances of 5.64% to 10.54%
200 (Supplementary Material, Table 2). BI analysis with concatenated data recognized
201 seven highly supported lineages, with *O. bicolor* and *O. cleberi* recovered as distinct
202 lineages (Fig. 3). Genetic mean distances varied from 4.84% to 11.68% among the
203 lineages recovered in the concatenated data analysis (Supplementary Material,
204 Table 3).

205 Specimens of *O. cleberi*, *O. roberti* and *O. tapajinus* from the Tapajós River
206 basin were not recovered as monophyletic groups (Fig. 2). In the BI analysis with
207 *cytb*, *O. cleberi* specimens from Aripuanã and Cotriguaçu (localities 23 and 24,
208 respectively; Figs. 1 and 2) grouped in a clade with individuals from south-central
209 Brazil (States of Goiás and São Paulo, and the Federal District). In addition, *O.*
210 *cleberi* specimens from the east bank of the Tapajós and Juruena Rivers (localities 1,
211 2, 3, 4, 24; Figs. 1 and 2) nested in a separate clade from the rest of the species.
212 Similarly, specimens of *O. roberti* from the Tapajós River basin (except for one
213 individual from locality 15) grouped with a sample from the Pantanal (HM594597).
214 Finally, the *O. tapajinus* clade included samples from the Tapajós River basin and
215 the Araguaia–Tocantins Rivers basin.

216 We recorded *O. bicolor*, *O. paricola* and *O. tapajinus* in sympatry on the east
217 bank of the Tapajós River, whereas only *O. cleberi* specimens were recorded on the
218 west bank. In the middle east Teles Pires River, we recorded *O. bicolor*, *O. paricola*
219 and *O. roberti*. In the low east Teles Pires River we recorded *Oecomys* aff.
220 *catherinae*, *O. paricola* and *O. roberti*. In the Teles Pires–Juruena interfluve, we
221 recorded *Oecomys* aff. *catherinae*, *O. cleberi*, *O. paricola* and *O. roberti*. Finally, on
222 the west bank of the Juruena River we recorded *Oecomys* aff. *catherinae*, *O.*
223 *catherinae* and *O. cleberi* (Fig. 1; Supplementary Material, Table 1).

224 **Population structure of *O. bicolor*, *O. cleberi* and *O. paricola* from the Tapajós**
225 **River basin**

226 The AMOVA of the *O. bicolor/O. cleberi* complex indicated greater variation
227 between these groups (56.26%), followed by the variation between populations within
228 groups (26.73%) and the variation within the populations (17.01%; Table 1),
229 supporting the differentiation between these two species that appeared separated by
230 25 mutational steps in the haplotypes network.

231 The species *O. cleberi* presented two haplogroups in the Teles Pires–Juruena
232 interfluvium (haplogroups B and D, Fig. 4), separated by 19 mutational steps.
233 Individuals from the west bank of the Juruena River were separated into two
234 haplogroups (A and C, Fig. 4), with one individual from this region grouped with the
235 west bank of the Tapajós River (haplogroups C, Fig. 4), indicating the presence of
236 gene flow between populations on the west bank of the Juruena and Tapajós Rivers.
237 Despite the haplogroups B and D occur in the same region, the former is closer to
238 the haplogroups A and C, from which it differs by 11 and seven mutational steps
239 respectively, evidencing the absence of geographic structure in the species. We
240 found no evidence of haplotype sharing across the Juruena River opposite banks.

241 Although one haplotype from the west bank of the Juruena River nests with
242 haplotypes of the west bank of the Tapajós River forming the haplogroup C, the
243 greatest genetic differentiation (F_{st} value of 0.62; Supplementary Material, Table 4)
244 was found between the populations on the west bank of the Tapajós and Juruena
245 Rivers. The Mantel test was not significant ($r= 0.124$ $p= 0.09$), indicating the absence
246 of isolation by distance in populations of the species.

247 The species *O. bicolor* was represented by two haplogroups separated by nine
248 mutational steps (haplogroups E and F, Fig. 4), which presented F_{st} equal to 0.84
249 (Supplementary Material, Table 4). The Mantel test showed high correlation between
250 genetic and geographical distance in populations of the species ($r= 0.585$ $p= 0.0009$).

251 The haplotypes network of *O. paricola* did not reveal geographic structure (Fig.
252 5), with haplotypes shared between individuals from opposite banks of the Teles
253 Pires River. According to the AMOVA, high genetic variation (62.65%) occurs within
254 the populations (Table 1), with the highest F_{st} (0.65) recovered between the
255 populations from the middle and low Teles Pires River, and the lowest value (0.25)
256 found between the populations from the middle Tapajós River and low Teles Pires

257 River (Supplementary Material, Table 4). We also did not find significant values in the
258 genetic isolation test for geographical distance ($r= 0.092$ $p= 0.09$).

259 Populations of the three analyzed species showed irregular and multimodal
260 mismatch distribution (Fig. 6) (*O. bicolor*: $r= 0.06$, $p= 0.06$; *O. cleberi*: $r= 0.005$, $p=$
261 0.94 ; *O. paricola*: $r= 0.009$, $p= 0.86$). Among the neutrality tests herein performed,
262 only the F_s showed significant results for *O. cleberi* and *O. paricola*. The haplotype
263 diversity was high and nucleotide diversity was low for the three species (Table 2).

264 Discussion

265 Diversity of *Oecomys* in the Tapajós River basin

266 Our analyses confirmed the occurrence of seven species of *Oecomys* in the
267 Tapajós River basin. Among these species, two comprise specimens that have been
268 previously associated to the *O. catherinae* complex (Suárez-Villota et al., 2018). In
269 our analyses with *cytb* data, one species grouped with the lineage that represents *O.*
270 *catherinae* stricto sensu from eastern Brazil and, for that reason, it is herein called *O.*
271 *catherinae*. The other species forms a tritomy with *O. catherinae* and *O. rex* (Fig. 2).
272 Due to its morphological similarity and close relationship with *O. catherinae* pointed
273 out by Suárez-Villota et al. (2018), the species is herein referred as *Oecomys* aff.
274 *catherinae*. This species presented 8.94% of mean genetic divergence from *O.*
275 *catherinae* (Supplementary Material, Table 2), which is similar to the 7.2-8.87% of
276 mean genetic divergence values reported by Suárez-Villota et al. (2018) between the *O.*
277 *catherinae* western clade (= ours *Oecomys* aff. *catherinae*) and the other lineages
278 within the *O. catherinae* complex of the authors. In addition, the species was
279 recovered as the sister species of a clade composed of *O. bicolor*, *O. catherinae*, *O.*
280 *cleberi*, *O. franciscorum*, *O. paricola*, *O. roberti*, and *O. tapajinus* in our BI and MV
281 analyses with concatenated data (Fig. 3). Therefore, the relationship of *Oecomys* aff.
282 *catherinae* with other congeners needs further clarification.

283 *Oecomys paricola* has recently been revealed as a species complex by Rosa
284 et al. (2012), who found karyotypic differences and high intraspecific genetic distance
285 (3.9%) within the species. In turn, Suárez-Villota et al. (2018) recognized three
286 distinct lineages in *O. paricola* (northern, eastern, and western lineages of authors),
287 with genetic divergences varying from 2.9 to 6.2% among them. Our specimens
288 grouped with the *O. paricola* western clade of the authors, evidencing that this

289 lineage extends to the right bank of the Tapajós River (Fig. 1). The species
290 presented 1.83% of intraspecific genetic divergence, notably lower than the 3.6% and
291 4.1% internal divergences found by Rocha et al. (2011) and Rocha et al. (2012),
292 respectively.

293 Based on the *cytb* marker and 11 specimens, Rocha et al. (2012) recovered
294 *O. bicolor* and *O. cleberi* as reciprocal monophyletic groups with high support values
295 and 6.8% of mean genetic distance. Despite of Rocha´s et al. (2012) promising
296 results, Suarez-Villota et al. (2018) were not able to separate these species
297 employing *cytb* and two nuclear markers of 24 specimens. Therefore, the latter
298 authors included both species in a single species complex, in which they recognized
299 two lineages associated to *O. cleberi* and six lineages associated to *O. bicolor*, with
300 genetic distances varying from 3.3% to 6.9% among them. Our *cytb* analyses did not
301 recover *O. bicolor* and *O. cleberi* as reciprocal monophyletic groups either (Fig. 2).
302 By contrast, our BI analysis with concatenated data recovered both species as
303 monophyletic, with high support and 4.84% of mean genetic divergence.
304 Interestingly, specimens of *O. bicolor* central and western clades of Suarez-Villota et
305 al. (2018) nested within our *O. cleberi* clade (Fig. 3). These results were also
306 obtained by our populational analyses, discussed below. Therefore, based on our BI
307 and populational analyses, we recognize the presence of both *O. bicolor* and *O.*
308 *cleberi* in the Tapajós River basin. These analyses also showed that *O. cleberi*
309 geographic distribution, currently restricted to south-central Brazil and sothern
310 Amazonia (Pardiñas et al., 2017; Suárez-Villota et al., 2018), extends to the west
311 bank of the Tapajós River (Fig. 1).

312 *Oecomys roberti* has recently been recognized as a species complex by
313 Suarez-Villota et al. (2018), composed of three distinct lineages called eastern,
314 central, and western clades by the authors, with genetic distances varying from 5.2%
315 to 9.1% among them. Our samples of *O. roberti* grouped with the authors´ central
316 clade, while our samples of *O. tapajinus* grouped with the author´s eastern clade. In
317 this sense, this latter clade of Suarez-Villota et al. (2018) corresponds to *O.*
318 *tapajinus*, a species revalidated by Rocha et al. (2018). Additionally, *O. tapajinus* was
319 recovered as sister to *O. roberti* in our BI and MV analyses with concatenated data
320 and our BI analysis with *cytb* data, supporting the close relation between these
321 species previously reported in the literature (Rocha et al., 2012; Rocha et al., 2018;
322 Suarez-Villota et al., 2018).

323 Despite Carleton and Musser (2015) report of *O. trinitatis* in Humboldt
324 Laboratory, Aripuanã, state of Mato Grosso, and even southward in Maracaju, state
325 of Mato Grosso do Sul, we did not find individuals of this species in our samples.
326 According to the authors, *O. trinitatis* exhibits dorsal fur soft and dense (10–13 mm
327 over middle rump), ventral fur that ranges from dark grayish white to rich ochraceous
328 gray, and robust skull, with narrow interorbit and distinct supraorbital ridges or
329 shelves that strongly diverge caudally to join prominent temporal ridges. All these
330 characters also apply to specimens of the *O. catherinae* complex, which Carleton
331 and Musser (2015) discriminate from *O. trinitatis* on the basis of a supposed smaller
332 size exhibited by the latter species. Considering that (i) we were not able to
333 confidently associate any of our specimens to *O. trinitatis*, (ii) there are no molecular
334 studies reporting this species to the state of Mato Grosso or farthest south, and (iii)
335 the diagnostic characters provided by Carleton and Musser (2015) cannot confidently
336 discriminate *O. trinitatis* from *O. catherinae*, we argue that the presence of the former
337 species in the Tapajós River basin still needs to be confirmed.

338 Species of *Oecomys* traditionally not recognized to occur in the Tapajós River
339 basin, such as *O. auyantepui*, *O. concolor*, *O. franciscorum*, *O. mamorae*, *O. rex*, *O.*
340 *rutilus*, *O. superans*, and *O. sydandersoni* were not identified in our samples. Also,
341 we were not able to associate any of our specimens to the three unnamed lineages
342 (*Oecomys* sp.1, *Oecomys* sp.2 e *Oecomys* sp.3) recognized by Suárez-Villota et al.
343 (2018).

344 Our results show the occurrence of up to four sympatric species in the Tapajós
345 River basin. Four to five *Oecomys* species in sympatry have already been reported
346 by Patton et al. (2000) in Colocação Vira-Volta, left bank the Juruá River, Amazonas
347 state, Brazil (four species); by Voss et al. (2001) in Kartabo, Guyana (five species), in
348 Arataye, French Guiana (four species), and in 52 km SSW Altamira, right bank of the
349 Xingu River, Brazil (four species); by Silva et al. (2013) in Cachoeira Santo Antônio,
350 Amapá state, Brazil; and by Suárez-Villota et al. (2018) in Cláudia, state of Mato
351 Grosso, Brazil.

352 According to Carleton and Musser (2015), species of *Oecomys* may be
353 classified as small-sized (head and body length 84–105 mm), medium-sized (head
354 and body length 109–125 mm) and large-sized (head and body length 125–150 mm).
355 In the Juruena–Teles Pires interfluve, we observed sympatry among *Oecomys*

356 species of the three body size classes, namely *O. cleberi* (small), *O. paricola* and *O.*
357 *roberti* (medium), and *Oecomys* aff. *catherinae* (large).

358 The sympatry among different-sized species of *Oecomys* were already
359 mentioned by Patton et al. (2000) and Suárez-Villota et al. (2018). As already
360 discussed by the latter authors, although there is no study of niche occupancy for
361 *Oecomys*, it is reasonable to infer that species with different body sizes explore
362 distinct resources, allowing their coexistence. Similarly, arboreality might be related
363 to the different ways species of *Oecomys* use the forest strata, favoring sympatry. In
364 a compilation of ecological studies on small nonvolant mammals from the Cerrado
365 biome, Alho (2015) pointed out that more than 80% of the captures of a small-sized
366 *Oecomys* species (identified by him as *O. bicolor*) occurred in the superior stratum,
367 while a medium-sized species (identified by him as *O. concolor*) were more
368 frequently captured in the inferior stratum, close to the ground.

369 Sympatry among *Oecomys* species with similar body size has also been
370 reported in the literature. Patton et al. (2000), for example, recorded two small-bodied
371 species (*O. bicolor* and *Oecomys* sp.2 of the authors) in Colocação Vira-Volta, left
372 bank the Juruá River. However, this sympatry has been more frequently recorded for
373 medium-sized species, such as *O. roberti* and *O. tapajinus* in localities of the mid-
374 Araguaia River basin (Rocha et al., 2014, 2018), *O. paricola* and *O. roberti* in both
375 banks of the Teles Pires River, and *O. paricola* and *O. tapajinus* in the east bank of
376 the Tapajós River (this study). Despite these recurrent records, the real causes for
377 the high level of sympatry found in *Oecomys*, which is a rare phenomenon for the
378 Sigmodontinae rodents, will only be unveiled if studies are carried out to investigate
379 the use of resources by its species.

380 **Population structure of *Oecomys* from the Tapajós River basin**

381 The geographic distributions of *O. bicolor* and *O. cleberi* appear to be shaped
382 by the Tapajós and Teles Pires Rivers, with the former species occurring on the east
383 bank and the latter species on the west bank of both rivers. Moreover, *O. cleberi* was
384 the only *Oecomys* species to be recorded on the west bank of the Tapajós River.
385 This pattern supports Oliveira's et al. (2017) argument that the major Amazonian
386 rivers coincides with breaks in species composition, acting as dispersal barriers for
387 some species. In particular, the Tapajós River have also been pointed out as a

388 barrier for some species of birds (Harvey and Brumfield, 2014, Ribas et al., 2012),
389 amphibians and squamates (Moraes et al., 2016).

390 Our results of populational analyses indicate the presence of gene flow
391 between populations of *O. cleberi* on the west bank of the Juruena and Tapajós
392 Rivers, and absence of gene flow between populations of *O. bicolor* on the east bank
393 of the Teles Pires and Tapajós Rivers. These results may be related to the great
394 geographical distance between the two populations of *O. bicolor* herein analyzed,
395 namely East Tapajós and Middle East Teles Pires (Fig. 4). Similar results were
396 obtained by Rocha et al. (2014), who studied the populational structure of *Oecomys*
397 *aff. roberti* (= *O. tapajinus*) along the mid-Araguaia river basin. However, by analysing
398 a greater number of populations, Rocha et al. (2018) refuted the scenario of isolation
399 by distance for this species.

400 One implication of the riverside hypothesis is the existence of unique
401 haplotypes in monophyletic clades and on opposite river banks (Antonelli et al., 2010;
402 Patton et al., 2000). The Araguaia River has already been considered a barrier for
403 rodents of the genus *Rhipidomys* (Rocha et al., 2011) and small marsupials with
404 specialized habits, like *Gracilinanus* (Rocha et al., 2015). On the other hand, this
405 river does not constitute a barrier for large-sized marsupials with generalist habits,
406 such as *Didelphis* (Rocha et al., 2015), nor for the rodents *Hylaeamys*
407 *megacephalus* (Rocha et al., 2014). For *O. tapajinus*, Rocha et al. (2014)
408 demonstrated shared haplotypes in populations from opposite banks of the Araguaia
409 River, rejecting this hypothesis for the diversification of the species. Similarly, we
410 found that individuals of *O. paricola* from opposite banks of the Teles Pires River
411 share the same haplotype, indicating that this river does not act as a barrier for this
412 species.

413 According to Haffer (2008), the number of species delimited by Amazonian
414 rivers is proportional to the width of the rivers, that is, narrower rivers may not act as
415 barriers for certain groups. Bates et al. (2004) emphasized that the Teles Pires River
416 is a narrow tributary (100-300 m wide) that can be easily crossed, rejecting the
417 hypothesis that this river acts as a barrier for birds. The absence of structure of the
418 populations of *O. paricola* herein analyzed support this idea.

419 The distribution of *Oecomys* species might also be associated with
420 evolutionary factors, such as species population expansion, which was not confirmed
421 by the mismatch analysis. Nevertheless, the existence of population expansion

422 cannot be completely discarded, since F_u 's F_s were significant for *O. cleberi* and *O.*
 423 *paricola*. A scenario of population expansion have already been proposed for *O.*
 424 *tapajinus* by Rocha et al. (2018), who suggested that this scenario may be linked to
 425 ecological characteristics of *Oecomys* that are subjected to the expansion and
 426 retraction of forests during glacial cycles, such as the arboreal habits and forest
 427 speciality.

428 In short, our results show high diversity of *Oecomys* species in the Tapajós
 429 River basin, consisting of at least seven species. Our results also refute the
 430 hypothesis that the Teles Pires River is a barrier to gene flow for *O. paricola* and
 431 indicate that the Tapajós River shape the geographical distribution of *Oecomys*
 432 species in this region.

433 **Acknowledgements**

434 We would like to thank Cleuton Lima Miranda for previous discussion of the project
 435 that resulted in this manuscript. This study was supported by the Fundação de Amparo
 436 à Pesquisa do Estado de Mato Grosso (FAPEMAT, process #477017/2011), and
 437 partially by the Coordenação de Aperfeiçoamento de Pessoal de Nível Superior - Brasil
 438 (CAPES) - Finance Code 001.

439 **References**

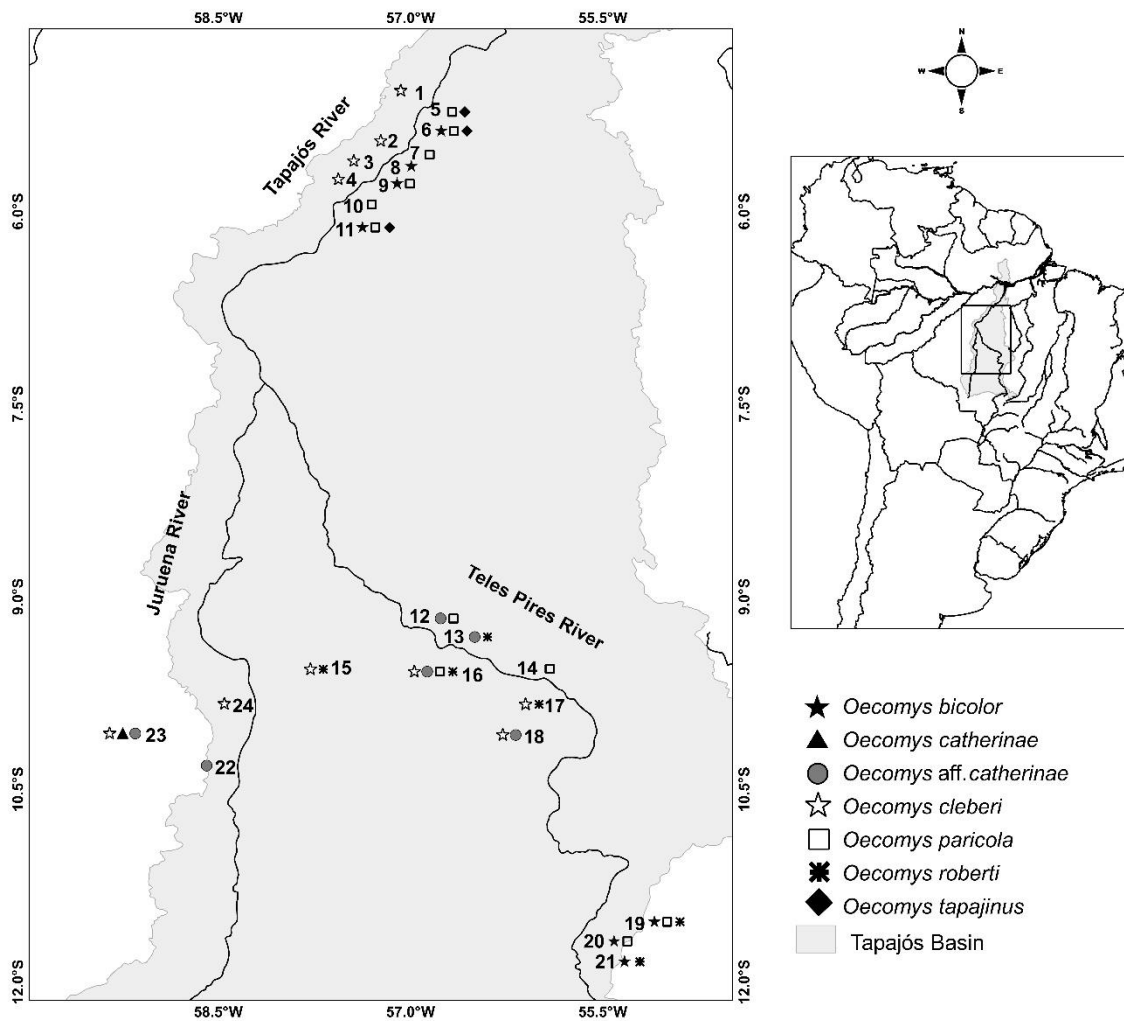
- 440 Alho, C.J.R., 2005. Intergradation of habitats of non-volant small mammals in the
 441 patchy cerrado landscape. *Arq. Mus. Nac.*, Rio de Janeiro. 63(1), 41–48.
- 442 Aljanabi, S.M., Martinez, I., 1997. Universal and rapid salt-extraction of high quality
 443 genomic DNA for PCR-based techniques. *Nucleic Acids Res.* 25, 4692–4693.
- 444 Antonelli, A., Quijada-Mascareñas, A., Crawford, A.J., Bates, J.M., Velazco, P.M.,
 445 Wüster, W., 2010. Molecular studies and phylogeography of Amazonian tetrapods
 446 and their relation to geological and climatic models, in: Hoorn, C., Wesselingh, F.P.
 447 (Eds.), *Amazônia, Landscape and Species Evolution: A Look into the Past*, first ed.
 448 Wiley-Blackwell, pp. 386–404.
- 449 Asfora, P.H., Palma, A.R.T., Astúa, D., Geise, R., 2011. Distribution of *Oecomys*
 450 *catherinae* Thomas, 1909 (Rodentia: Cricetidae) in northeastern Brazil with
 451 karyotypical and morphometrical notes. *Biota Neotrop.* 11(2), 415–424.
- 452 Bandelt, H.J., Forster, P., Röhl, A., 1999. Median-joining networks for inferring
 453 intraspecific phylogenies. *Mol. Biol. Evol.* 16(1), 37–48.
- 454 Bates, J.M., Haffer, J., Grisme, E., 2004. Avian mitochondrial DNA sequence
 455 divergence across a headwater stream of the rio Tapajós, a major Amazonian river.
 456 *J. Ornithol.* 145, 199–205.

- 457 Bonvicino, C.R., Oliveira, J.A., D'andrea, P.S., 2008. Guia dos roedores do Brasil,
458 com chaves para gêneros baseadas em caracteres externos. Rio de Janeiro: Centro
459 Pan-Americano de Febre Aftosa – OPAS/OMS.
- 460 Carleton, M.D., Musser, G.G., 2015. Genus *Oecomys* Thomas, 1906, in: Patton, J.,
461 Pardiñas, U. F. J., D'Elía, G. (Eds.), Mammals of South America, vol.2, rodents.
462 University of Chicago Press, Chicago, Illinois. pp. 393–417.
- 463 Excoffier, L., Lischer, H.E.L., 2010. Arlequin suite ver 3.5: A new series of programs
464 to perform population genetics analyses under Linux and Windows. Mol. Ecol.10,
465 564–567.
- 466 Excoffier, L., Smouse, P., Quattro, J., 1992. Analysis of molecular variance inferred
467 from metric distances among DNA haplotypes: Application to human mitochondrial
468 DNA restriction data. Genet. 131, 479–491.
- 469 Fu, Y.X., 1997. Statistical tests of neutrality of mutations against population growth,
470 Hitchhiking and Background Selection. Genet. 147, 915–925.
- 471 Haffer, J., 2008. Hypotheses to explain the origin of species in Amazonia. Braz. J.
472 Biol. 68(4), 917–947.
- 473 Hall, T.A., 1999. BioEdit: A user-friendly biological sequence alignment editor and
474 analysis program for Windows 85/98/NT. Nucleic Acids Symp. Ser. 41, 95–98.
- 475 Harpending, H.C., 1994. Signature of ancient population growth in a low-resolution
476 mitochondrial DNA mismatch distribution. Hum Biol. 66, 591–600.
- 477 Harvey, M.G., Brumfield, R.T., 2014. Genomic variation in a widespread Neotropical
478 bird (*Xenops minutus*) reveals divergence, population expansion, and gene flow. Mol.
479 Phylogenet. Evol. 38, 305-316.
- 480 Kumar, S., Stecher, G., Tamura, K., 2016. MEGA7: molecular evolutionary genetics
481 analysis version 7.0 for bigger datasets. Mol. Biol. Evol. 33, 1870–1874.
- 482 Malcher, M.S., Pieczarka, J.C., Geise, L., Rossi, R.V., Pereira, A.L., O'Brien, P.C.M.,
483 Asfora, P.H., Silva, V.F., Sampaio, M.I., Ferguson-Smith, M.A., Nagamachi, C.Y.,
484 2017. *Oecomys catherinae* (Sigmodontinae, Cricetidae): Evidence for chromosomal
485 speciation? PLoS ONE, <https://doi.org/10.1371/journal.pone.0181434>
- 486 Matocq, M.D., Shurtliff, Q.R., Feldman, C.R., 2007. Phylogenetics of the woodrat
487 genus *Neotoma* (Rodentia: Muridae): Implications for the evolution of phenotypic
488 variation in male external genitalia. Mol. Phylogenet. Evol. 42, 637–652.
- 489 Miller, M.P., 2005. Alleles In Space (AIS): Computer Software for the Joint Analysis
490 of Interindividual Spatial and Genetic information. J. Hered. 96, 722–724.
- 491 Moraes, L.J.C.L., Pavan, D., Barros, M.C., Ribas, C.C., 2016. The combined
492 influence of riverine barriers and flooding gradients on biogeographical patterns for
493 amphibians and squamates in south-eastern Amazonia. J. Biogeogr. 43, 2113-2124.
- 494 Oliveira, J.A., Bonvicino, C.R., 2011. Ordem Rodentia, in: Reis, N.R., Peracchi, A.L.,
495 Pedro, W.A., Lima, I.P., (Eds.), Mamíferos do Brasil. second ed. Londrina (PR),
496 Universidade Estadual de Londrina, pp. 358–415.
- 497 Oliveira, U., Vasconcelos, M.F., Santos, A.J., 2017. Biogeography of Amazon birds:
498 rivers limit species composition, but not areas of endemism. Sci. Rep. 7, 2992.

- 499 Paglia, A.P., Fonseca, G.A.B., Rylands, A.B., Herrmann, G., Aguiar, L.M.S.,
 500 Chiarello, A.G., Leite, Y.L.R., Costa, L.P., Siciliano, S., Kierulff, M.C.M., Mendes,
 501 S.L., Tavares, V.C., Mittermeier, R.A., Patton, J.L., 2012. Annotated checklist of
 502 brazilian mammals, second ed. *Occas. Pap. Conserve. Biol.* 6, 1–76.
- 503 Pardiñas, U., Ruelas, D., Brito, J., Bradley, L., Bradley, R., Garza, N.O., Kryštufek,
 504 B., Cook, J., Soto, E.C., Salazar-Bravo, J., Shenbrot, G., Chiquito, E., Percequillo, A.,
 505 Prado, J., Haslauer, R., Patton, J., León-Paniagua, L., 2017. Species Accounts of
 506 Cricetidae, in Wilson, D.E., Lacher, T.E., Mittermeier, R.A. (Eds.), *Handbook of*
 507 *mammals of the world, Vol.7, Rodents II.* Lynx Edicions, Barcelona, Spain. pp. 281–
 508 535.
- 509 Patton, J.L., Da Silva, M.N.F., Malcom, J.R., 2000. Mammals of the rio Juruá and the
 510 evolutionary and ecological diversification of Amazonia. *Bull. Am. Mus. Nat. Hist.*
 511 244, 1–306.
- 512 PERH–MDA. 2011. Plano Estratégico de Recursos Hídricos da Bacia Amazônica:
 513 Afluentes da margem direita – Volume I: Descrição das bacias e aspectos físicos.
 514 <http://margemdireita.ana.gov.br/> (accessed 24 April 2018).
- 515 Posada, D., 2008. jModelTest: Phylogenetic Model Averaging. *Mol. Biol. Evol.* 25(7),
 516 1253–1256. doi.org/10.1093/molbev/msn083
- 517 Rambaut, A., 2016. FigTree v1.4.3 2006–2016.
 518 <http://tree.bio.ed.ac.uk/software/figtree/> (accessed 24 April 2018).
- 519 Ribas, C.C., Aleixo, A., Nogueira, A.C.R., Miyaki, C.Y., Cracraft, J., 2012. A
 520 palaeobiogeographic model for biotic diversification within Amazonia over the past
 521 three million years. *Proc. R. Soc. B.* 279, 681–689.
- 522 Rocha, R.G., Duda, R., Flores, T., Rossi, R., Sampaio, I., Mendes–Oliveira, A.C.,
 523 Leite, Y.L.R., Costa, L. P., 2018. Cryptic diversity in the *Oecomys roberti* complex:
 524 revalidation of *Oecomys tapajinus* (Rodentia, Cricetidae). *J. Mammal.* 99, 174–186.
- 525 Rocha, R.G., Ferreira, E., Costa, B.M.A., Martins, I.C.M., Leite, Y.L.R., Costa, L.P.,
 526 Fonseca, C., 2011. Small mammals of the mid–Araguaia River in central Brazil, with
 527 the description of a new species of climbing rat. *Zootaxa.* 2789, 1–34.
- 528 Rocha, R.G., Ferreira, E., Fonseca, C., Justino, J., Leite, Y.L.R., Costa, L.P., 2014.
 529 Seasonal flooding regime and ecological traits influence genetic structure of two
 530 small rodents. *Ecol. Evol.* 4(24), 4598–4608.
- 531 Rocha, R.G., Ferreira, E., Loss, A.C., Heller, R., Fonseca, C., Costa, L.P., 2015. The
 532 Araguaia River as an Important Biogeographical Divide for Didelphid Marsupials in
 533 Central Brazil. *J. Hered.* 106(5), 593–607.
- 534 Rocha, R.G., Fonseca, C., Zhou, Z., Leite, Y.L.R., Costa, L.P., 2012. Taxonomic and
 535 conservation status of the elusive *Oecomys cleberi* (Rodentia, Sigmodontinae) from
 536 central Brazil. *Mamm. Biol.* 77, 414–419.
- 537 Ronquist, F., Huelsenbeck, J.F., 2003. MrBayes: Bayesian phylogenetic inference
 538 under mixed models. *Bioinform.* 19(12), 1572–1574.
- 539 Rosa, C.C., Flores, T., Pieczarka, J.C., Rossi, R.V., Sampaio, M.I.C., Rissino, J.D.,
 540 Amaral, P.J.S., Nagamachi, C.Y., 2012. Genetic and morphological variability in

- 541 South American rodent *Oecomys* (Sigmodontinae, Rodentia): evidence for a complex
542 of species. *J. Genet.* 91(3), 265–277.
- 543 Rozas, J., Ferrer–Mata, A., Sánchez–DelBarrio, J.C., Guirao–Rico, S., Librado, P.,
544 Ramos–Onsins, S.E., Sánchez–Gracia, A., 2017. DnaSP v6: DNA sequence
545 polymorphism analyses of large datasets. *Mol. Biol.* 34, 3299–3302.
- 546 Silva, C.R., Martins, A.C.M., Castro, I.J., Bernard, E., Cardoso, E.M., Lima, D.S.,
547 Gregorin, R., Rossi, R.V., Percequillo, A.R., Castro, K.C., 2013. Mammals of Amapá
548 State, Eastern Brazilian Amazonia: a revised taxonomic list with comments on
549 species distributions. *Mamm.* 77, 409–424.
- 550 Silva, J.M.C., Rylands, A.B., Fonseca, G.A.B., 2005. The Fate of the Amazonian
551 Areas of Endemism. *Conserv. Biol.* 19(3), 689–694.
- 552 Smith, M.F., Patton, J.L., 1993. The diversification of South American murid rodents:
553 Evidence from mitochondrial DNA sequence data for Akodontine tribe. *Biol. J. Linn.*
554 *Soc.* 50, 149–177.
- 555 Suárez–Villota, E.Y., Carmignotto, A.P., Brandão, M.V., Percequillo, A.R., Silva,
556 M.J.J., 2018. Systematics of the genus *Oecomys* (Sigmodontinae: Oryzomyini):
557 molecular phylogenetic, cytogenetic and morphological approaches reveal cryptic
558 species. *Zool. J. Linn. Soc.* 184, 182–210.
- 559 Tajima, F., 1989. Statistical method for testing the neutral mutation hypothesis by
560 DNA polymorphism. *Genet.* 123, 585–595.
- 561 Voss, R.S., Lunde, D.P., Limmons, N.B., 2001. The mammals of paracou, french
562 guiana: a neotropical lowland rainforest fauna part 2. Nonvolant species. *Bull. Am.*
563 *Mus. Nat. Hist.* 263, 1–236.
- 564 Wallace, A.R., 1852. On the monkeys of the Amazon. *Proc. Zool. Soc. Lond.* 20,
565 107–110.
- 566 Weir, B.S., Cockerham, C.C., 1984. Estimating F–Statistics for the Analysis of
567 Population Structure. *Evol.* 38(6), 1358–1370.
- 568 Xia, X., 2013. DAMBE5: A Comprehensive Software Package for Data Analysis in
569 Molecular Biology and Evolution. *Mol. Biol. Evol.* 30(7), 1720–1728.
- 570 Zwickl, D.J., 2006. Genetic algorithm approaches for the phylogenetic analysis of
571 large biological sequence datasets under the maximum likelihood criterion. Ph.D.
572 dissertation. The University of Texas at Austin. pp. 1–125.

573 Figures

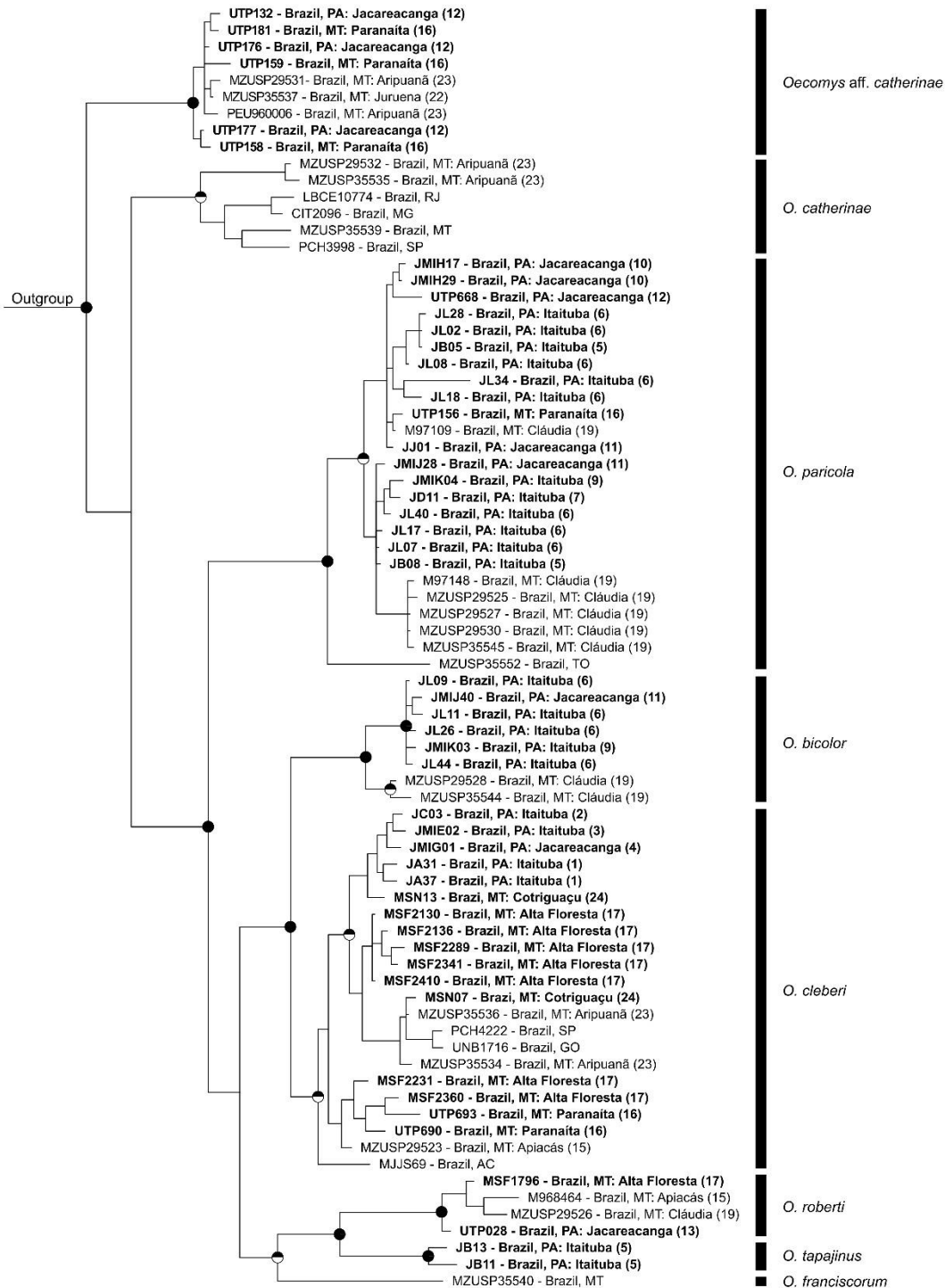


574

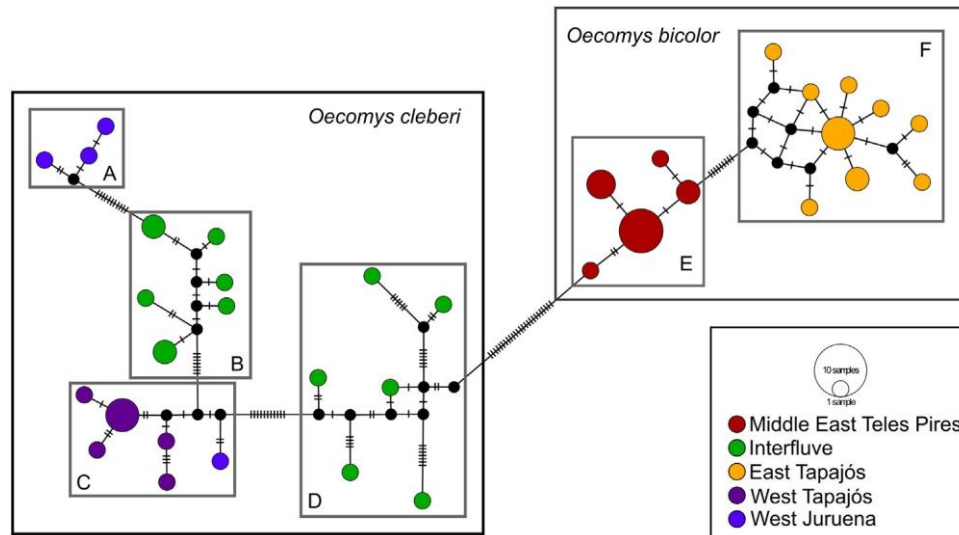
575 **Fig. 1.** Map indicating the main rivers in the Tapajós River basin and sampled
 576 localities. Numbers indicate the collection points and the symbols indicate the
 577 species collected at these points. Coordinates and number of locations are listed in
 578 Supplementary Material, Table 1.



580 **Fig. 2.** Bayesian Inference topology based on *Oecomys* cytochrome b gene data.
 581 Rigid circles indicate posterior probability greater than 0.95 and maximum likelihood
 582 bootstrap of more than 80%. Half black circles indicate posterior probability above
 583 0.95. Numbers in parentheses refer to the localities from the Tapajós River basin
 584 indicated in Fig. 1. Boldfaced samples indicate sequences obtained in this study.
 585 Identification of samples and their locations are listed in Supplementary Material,
 586 Table 1.

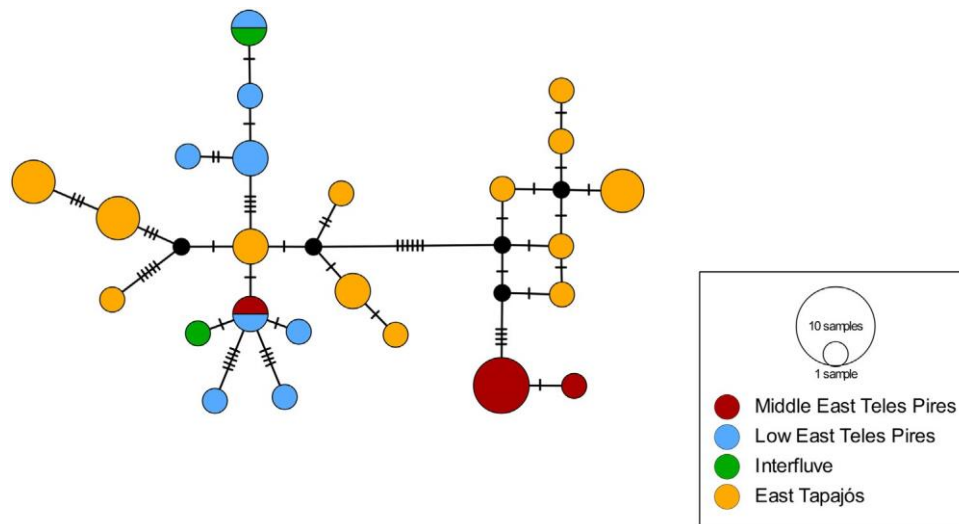


588 **Fig. 3.** Bayesian Inference topology based on concatenated data from cytochrome b
 589 gene and nuclear marker intron 7 β -fibrinogen gene of *Oecomys*. Circles indicate
 590 posterior probability greater than 0.95 and maximum likelihood bootstrap greater than
 591 80%. Half black circles indicate posterior probability above 0.95. Numbers in
 592 parentheses refer to the localities from the Tapajós River basin indicated in Fig. 1.
 593 Boldfaced samples indicate sequences obtained in this study. Identification of
 594 samples and their locations are listed in Supplementary Material, Table 1.



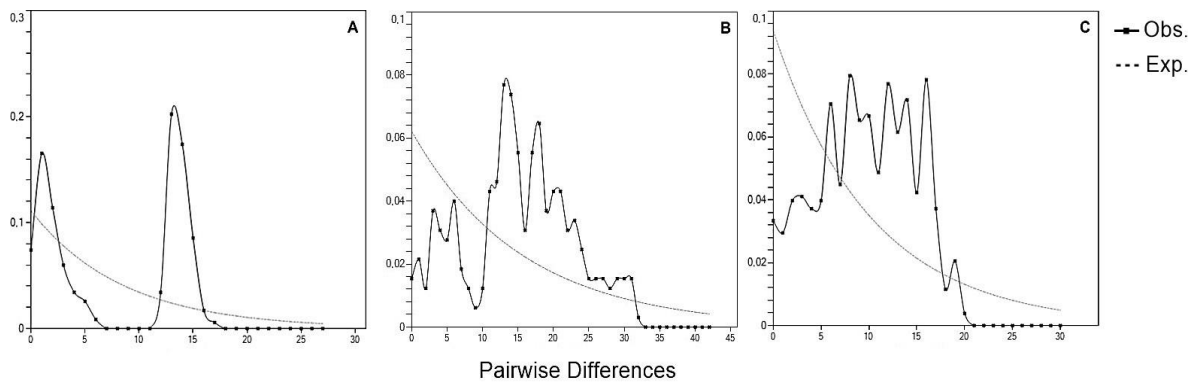
595

596 **Fig. 4.** Median-joining haplotype network based on cytochrome b gene data,
 597 representing the relationships in the *Oecomys bicolor/Oecomys cleberi* species
 598 complex. The size of the circle is proportional to the frequency of the haplotypes and
 599 the colors correspond to the localities. The mutational steps are indicated on the
 600 branches.



601

602 **Fig. 5.** Median-joining haplotype network based on data from the cytochrome b gene
 603 of *Oecomys paricola*. The size of the circle is proportional to the frequency of the
 604 haplotypes and the colors correspond to the localities. The mutational steps are
 605 indicated on the branches.



606

607 **Fig. 6.** Mismatch distribution graphs based on cytochrome b data from *Oecomys*
 608 *bicolor* (A), *Oecomys cleberi* (B) and *Oecomys paricola* (C). Dotted gray line
 609 indicates the expected distribution and solid black line indicates the frequency of
 610 distribution observed.

611 Tables

612 **Table 1.** Percentage of variation and fixation index of Analysis of Molecular Variance
 613 (AMOVA) based on cytochrome b data of the *Oecomys bicolor/Oecomys cleberi*
 614 complex (2 groups) and *O. paricola*. *Significant values ($p < 0.05$).

615

	<i>O. bicolor/O. cleberi</i>		<i>O. paricola</i>	
	% Variation	Fixation index	% Variation	Fixation index
Among groups	56.26*	Φ_{CT} 0.56*		
Among populations	26.73*	Φ_{ST} 0.83*	37.35*	Φ_{ST} 0.37*
Within populations	17.01*	Φ_{SC} 0.61*	62.65*	

616

617 **Table 2.** Genetic diversity indices and demographic expansion of *Oecomys bicolor*,
 618 *O. cleberi* and *O. paricola* based on cytochrome b data. N: Sample number; H:
 619 number of haplotypes; h: haplotype diversity, π : nucleotide diversity. *Significant
 620 values ($p < 0.05$).

621

	N	H	$h^* \pm DP$	$\pi^* \pm DP$	D (Tajima)	ρ	Fs (Fu)	p
<i>Oecomys bicolor</i>	27	17	0.954 ± 0.022	0.011 ± 0.006	0.46	0.72	-2.71	0.13
<i>Oecomys cleberi</i>	26	17	0.991 ± 0.015	0.021 ± 0.010	-0.20	0.52	-8.71	0.007*
<i>Oecomys paricola</i>	39	29	0.975 ± 0.013	0.014 ± 0.007	0.68	0.26	-10.28	0.001*

622

623 **Supplementary Material**

624 **Table 1.** Field number, voucher number, GenBank accession number, geographical coordinates, region and locality of specimens included in
 625 this study. Localities are indicated in Figure 1 (map). MT: Mato Grosso; PA: Pará; BR: Brazil.

Species	Field number	Voucher number	GenBank Cytb	GenBank iBF7	Coordinates	Map	Region	Locality	Reference
<i>Oecomys cleberi</i>	JA31	UFPAM1560	MK874374	MK874455	-5,062 -56,879	1	West Tapajós River	PA: Itaituba	This study
<i>Oecomys cleberi</i>	JA37	UFPAM1566	MK874375	MK874456	-5,062 -56,879	1	West Tapajós River	PA: Itaituba	This study
<i>Oecomys cleberi</i>	JC03	UFPAM1407	MK874376	MK874457	-5,453 -57,085	2	West Tapajós River	PA: Itaituba	This study
<i>Oecomys cleberi</i>	JMIE02	UFPAM1163	MK874380	MK874458	-5,610 -57,296	3	West Tapajós River	PA: Itaituba	This study
<i>Oecomys cleberi</i>	JG09	UFPAM1459	MK874377	-	-5,722 -57,366	4	West Tapajós River	PA: Jacareacanga	This study
<i>Oecomys cleberi</i>	JG14	-	MK874378	-	-5,722 -57,366	4	West Tapajós River	PA: Jacareacanga	This study
<i>Oecomys cleberi</i>	JG21	UFPAM1627	MK874379	-	-5,722 -57,366	4	West Tapajós River	PA: Jacareacanga	This study
<i>Oecomys cleberi</i>	JMIG01	UFPAM1177	MK874381	MK874459	-5,722 -57,366	4	West Tapajós River	PA: Jacareacanga	This study
<i>Oecomys paricola</i>	JB05	UFPAM1390	MK874397	MK874471	-5,227 -56,929	5	East Tapajós River	PA: Itaituba	This study
<i>Oecomys paricola</i>	JB08	UFPAM1393	MK874398	MK874472	-5,227 -56,929	5	East Tapajós River	PA: Itaituba	This study
<i>Oecomys tapajinus</i>	JB11	UFPAM1396	MK874439	MK874491	-5,227 -56,929	5	East Tapajós River	PA: Itaituba	This study
<i>Oecomys tapajinus</i>	JB13	UFPAM1398	MK874440	MK874492	-5,227 -56,929	5	East Tapajós River	PA: Itaituba	This study
<i>Oecomys bicolor</i>	JL09	UFPAM1526	MK874341	-	-5,376 -56,923	6	East Tapajós River	PA: Itaituba	This study
<i>Oecomys bicolor</i>	JL10	UFPAM1527	MK874342	-	-5,376 -56,923	6	East Tapajós River	PA: Itaituba	This study
<i>Oecomys bicolor</i>	JL11	UFPAM1528	MK874343	MK874444	-5,376 -56,923	6	East Tapajós River	PA: Itaituba	This study
<i>Oecomys bicolor</i>	JL15	UFPAM1531	MK874344	-	-5,376 -56,923	6	East Tapajós River	PA: Itaituba	This study
<i>Oecomys bicolor</i>	JL22	UFPAM1538	MK874345	-	-5,376 -56,923	6	East Tapajós River	PA: Itaituba	This study
<i>Oecomys bicolor</i>	JL24	UFPAM1540	MK874346	-	-5,376 -56,923	6	East Tapajós River	PA: Itaituba	This study
<i>Oecomys bicolor</i>	JL25	UFPAM1541	MK874347	-	-5,376 -56,923	6	East Tapajós River	PA: Itaituba	This study
<i>Oecomys bicolor</i>	JL26	UFPAM1542	MK874348	MK874445	-5,376 -56,923	6	East Tapajós River	PA: Itaituba	This study
<i>Oecomys bicolor</i>	JL44	UFPAM1708	MK874349	MK874446	-5,376 -56,923	6	East Tapajós River	PA: Itaituba	This study
<i>Oecomys paricola</i>	JL02	UFPAM1519	MK874402	MK874475	-5,376 -56,923	6	East Tapajós River	PA: Itaituba	This study
<i>Oecomys paricola</i>	JL07	UFPAM1524	MK874403	MK874476	-5,376 -56,923	6	East Tapajós River	PA: Itaituba	This study
<i>Oecomys paricola</i>	JL08	UFPAM1525	MK874404	MK874477	-5,376 -56,923	6	East Tapajós River	PA: Itaituba	This study
<i>Oecomys paricola</i>	JL16	UFPAM1532	MK874405	-	-5,376 -56,923	6	East Tapajós River	PA: Itaituba	This study

Species	Field number	Voucher number	GenBank Cytb	GenBank iBF7	Coordinates	Map	Region	Locality	Reference
<i>Oecomys paricola</i>	JL17	UFPAM1533	MK874406	MK874478	-5,376 -56,923	6	East Tapajós River	PA: Itaituba	This study
<i>Oecomys paricola</i>	JL18	UFPAM1534	MK874407	MK874479	-5,376 -56,923	6	East Tapajós River	PA: Itaituba	This study
<i>Oecomys paricola</i>	JL20	UFPAM1536	MK874408	-	-5,376 -56,923	6	East Tapajós River	PA: Itaituba	This study
<i>Oecomys paricola</i>	JL21	UFPAM1537	MK874409	-	-5,376 -56,923	6	East Tapajós River	PA: Itaituba	This study
<i>Oecomys paricola</i>	JL28	UFPAM1544	MK874410	MK874480	-5,376 -56,923	6	East Tapajós River	PA: Itaituba	This study
<i>Oecomys paricola</i>	JL34	UFPAM1698	MK874411	MK874481	-5,376 -56,923	6	East Tapajós River	PA: Itaituba	This study
<i>Oecomys paricola</i>	JL40	UFPAM1704	MK874412	MK874482	-5,376 -56,923	6	East Tapajós River	PA: Itaituba	This study
<i>Oecomys tapajinus</i>	JL19	UFPAM1535	MK874442	MK874493	-5,376 -56,923	6	East Tapajós River	PA: Itaituba	This study
<i>Oecomys paricola</i>	JD11	UFPAM1734	MK874399	MK874473	-5,580 -57,123	7	East Tapajós River	PA: Itaituba	This study
<i>Oecomys bicolor</i>	JF07	UFPAM1446	MK874340	-	-5,661 -57,247	8	East Tapajós River	PA: Itaituba	This study
<i>Oecomys bicolor</i>	JMIK03	UFPAM1164	MK874351	MK874448	-5,766 -57,277	9	East Tapajós River	PA: Itaituba	This study
<i>Oecomys bicolor</i>	JMIK08	UFPAM1165	MK874352	-	-5,766 -57,277	9	East Tapajós River	PA: Itaituba	This study
<i>Oecomys paricola</i>	JMIK04	UFPAM1166	MK874418	MK874486	-5,766 -57,277	9	East Tapajós River	PA: Itaituba	This study
<i>Oecomys paricola</i>	JH55	UFPAM1662	MK874400	-	-5,817 -57,395	10	East Tapajós River	PA: Jacareacanga	This study
<i>Oecomys paricola</i>	JMIH17	UFPAM1171	MK874413	MK874483	-5,817 -57,395	10	East Tapajós River	PA: Jacareacanga	This study
<i>Oecomys paricola</i>	JMIH26	UFPAM1168	MK874414	-	-5,817 -57,395	10	East Tapajós River	PA: Jacareacanga	This study
<i>Oecomys paricola</i>	JMIH29	UFPAM1173	MK874415	MK874484	-5,817 -57,395	10	East Tapajós River	PA: Jacareacanga	This study
<i>Oecomys paricola</i>	JMIH39	UFPAM1167	MK874416	-	-5,817 -57,395	10	East Tapajós River	PA: Jacareacanga	This study
<i>Oecomys bicolor</i>	JMIJ40	UFPAM1162	MK874350	MK874447	-6,127 -57,588	11	East Tapajós River	PA: Jacareacanga	This study
<i>Oecomys paricola</i>	JJ01	UFPAM1504	MK874401	MK874474	-6,127 -57,588	11	East Tapajós River	PA: Jacareacanga	This study
<i>Oecomys paricola</i>	JMIJ28	UFPAM1172	MK874417	MK874485	-6,127 -57,588	11	East Tapajós River	PA: Jacareacanga	This study
<i>Oecomys tapajinus</i>	JJ02	UFPAM1505	MK874441	-	-6,127 -57,588	11	East Tapajós River	PA: Jacareacanga	This study
<i>Oecomys aff. catherinae</i>	UTP132	UFMT1686	MK874367	MK874449	-9,311 -56,768	12	Low East Teles Pires River	PA: Jacareacanga	This study
<i>Oecomys aff. catherinae</i>	UTP176	UFMT1775	MK874371	MK874452	-9,311 -56,768	12	Low East Teles Pires River	PA: Jacareacanga	This study
<i>Oecomys aff. catherinae</i>	UTP177	UFMT1776	MK874372	MK874453	-9,311 -56,768	12	Low East Teles Pires River	PA: Jacareacanga	This study
<i>Oecomys paricola</i>	UTP685	UFMT1780	MK874427	-	-9,311 -56,768	12	Low East Teles Pires River	PA: Jacareacanga	This study
<i>Oecomys paricola</i>	UTP119	UFMT1685	MK874422	-	-9,311 -56,768	12	Low East Teles Pires River	PA: Jacareacanga	This study
<i>Oecomys paricola</i>	UTP666	UFMT1778	MK874424	-	-9,311 -56,768	12	Low East Teles Pires River	PA: Jacareacanga	This study
<i>Oecomys paricola</i>	UTP668	UFMT1779	MK874425	MK874488	-9,311 -56,768	12	Low East Teles Pires River	PA: Jacareacanga	This study
<i>Oecomys aff. catherinae</i>	UTP002	UFMT1680	MK874366	-	-9,385 -56,732	13	Low East Teles Pires River	PA: Jacareacanga	This study

Species	Field number	Voucher number	GenBank Cytb	GenBank iBF7	Coordinates	Map	Region	Locality	Reference
<i>Oecomys roberti</i>	UTP028	UFMT1682	MK874437	MK874490	-9,385 -56,732	13	Low East Teles Pires River	PA: Jacareacanga	This study
<i>Oecomys paricola</i>	LPC559	MVZ197507	HM594592	-	-9,583 -55,917	14	Low East Teles Pires River	MT: Alta Floresta	Rocha et al. (2011)
<i>Oecomys paricola</i>	LPC570	MVZ197507	HM594593	-	-9,583 -55,917	14	Low East Teles Pires River	MT: Alta Floresta	Rocha et al. (2011)
<i>Oecomys paricola</i>	LPC525	UFMG2841	HM594591	-	-9,583 -55,917	14	Low East Teles Pires River	MT: Alta Floresta	Rocha et al. (2011)
<i>Oecomys paricola</i>	RVR 38	UFMT4116	MK874419	-	-9,604 -56,090	14	Low East Teles Pires River	MT: Alta Floresta	This study
<i>Oecomys cleberi</i>	M968410	MZUSP29523	MG323750	MG323834	-9,567 -57,383	15	Interfluve (Teles Pires - Juruena)	MT: Apicás	Suárez-Villota et al. (2018)
<i>Oecomys paricola</i>	RVR 94	UFMT4112	MK874420	-	-9,604 -56,090	15	Low East Teles Pires River	MT: Alta Floresta	This study
<i>Oecomys roberti</i>	M968464	-	MG323719	MG323806	-9,567 -57,383	15	Interfluve (Teles Pires - Juruena)	MT: Apicás	Suárez-Villota et al. (2018)
<i>Oecomys aff. catherinae</i>	UTP158	UFMT1772	MK874368	MK874450	-9,485 -56,472	16	Interfluve (Teles Pires - Juruena)	MT: Paranaíta	This study
<i>Oecomys aff. catherinae</i>	UTP159	UFMT1773	MK874369	MK874451	-9,485 -56,472	16	Interfluve (Teles Pires - Juruena)	MT: Paranaíta	This study
<i>Oecomys aff. catherinae</i>	UTP162	UFMT1774	MK874370	-	-9,485 -56,472	16	Interfluve (Teles Pires - Juruena)	MT: Paranaíta	This study
<i>Oecomys aff. catherinae</i>	UTP181	UFMT1806	MK874373	MK874454	-9,485 -56,472	16	Interfluve (Teles Pires - Juruena)	MT: Paranaíta	This study
<i>Oecomys cleberi</i>	UTP664	UFMT1777	MK874394	-	-9,485 -56,472	16	Interfluve (Teles Pires - Juruena)	MT: Paranaíta	This study
<i>Oecomys cleberi</i>	UTP690	UFMT1781	MK874395	MK874469	-9,485 -56,472	16	Interfluve (Teles Pires - Juruena)	MT: Paranaíta	This study
<i>Oecomys cleberi</i>	UTP693	UFMT1782	MK874396	MK874470	-9,485 -56,472	16	Interfluve (Teles Pires - Juruena)	MT: Paranaíta	This study
<i>Oecomys paricola</i>	UTP669	UFMT1848	MK874426	-	-9,485 -56,472	16	Interfluve (Teles Pires - Juruena)	MT: Paranaíta	This study
<i>Oecomys paricola</i>	UTP156	UFMT1771	MK874423	MK874487	-9,485 -56,472	16	Interfluve (Teles Pires - Juruena)	MT: Paranaíta	This study
<i>Oecomys roberti</i>	UTP696	UFMT1783	MK874438	-	-9,485 -56,472	16	Interfluve (Teles Pires - Juruena)	MT: Alta Floresta	This study
<i>Oecomys cleberi</i>	MSF2130	-	MK874382	MK874460	-9,757 -55,972	17	Interfluve (Teles Pires - Juruena)	MT: Alta Floresta	This study
<i>Oecomys cleberi</i>	MSF2136	-	MK874384	MK874461	-9,757 -55,972	17	Interfluve (Teles Pires - Juruena)	MT: Alta Floresta	This study
<i>Oecomys cleberi</i>	MSF2410	-	MK874389	MK874466	-9,798 -55,926	17	Interfluve (Teles Pires - Juruena)	MT: Alta Floresta	This study
<i>Oecomys cleberi</i>	MSF2289	-	MK874386	MK874463	-9,824 -55,893	17	Interfluve (Teles Pires - Juruena)	MT: Alta Floresta	This study
<i>Oecomys cleberi</i>	MSF2341	-	MK874387	MK874464	-9,824 -55,893	17	Interfluve (Teles Pires - Juruena)	MT: Alta Floresta	This study
<i>Oecomys cleberi</i>	MSF2132	-	MK874383	-	-9,757 -55,972	17	Interfluve (Teles Pires - Juruena)	MT: Alta Floresta	This study
<i>Oecomys cleberi</i>	MSF2231	-	MK874385	MK874462	-9,867 -55,900	17	Interfluve (Teles Pires - Juruena)	MT: Alta Floresta	This study
<i>Oecomys cleberi</i>	MSF2360	-	MK874388	MK874465	-9,867 -55,900	17	Interfluve (Teles Pires - Juruena)	MT: Alta Floresta	This study
<i>Oecomys roberti</i>	MSF1796	-	MK874430	MK874489	-9,840 -56,005	17	Interfluve (Teles Pires - Juruena)	MT: Alta Floresta	This study
<i>Oecomys aff. catherinae</i>	RVR 89	UFMT4118	MK874365	-	-10,007 -56,038	18	Interfluve (Teles Pires - Juruena)	MT: Alta Floresta	This study
<i>Oecomys cleberi</i>	RVR 49	UFMT4111	MK874392	-	-9,978 -56,083	18	Interfluve (Teles Pires - Juruena)	MT: Alta Floresta	This study

Species	Field number	Voucher number	GenBank Cytb	GenBank iBF7	Coordinates	Map	Region	Locality	Reference
<i>Oecomys cleberi</i>	RVR 75	UFMT4117	MK874393	-	-9,978 -56,083	18	Interfluve (Teles Pires - Juruena)	MT: Alta Floresta	This study
<i>Oecomys bicolor</i>	M97074	MZUSP29528	MG323726	MG323812	-11,583 -55,167	19	Middle East Teles Pires River	MT: Cláudia	Suárez-Villota et al. (2018)
<i>Oecomys bicolor</i>	M97107	MZUSP35544	MG323725	MG323785	-11,583 -55,167	19	Middle East Teles Pires River	MT: Cláudia	Suárez-Villota et al. (2018)
<i>Oecomys paricola</i>	M97023	MZUSP29525	MG323713	MG323802	-11,583 -55,167	19	Middle East Teles Pires River	MT: Cláudia	Suárez-Villota et al. (2018)
<i>Oecomys paricola</i>	M97073	MZUSP29527	MG323711	MG323800	-11,583 -55,167	19	Middle East Teles Pires River	MT: Cláudia	Suárez-Villota et al. (2018)
<i>Oecomys paricola</i>	M97109	-	MG323708	MG323798	-11,583 -55,167	19	Middle East Teles Pires River	MT: Cláudia	Suárez-Villota et al. (2018)
<i>Oecomys paricola</i>	M97141	MZUSP29530	MG323709	MG323799	-11,583 -55,167	19	Middle East Teles Pires River	MT: Cláudia	Suárez-Villota et al. (2018)
<i>Oecomys paricola</i>	M97148	-	MG323710	MG323776	-11,583 -55,167	19	Middle East Teles Pires River	MT: Cláudia	Suárez-Villota et al. (2018)
<i>Oecomys paricola</i>	M976296	MZUSP35545	MG323712	MG323801	-11,583 -55,167	19	Middle East Teles Pires River	MT: Cláudia	Suárez-Villota et al. (2018)
<i>Oecomys roberti</i>	M97060	MZUSP29526	MG323720	MG323807	-11,583 -55,167	19	Middle East Teles Pires River	MT: Cláudia	Suárez-Villota et al. (2018)
<i>Oecomys bicolor</i>	RVR133	UFMT4313	MK874353	-	-11,677 -55,333	20	Middle East Teles Pires River	MT: Sinop	This study
<i>Oecomys bicolor</i>	RVR145	UFMT4316	MK874355	-	-11,677 -55,333	20	Middle East Teles Pires River	MT: Sinop	This study
<i>Oecomys bicolor</i>	RVR146	UFMT4333	MK874356	-	-11,697 -55,277	20	Middle East Teles Pires River	MT: Sinop	This study
<i>Oecomys bicolor</i>	RVR148	UFMT4318	MK874357	-	-11,677 -55,333	20	Middle East Teles Pires River	MT: Sinop	This study
<i>Oecomys bicolor</i>	RVR169	UFMT4321	MK874358	-	-11,666 -55,280	20	Middle East Teles Pires River	MT: Sinop	This study
<i>Oecomys bicolor</i>	RVR214	UFMT4639	MK874361	-	-11,671 -55,525	20	Middle East Teles Pires River	MT: Sinop	This study
<i>Oecomys bicolor</i>	RVR244	UFMT4642	MK874362	-	-11,697 -55,277	20	Middle East Teles Pires River	MT: Sinop	This study
<i>Oecomys bicolor</i>	RVR260	UFMT4646	MK874363	-	-11,697 -55,277	20	Middle East Teles Pires River	MT: Sinop	This study
<i>Oecomys bicolor</i>	RVR264	UFMT4647	MK874364	-	-11,697 -55,277	20	Middle East Teles Pires River	MT: Sinop	This study
<i>Oecomys paricola</i>	RVR167	UFMT4320	MK874421	-	-11,665 -55,511	20	Middle East Teles Pires River	MT: Sinop	This study
<i>Oecomys bicolor</i>	RVR142	UFMT4314	MK874354	-	-11,733 -55,360	21	Middle East Teles Pires River	MT: Sinop	This study
<i>Oecomys bicolor</i>	RVR186	UFMT4636	MK874359	-	-11,733 -55,360	21	Middle East Teles Pires River	MT: Sinop	This study
<i>Oecomys bicolor</i>	RVR205	UFMT4638	MK874360	-	-11,714 -55,402	21	Middle East Teles Pires River	MT: Sinop	This study
<i>Oecomys roberti</i>	RVR122	UFMT4311	MK874431	-	-11,817 -55,411	21	Middle East Teles Pires River	MT: Sinop	This study
<i>Oecomys roberti</i>	RVR123	UFMT4312	MK874432	-	-11,742 -55,229	21	Middle East Teles Pires River	MT: Sinop	This study

Species	Field number	Voucher number	GenBank Cytb	GenBank iBF7	Coordinates	Map	Region	Locality	Reference
<i>Oecomys roberti</i>	RVR143	UFMT4315	MK874433	-	-11,677 -55,333	21	Middle East Teles Pires River	MT: Sinop	This study
<i>Oecomys roberti</i>	RVR147	UFMT4317	MK874434	-	-11,733 -55,360	21	Middle East Teles Pires River	MT: Sinop	This study
<i>Oecomys roberti</i>	RVR149	UFMT4319	MK874435	-	-11,794 -55,413	21	Middle East Teles Pires River	MT: Sinop	This study
<i>Oecomys roberti</i>	RVR263	UFMT4651	MK874436	-	-11,697 -55,277	21	Middle East Teles Pires River	MT: Sinop	This study
<i>Oecomys aff. catherinae</i>	APC145	MZUSP35537	MG323757	MG323779	-10,317 -58,483	22	West Juruena River	MT: Juruena	Suárez-Villota et al. (2018)
<i>Oecomys aff. catherinae</i>	APC244	MZUSP29531	MG323756	MG323777	-10,167 -59,450	23	West Juruena River	MT: Aripuanã	Suárez-Villota et al. (2018)
<i>Oecomys aff. catherinae</i>	PEU960006	-	MG323755	MG323839	-10,167 -59,450	23	West Juruena River	MT: Aripuanã	Suárez-Villota et al. (2018)
<i>Oecomys catherinae</i>	APC243	MZUSP35535	MG323759	MG323841	-10,167 -59,450	23	West Juruena River	MT: Aripuanã	Suárez-Villota et al. (2018)
<i>Oecomys catherinae</i>	APC249	MZUSP29532	MG323758	MG323840	-10,167 -59,450	23	West Juruena River	MT: Aripuanã	Suárez-Villota et al. (2018)
<i>Oecomys cleberii</i>	APC210	MZUSP35534	MG323745	MG323829	-10,167 -59,450	23	West Juruena River	MT: Aripuanã	Suárez-Villota et al. (2018)
<i>Oecomys cleberii</i>	PEU960047	MZUSP35536	MG323744	MG323828	-10,167 -59,450	23	West Juruena River	MT: Aripuanã	Suárez-Villota et al. (2018)
<i>Oecomys cleberii</i>	MSN07	UFMT1363	MK874390	MK874467	-9,836 -58,253	24	West Juruena River	MT: Cotriguaçu	This study
<i>Oecomys cleberii</i>	MSN13	UFMT1366	MK874391	MK874468	-9,836 -58,253	24	West Juruena River	MT: Cotriguaçu	This study
<i>Oecomys auyantepui</i>	-	CN120	JF759666	-	1,167 -55,650	-	-	Pará, BR	Rosa et al. (2012)
<i>Oecomys auyantepui</i>	-	V-1001	AJ496305	-	4,083 -52,683	-	-	French Guiana	Mauffrey et al. (unpubl.)
<i>Oecomys bicolor</i>	FSF34r	-	KR190445	-	-9,630 -50,144	-	-	Pará, BR	Rocha et al. (2015)
<i>Oecomys bicolor</i>	-	MVZ154990	JQ312123	-	-5,517 -79,817	-	-	Peru	Rocha et al. (2012)
<i>Oecomys bicolor</i>	-	MVZ154999	AF108699	-	-5,517 -79,817	-	-	Peru	Smith and Patton (1999)
<i>Oecomys catherinae</i>	-	MN36747	FJ361068	-	-13,517 -48,217	-	-	Goiás, BR	Miranda et al. (unpubl.)
<i>Oecomys catherinae</i>	PCH3998	-	MG323764	MG323846	-20,483 -47,850	-	-	São Paulo, BR	Suárez-Villota et al. (2018)
<i>Oecomys catherinae</i>	CIT2096	-	MG323772	MG323774	-19,533 -42,533	-	-	Minas Gerais, BR	Suárez-Villota et al. (2018)
<i>Oecomys catherinae</i>	-	LBCE10774	MG323771	MG323852	-23,217 -44,717	-	-	Rio de Janeiro, BR	Suárez-Villota et al. (2018)
<i>Oecomys catherinae</i>	APC289	MZUSP35539	MG323766	MG323848	-10,017 -51,117	-	-	Mato Grosso, BR	Suárez-Villota et al. (2018)

Species	Field number	Voucher number	GenBank Cytb	GenBank iBF7	Coordinates	Map	Region	Locality	Reference
<i>Oecomys catherinae</i>	-	USNM549530	KT737238	-	-3,650 -52,367	-	-	Pará, BR	Pardiñas et al. (2016)
<i>Oecomys cleberii</i>	-	AMNH269823	AJ496307	-	-4,083 -52,683	-	-	French Guiana	Mauffrey et al. (unpubl.)
<i>Oecomys cleberii</i>	MJJS69	-	MG323749	MG323833	-9,333 -68,317	-	-	Acre, BR	Suárez-Villota et al. (2018)
<i>Oecomys cleberii</i>	MTR19074	-	MG323752	MG323836	-4,717 -62,117	-	-	Amazonas, BR	Suárez-Villota et al. (2018)
<i>Oecomys cleberii</i>	-	MN24131	JQ312125	-	-15,950 -47,933	-	-	Distrito Federal, BR	Rocha et al. (2012)
<i>Oecomys cleberii</i>	APC553	UNB1716	MG323734	MG323818	-18,100 -52,917	-	-	Goiás, BR	Suárez-Villota et al. (2018)
<i>Oecomys cleberii</i>	-	UFMG2802	HM594608	-	-15,633 -52,350	-	-	Mato Grosso, BR	Rocha et al. (2011)
<i>Oecomys cleberii</i>	PCH4222	-	MG323741	MG323825	-20,500 -47,833	-	-	São Paulo, BR	Suárez-Villota et al. (2018)
<i>Oecomys concolor</i>	JLP16728	-	HM594614	-	-2,217 -62,383	-	-	Amazonas, BR	Rocha et al. (2011)
<i>Oecomys concolor</i>	JLP16729	-	HM594617	-	-2,217 -62,383	-	-	Amazonas, BR	Rocha et al. (2011)
<i>Oecomys concolor</i>	JLP16806	-	HM594615	-	-2,217 -62,383	-	-	Amazonas, BR	Rocha et al. (2011)
<i>Oecomys franciscorum</i>	roe224	-	KF207846	-	-25,917 -58,933	-	-	Argentina	Orozco et al. (2014)
<i>Oecomys franciscorum</i>	-	MACN26663	KT737232	-	-25,967 -58,167	-	-	Argentina	Pardiñas et al. (2016)
<i>Oecomys franciscorum</i>	PNPA300	MZUSP35540	MG323716	MG323786	-17,650 -57,433	-	-	Mato Grosso, BR	Suárez-Villota et al. (2018)
<i>Oecomys mamorae</i>	PZ94	-	KT737226	-	-14,150 -67,917	-	-	Bolivia	Pardiñas et al. (2016)
<i>Oecomys mamorae</i>	PZ316	-	KT737225	-	-15,283 -68,383	-	-	Bolivia	Pardiñas et al. (2016)
<i>Oecomys mamorae</i>	-	MVZ197505	HM594605	-	-17,120 -56,946	-	-	Mato Grosso, BR	Rocha et al. (2011)
<i>Oecomys mamorae</i>	-	MSB63354	KT737228	-	-19,550 -64,133	-	-	Bolivia	Pardiñas et al. (2016)
<i>Oecomys paricola</i>	BAR013	-	JF759675	-	-1,500 -48,667	-	-	Pará, BR	Rosa et al. (2012)
<i>Oecomys paricola</i>	APC1240	MZUSP35552	MG323702	MG323794	-11,233 -46,850	-	-	Tocantins, BR	Suárez-Villota et al. (2018)
<i>Oecomys paricola</i>	-	MPEG40843	JF759669	-	-0,650 -50,183	-	-	Pará, BR	Rosa et al. (2012)
<i>Oecomys rex</i>	RC01	-	MK874429	-	-	-	-	Pará, BR	This study
<i>Oecomys rex</i>	CSA22	-	MK874428	-	-	-	-	Pará, BR	This study
<i>Oecomys roberti</i>	-	UFMG2845	HM594597	-	-17,120 -56,946	-	-	Mato Grosso, BR	Rocha et al. (2011)

Species	Field number	Voucher number	GenBank Cytb	GenBank iBF7	Coordinates	Map	Region	Locality	Reference
<i>Oecomys roberti</i>	JLP15241	MVZ200947	U58384	-	-6,833 -70,750	-	-	Amazonas, BR	Patton and Da Silva (1995)
<i>Oecomys rutilus</i>	CN123	-	JF759665	-	-1,167 -55,650	-	-	Pará, BR	Rosa et al. (2012)
<i>Oecomys rutilus</i>	-	MNHN1995.3236	AJ496309	-	-	-	-	French Guiana	Mauffrey et al. (unpubl.)
<i>Oecomys superans</i>	-	MVZ200944	U58385	-	-6,833 -70,750	-	-	Amazonas, BR	Patton and Da Silva (1995)
<i>Oecomys superans</i>	-	MVZ155006	AY275123	-	-5,517 -79,817	-	-	Peru	D'Elía (2003)
<i>Oecomys sydandersoni</i>	-	USNM584557	KT737234	-	-15,250 -61,017	-	-	Bolivia	Pardiñas et al. (2016)
<i>Oecomys sydandersoni</i>	-	USNM588189	KT737235	-	-14,767 -61,033	-	-	Bolivia	Pardiñas et al. (2016)
<i>Oecomys tapajinus</i>	FSF53r	-	KR190448	-	-9,630 -50,144	-	-	Pará, BR	Rocha et al. (2015)
<i>Oecomys tapajinus</i>	-	UFES1354	HM594598	-	-9,970 -50,069	-	-	Tocantins - BR	Rocha et al. (2011)
<i>Oecomys trinitatis</i>	-	MUSM13320	GU126527	-	-5,200 -72,883	-	-	Peru	Percequillo et al. (2011)
<i>Oecomys trinitatis</i>	-	MVZ200948	OTU58390	-	-8,667 -72,783	-	-	Acre, BR	Patton and Da Silva (1995)
<i>Oecomys</i> sp. 1	-	MVZ155005	JF693876	-	-5,517 -79,817	-	-	Peru	Pine et al. (2012)
<i>Oecomys</i> sp. 2	JUR354	MVZ200905	U58388	-	-3,317 -66,017	-	-	Amazonas, BR	Patton and Da Silva (1995)
<i>Oecomys</i> sp. 3	-	MSB68480	KT737233	-	-15,117 -68,867	-	-	Bolivia	Pardiñas et al. (2016)
<i>Euryoryzomys macconnelli</i>	LGV151	-	MK874443	-	-	-	-	Pará, BR	This study
<i>Handleyomys intectus</i>	-	CADV088	EU579490	-	-	-	-	Colombia	Hanson and Bradley (unpub.)
<i>Handleyomys melanotis</i>	-	ASNHC3419	KF658409	KF658415	-	-	-	México	Almendra et al. (2014)
<i>Oligoryzomys utiaritensis</i>	-	MN75625	JQ013752	JQ282893	-	-	-	Mato Grosso, BR	Agrellos et al. (2012)

627 **Table 2.** Kimura 2 parameters genetic distance among and within (bold numbers) *Oecomys* clades based on cytochrome b. Values in
 628 percentage. Standard deviation values are shown above boldfaced numbers.

		1	2	3	4	5	6	7	8	9	10	11	12	13	14	15	16	17	18
1	<i>O. auyantepui</i>	1.00	1.70	2.26	1.83	1.80	1.96	1.81	1.83	1.81	1.83	2.26	1.96	2.11	1.95	1.95	1.88	1.87	1.77
2	<i>O. bicolor / O. cleberi</i>	10.62	3.15	1.77	1.51	1.13	1.57	1.40	1.50	1.72	1.26	1.53	1.19	1.33	1.08	1.32	1.74	1.12	1.57
3	<i>O. aff. catherinae</i>	14.19	10.91	0.70	1.55	2.00	1.96	2.05	1.76	1.74	1.85	2.12	2.19	2.39	2.06	1.83	2.29	1.84	1.83
4	<i>O. catherinae</i>	11.54	9.66	8.94	3.51	1.27	1.76	1.62	1.62	1.39	1.73	1.74	1.74	1.63	1.66	1.81	1.83	1.68	1.81
5	<i>O. concolor</i>	9.85	5.60	10.66	6.89	0.00	1.37	1.32	1.52	1.60	1.31	1.69	1.50	1.34	1.37	1.65	1.69	1.37	1.44
6	<i>O. franciscorum</i>	11.57	9.12	11.54	10.48	6.64	0.33	0.87	1.59	1.91	1.67	2.02	1.80	1.49	1.46	1.84	1.64	1.68	1.57
7	<i>O. mamorae</i>	11.17	8.89	12.62	10.64	7.20	4.21	3.71	1.49	1.79	1.47	1.86	1.57	1.46	1.35	1.71	1.59	1.53	1.48
8	<i>O. paricola</i>	11.09	9.44	10.44	10.12	8.17	8.76	9.18	1.83	1.80	1.45	2.15	1.74	1.71	1.72	1.62	1.69	1.58	1.43
9	<i>O. rex</i>	10.24	10.17	9.49	8.23	8.14	11.12	11.23	10.56	0.74	1.80	1.97	1.97	1.89	1.90	1.69	2.22	1.94	1.76
10	<i>O. roberti</i>	10.13	7.02	10.54	10.41	5.99	8.59	8.20	7.87	9.70	0.61	1.88	1.30	1.76	1.68	1.36	1.79	1.16	1.48
11	<i>O. rutilus</i>	14.09	8.88	12.13	10.64	8.56	12.02	11.42	13.24	11.65	10.30	0.25	2.05	1.99	1.56	1.87	2.19	1.70	2.04
12	<i>Oecomys</i> sp.1	11.22	6.16	12.75	10.39	7.09	9.55	9.00	9.87	10.73	5.97	11.48	n/c	1.75	1.69	1.57	1.61	1.31	1.70
13	<i>Oecomys</i> sp.2	12.25	6.68	13.33	8.84	5.64	7.07	8.01	9.46	10.09	9.30	10.55	8.65	n/c	1.57	1.76	1.78	1.59	1.55
14	<i>Oecomys</i> sp.3	12.16	5.71	12.19	10.19	6.46	7.33	7.65	10.00	10.36	8.75	7.78	8.54	7.09	n/c	1.58	1.89	1.50	1.86
15	<i>O. superans</i>	11.90	7.51	10.58	11.44	8.58	11.04	10.80	9.83	8.94	7.05	10.23	8.02	9.37	8.26	2.29	1.93	1.62	1.51
16	<i>O. sydandersoni</i>	11.38	10.78	14.32	11.60	8.91	8.88	9.61	9.82	13.18	9.74	13.48	8.45	9.80	10.57	11.58	2.28	1.70	1.57
17	<i>O. tapajinus</i>	11.22	6.37	10.36	10.32	6.54	9.12	8.96	8.78	11.25	5.64	9.54	6.15	8.02	7.86	9.34	9.56	0.95	1.58
18	<i>O. trinitatis</i>	10.37	9.03	9.86	11.16	6.69	8.15	8.67	7.69	9.51	7.44	12.04	8.80	7.86	10.79	8.36	8.77	8.17	0.25

630 **Table 3.** Kimura 2 parameters genetic distance among and within (boldfaced numbers) *Oecomys* clades based on cytochrome b of samples
 631 used in concatenated analyzes. Values in percentage. Standard deviation values are shown above boldfaced numbers.

		1	2	3	4	5	6	7	8
1	<i>O. bicolor</i>	1.12	1.55	1.45	0.76	1.30	1.43	1.26	1.15
2	<i>O. aff catherinae</i>	11.43	0.60	1.18	1.37	1.51	1.48	1.54	1.39
3	<i>O. catherinae</i>	11.65	8.38	3.36	1.15	1.43	1.30	1.35	1.48
4	<i>O. cleberi</i>	4.84	9.98	9.20	2.12	1.03	1.11	1.17	1.09
5	<i>O. franciscorum</i>	9.08	10.91	11.47	7.52	n/c	1.31	1.36	1.39
6	<i>O. paricola</i>	11.08	11.68	10.87	8.97	10.16	1.78	1.22	1.36
7	<i>O. roberti</i>	9.18	10.71	10.61	8.56	10.05	9.31	1.00	1.09
8	<i>O. tapajinus</i>	7.31	9.73	11.47	7.29	9.63	9.81	6.99	1.20

632 **Table 4.** Fst values based on cytochrome b sequences of *Oecomys bicolor*, *O. cleberi* and *O. paricola* from the Tapajós River basin.
 633

	<i>O. bicolor</i>		<i>O. cleberi</i>		<i>O. paricola</i>	
	Middle Teles Pires	West Juruena	Interfluve	Middle Teles Pires	Low Teles Pires	
East Tapajós	0.83895	0.62055	0.42155	0.40981	0.25431	
West Juruena	-	-	0.27168	-	-	
Low Teles Pires	-	-	-	0.65305	-	

634

CAPÍTULO II

**Integrative analysis supports a new species of the *Oecomys catherinae* complex
(Rodentia, Cricetidae) from Amazonia**

Manuscrito aceito para publicação pela revista *Journal of Mammalogy*

ISSN: 1545-1542; classificação CAPES: A2

1 Contact information of corresponding author:
2 Universidade Federal de Mato Grosso
3 Instituto de Biociências, Departamento de Biologia e Zoologia
4 Av. Fernando Correa da Costa, 2367
5 Cuiabá, MT, Brasil, CEP 78060-900
6 rogerrossi@gmail.com
7

8 **Running Header:** A new Amazonian *Oecomys* species

9

10 **Integrative analysis supports a new species of the *Oecomys catherinae* complex**
11 **(Rodentia, Cricetidae) from Amazonia**

12

13 JULIANE SALDANHA AND ROGÉRIO VIEIRA ROSSI*

14

15 *Laboratório de Mastozoologia, Instituto de Biociências, Universidade Federal do Mato*
16 *Grosso, Cuiabá, Mato Grosso, Brazil (JS-RVR)*

17 *Laboratório de Citogenética e Genética Animal, Instituto de Biociências, Universidade*
18 *Federal do Mato Grosso, Cuiabá, Mato Grosso, Brazil (JS)*

19

20 **Correspondent: rogerrossi@gmail.com*

21

22 The sigmodontine rodent *Oecomys catherinae* has been recognized as a species complex that
23 includes five different lineages distributed throughout Brazil south of the Amazon river,
24 named in literature according to their geographic position (central, eastern, northern, western,
25 and westernmost). The western lineage has also been referred as *Oecomys* aff. *catherinae* in
26 literature, because it may represent a distinct species. Herein, we used molecular and
27 morphological data to investigate the possible species distinctiveness within the *O. catherinae*
28 complex. From molecular analyses, we recovered the western lineage as a monophyletic

29 group with high genetic divergence from the other lineages of the complex. This lineage can
30 be differentiated from other lineages of the *O. catherinae* complex and other congeners
31 through a combination of morphometric and morphological characters that includes: smaller
32 size; posterior margin of nasals usually surpassing the maxillary-frontal suture; supraorbital
33 crest moderately developed, similar to the temporal crest; parietal slightly expanded laterally;
34 subsquamosal fenestra present; alisphenoid strut absent; and anterior cingulum of M1 present.
35 The western lineage occurs in the southern Amazonia, in sympatry with the westernmost
36 lineage and other species of *Oecomys*. Herein we describe this lineage as a new species,
37 increasing to 19 the number of species within *Oecomys*.

38

39 Key words: Sigmodontinae, Oryzomyini, Species delimitation, Taxonomy.

40

41 O roedor sigmodontíneo *Oecomys catherinae* foi reconhecido como um complexo de espécies
42 que inclui cinco linhagens distintas distribuídas ao sul do rio Amazonas, referidas na literatura
43 de acordo com sua posição geográfica (central, leste, norte, oeste e extremo oeste). A
44 linhagem oeste também já foi referida na literatura como *Oecomys* aff. *catherinae*, uma vez
45 que pode representar uma espécie distinta. Neste estudo, utilizamos dados moleculares e
46 morfológicos para investigar a possível distinção de espécies dentro do complexo *O.*
47 *catherinae*. Nas análises moleculares recuperamos a linhagem oeste como um grupo
48 monofilético, com alta divergência genética das demais linhagens do complexo. Esta
49 linhagem pode ser diferenciada dos demais clados dentro do complexo *O. catherinae* e de
50 outros congêneres a partir de uma combinação de caracteres morfométricos e morfológicos,
51 que inclui: tamanho menor; margem posterior dos nasais geralmente ultrapassando a sutura
52 maxilar-frontal; crista supraorbital levemente desenvolvida, similar à crista temporal; parietal
53 com pequena expansão lateral; fenestra subesquamosal presente; barra do alisfenóide ausente;

54 e cíngulo anterior do M1 presente. A linhagem oeste ocorre na Amazônia meridional, em
55 simpatria com a linhagem extremo oeste e outras espécies do gênero *Oecomys*. Aqui nós
56 descrevemos esta linhagem como uma nova espécie, elevando para 19 o número de espécies
57 em *Oecomys*.

58

59 **Palavras-chave:** Delimitação de espécies, Oryzomyini, Sigmodontinae, Taxonomia.

60

61 In a recent literature review on rodent systematics, D'Elía et al. (2019) showed that
62 integrative taxonomy with molecular, karyotypes, and morphological, data provides a better
63 understanding of the diversification of this group, including aspects of morphological
64 evolution. In a similar way, Rocha et al. (2018) stated that analyses of morphological and
65 molecular variation through space are essential in the identification of cryptic species, such as
66 those belonging to the genus *Oecomys*.

67 Since Musser and Carleton (1993, 2005) consolidated *Oecomys* as a genus with 15
68 valid species, *O. sydandersoni* and *O. franciscorum* were described, and *O. tapajinus* was
69 revalidated, the latter two based on molecular, morphological, and morphometric, data
70 (Carleton et al. 2009; Pardiñas et al. 2016; Rocha et al. 2018, respectively). Thus, the genus
71 *Oecomys* currently is one of the most diverse in the tribe Oryzomyini, with 18 recognized
72 species (Pardiñas et al. 2017; Rocha et al. 2018), most of which are distributed in the Amazon
73 Basin (Carleton and Musser 2015; Pardiñas et al. 2017).

74 Based on a systematic study of *Oecomys* integrating morphological, karyotypic, and
75 molecular data, Suárez-Villota et al. (2018) recognized seven valid species, three undescribed
76 species, and five species complexes, which altogether account 15 species. One of these
77 species complexes is *O. catherinae* (hereafter referred to as the *O. catherinae* complex *sensu*
78 *lato* in this report), consisting of five lineages according to the authors. Despite great

79 morphological similarity, these lineages exhibit substantial molecular divergences (*Cytb* K2P:
80 1.6 – 8.7%), and different karyotypes ($2n = 54 - 62$) and distributions. Suárez-Villota et al.
81 (2018) treated these lineages as western, westernmost, northern, central, and eastern, clades.
82 The first two clades include specimens from the northern part of Mato Grosso state; the third
83 occurs in northwestern Mato Grosso and southeastern Pará states; the fourth lineage includes
84 specimens from the central region of Brazil; and the fifth lineage includes specimens from the
85 south and southeast of Brazil. The geographic distribution of the latter clade comprises the
86 type locality of *O. catherinae*, which is Joinville, Santa Catarina state (Thomas 1909).
87 Another available name for this species complex is *bahiensis* Hershkovitz, 1960, currently
88 recognized as a junior synonym of *O. catherinae* fide Carleton and Musser (2015). As a
89 nominal taxon also described from the Brazilian Atlantic Forest—particularly for Fazenda
90 Almada, Ilhéus, state of Bahia—*Oryzomys concolor bahiensis* probably applies to the eastern
91 clade of Suárez-Villota et al. (2018).

92 Populations of *O. catherinae* complex *s. l.* corresponding to the northern and eastern
93 clades already have been identified by Malcher et al. (2017) based on chromosomal
94 differences, but without consistent morphological and molecular differentiation, suggesting
95 that these populations may represent cryptic species. In addition, the western clade has been
96 suggested to represent a distinct taxonomic entity by Saldanha et al. (2019), based on its high
97 genetic divergence from the other clades within the complex.

98 During the morphological examination of samples from the western clade of Suárez-
99 Villota et al. (2018; = *Oecomys* aff. *catherinae* sequenced by Saldanha et al. 2019), we
100 realized that this form can consistently be distinguished from the other lineages within *O.*
101 *catherinae* complex *s. l.* and from other congeneric species. To investigate the molecular and
102 morphological distinctiveness within the *O. catherinae* complex *s. l.* and to evaluate whether
103 *Oecomys* aff. *catherinae* (sensu Saldanha et al. 2019) represents a new species, we analyzed

104 DNA sequences, and external and craniodental morphology of the largest sample from this
105 complex gathered to date, including the holotype of *O. catherinae*.

106 MATERIALS AND METHODS

107 *Phylogenetic Analysis.*—We used nucleotide sequences of the mitochondrial marker
108 Cytochrome *b* (*Cytb*) available from GenBank (<http://www.ncbi.nlm.nih.gov/genbank>). The
109 data matrix contains 71 specimens of the *O. catherinae* complex *s. l.*, including 14 individuals
110 referred as *Oecomys* aff. *catherinae* by Saldanha et al. (2019). In addition, we included four
111 sequences of *O. rex*, and two from each of the other species recognized in the genus with
112 available sequences, totaling 26 specimens. Sequences of *Euryoryzomys macconnelli*, *E.*
113 *nitidus*, *Handleyomys intectus*, and *Hylaeamys megacephalus*, were used as an external group
114 (Supplementary Data S1).

115 We also used nucleotide sequences from the nuclear marker intron 7 β -fibrinogen (*i7-*
116 *fgb*) available from GenBank and obtained sequence from the specimen UFMT 4118,
117 following the extraction, amplification and sequencing protocols described by Saldanha et al.
118 (2019). This sequence is available at Genbank under number MT978188. This data matrix
119 contains 28 specimens from the *O. catherinae* complex *s. l.*, including 12 individuals of
120 *Oecomys* aff. *catherinae*. We also included sequences of the other species from the genus
121 with available sequences. Sequences of *i7-fgb* and *Cytb* were concatenated into a single data
122 matrix based on the same *i7-fgb* matrix specimens. Sequences of *Oligoryzomys utiaritensis*,
123 “*Handleyomys*” *melanotis*, *Euryoryzomys nitidus*, and *Hylaeamys megacephalus*, were used
124 as an external group in the analyses of *i7-fgb* and concatenated data (Supplementary Data
125 SD1).

126 The three data sets of sequences (*Cytb*, *i7-fgb*, and concatenated data) were aligned in
127 the program BioEdit 7.0.5.3 (Hall 1999) with the ClustalW tool. Subsequently, the JModeltest
128 2.1.6 program (Darriba et al. 2012) was used to define the evolutionary model of each data

129 matrix in the CIPRES platform (Miller et al. 2010). The data matrix composed of 106
130 sequences with 801 *Cytb* base pairs was best represented by the GTR + I + G evolutionary
131 model. The data matrix composed of 46 sequences with 736 *i7-fgb* base pairs was best
132 represented by the HKY + G evolutionary model. The *Cytb* + *i7-fgb* concatenated data matrix,
133 consisting of 46 sequences with 1,537 base pairs, was best represented by the GTR + I + G
134 and HKY + G evolutionary models, respectively.

135 We carried out the Bayesian Inference (BI) analysis using the MrBayes 3.2.6 program
136 (Ronquist et al. 2012) on the CIPRES platform (Miller et al. 2010), enabling four chains, 50
137 million generations, sampling every 1000 generation, with 25% burnin. Maximum likelihood
138 analysis (ML) was obtained using the Garli program 2.0 (Zwickl 2006), with bootstrap of
139 1000 replicates and a majority consensus tree summarized in the SumTrees program
140 (Sukumaran and Holder 2010).

141 The resulting trees were visualized and edited in the FigTree program v1.4.3 (Rambaut
142 2016). Branch supports were evaluated by Bayesian Posterior Probability (BPP) values in BI
143 and bootstrap values in ML. The genetic distances within and among the clades were
144 calculated in the MEGA7 (Kumar et al. 2016) by uncorrected *p*-method.

145 To estimate putative species, we used *Cytb* sequences for Bayesian implementation of
146 Poisson Tree Processes (bPTP) analysis (Zhang et al. 2013) and Generalized Mixed Yule
147 Coalescent (GMYC) analysis (Fujisawa and Barraclough 2013). The bPTP method also was
148 used to delimit species with concatenated (*Cytb* + *i7-fgb*) data.

149 For the bPTP analysis, we used the concatenated tree and *Cytb* tree obtained by BI,
150 exported in Newick tree format. These trees were submitted as input file for the bPTP analysis
151 on the online platform <https://species.h-its.org/ptp/>.

152 For GMYC analysis, we used an ultrametric tree obtained from 84 sequences
153 (duplicates were removed) from the *Cytb* marker. From these sequences we generated an .xml

154 file in BEAUti v. 2.4.8 (Bouckaert et al. 2014) with the evolutionary model GTR + I + G,
155 uncorrelated lognormal Relaxed Clock, 20 million MCMC generations and a priori model of
156 Yule. The ultrametric tree was estimated in BEAST 2.4.8 (Bouckaert et al. 2014) on the
157 CIPRES platform (Miller et al. 2010) with three independent runs, subsequently combined
158 into a single run with 25% burnin. Tracer v1.6 (Rambaut et al. 2014) was used to check the
159 values and effective size of the samples (ESS) generated in BEAST. Trees were summarized
160 into a summary tree using TreeAnnotator v.1.8 (Drummond et al. 2012), visualized in FigTree
161 v1.4.3 (Rambaut 2016) and finally exported in Newick format for GMYC analysis on the
162 online platform <https://species.h-its.org/gmyc/> with the Single Threshold model.

163 *Morphological Analysis.*—We examined 116 specimens from the *O. catherinae*
164 complex *s. l.* and eight specimens of *O. rex*. This latter species was included in the examined
165 material for comparison purposes, because of the morphological similarity and putative sister-
166 species position with the *O. catherinae* complex *s. l.* previously reported in the literature. The
167 specimens, preserved as skins, skulls, and fluid, are deposited in the following institutions:
168 Museu Nacional da Universidade Federal do Rio de Janeiro (MN); Museu de Zoologia da
169 Universidade de São Paulo (MZUSP); Museu Paraense Emílio Goeldi (MPEG); Universidade
170 do Estado de Mato Grosso (Unemat); and Universidade Federal de Mato Grosso (UFMT). We
171 also examined the holotypes of *O. catherinae* (MNH 1909.11.19.24) and *O. rex* (MNH
172 1910.9.29.17), deposited in the Natural History Museum, London. Collection locations and
173 geographic coordinates were obtained from the labels of the specimens and inserted in the
174 QGIS 2.18 program (<https://www.qgis.org>) to produce maps of collecting localities of
175 vouchers and tissue samples included in this report (Fig. 1).

176 Some of the specimens of the *O. catherinae* complex *s. l.* included in this study were
177 collected by RVR in accordance with the guidelines of the American Society of
178 Mammalogists (Sikes et al. 2011). They were measured and weighed in the field and prepared

179 as skins and skeletons. Vouchers were deposited in the Coleção Zoológica da Universidade
180 Federal de Mato Grosso (UFMT).

181 In the specimens examined, we observed patterns of dorsal and ventral pelage
182 coloration, tail coloration, pattern of distribution of the caudal scales, and number and size of
183 caudal scale hairs. We observed aspects of cranial morphology such as bone shape, presence
184 and position of foramina, fenestrae, and sutures, development and morphology of crests, and
185 morphology of the auditory region and teeth. The nomenclature used to describe the skull and
186 its structures follows Voss et al. (2001) and Weksler (2006). Molar nomenclature follows
187 Reig (1977) and Pires et al. (2016).

188 *Morphometric Analysis.*—For the morphometric analyses, specimens were grouped
189 into five different age classes following Voss (1991). Only specimens considered adults (with
190 third upper molar completed erupted) were used. External measurements were obtained
191 directly from specimen label and include head and body length (HBL), length of tail (TL),
192 length of hindfoot with claw (HFL), length of ear (Ear), and mass (Weight). In the absence of
193 HBL, this measurement was calculated by subtracting the length of tail from the total length.

194 Thirty-one craniodental measurements were obtained using a 0.01 mm precision
195 caliper while specimens were being examined under a stereomicroscope. Thirteen of these
196 measurements were defined by Voss (1988), as follows: breadth across the exoccipital
197 condyles (BOC); breadth across the incisive foramina (BIF); breadth of incisor (BI); breadth
198 of M1 (BM1); breadth of nasals (BN); breadth of the zygomatic plate (BZP); condylo-incisive
199 length (CIL); coronal length of upper molars (CLM); greatest zygomatic breadth (ZB); least
200 interorbital breadth (LIB); length of incisive foramen (LIF); length of nasals (LN); and length
201 of upper diastema (LD). Four measurements followed Carleton and Musser (1995): bullar
202 breadth (BB); length of palatal bridge (LPB); length of rostrum (LR); and occipitonasal length
203 (ONL). The remaining 14 measurements were based on unpublished dissertations

204 (Percequillo 1988; Flores 2010). These measurements and their respective descriptions are:
205 braincase height (BH), measured from the basisphenoid-basioccipital suture to the frontal-
206 parietal suture on midline; breadth of interparietal (BIP), the greatest breadth of interparietal
207 bone; breadth of m1 (Bm1), the greatest crown breadth of the first lower molar; breadth of
208 rostrum at palate (BRP), measured between most posterior lower edges of infraorbital
209 foramina on ventral side of skull; breadth of rostrum (BR), the distance between the inside
210 margins of nasolachrymal capsule; condylo-zygomatic length (CZL), measured from the most
211 anterior point in anterior edge of zygomatic plate to the articular surface of the condyle on the
212 same side; coronal length of lower molars (CLLM), the crown length from m1 to m3; least
213 condyloid-Incisor breadth (LCIB), measured from the crown of the first cheektooth to the less
214 curvature of the incisor on the same side; length of interparietal (LIP), the greatest length of
215 interparietal bone; length of lower diastema (LLD), measured from the crown of the first
216 cheektooth to the less curvature; mandible height (MH), the distance across cranium at
217 mastoid processes; mastoid breadth (MB), measured from the angular process to the
218 condyloid process on the same side; orbital length (OL), the internal distance between anterior
219 and posterior margins of the orbit; and zygomatic length (ZL), the greatest transverse
220 dimension across the squamosal zygomatic process.

221 External and craniodental measurements were summarized as basic descriptive
222 statistics. Craniodental dimensions were used in uni- and multivariate statistical analyses.
223 Initially, we carried out a Kolmogorov-Smirnov test to assess the normal distribution of the
224 variables (Sokal and Rohlf 1981). Since most variables displayed a normal distribution, we
225 used the Student's *t*-test to evaluate sexual dimorphism from the total studied sample. This
226 was discarded for the tested variables, except BH and LPB. Subsequent analyses therefore
227 were carried out with males and females together.

228 Measurements were transformed into a base 10 logarithms to be used in Principal
229 Component Analysis (PCA) and Discriminant Analysis (DA), to investigate which variables
230 respond to most of the data variation and which have the greatest discrimination power among
231 the species, respectively. Scatter plots were provided to visualize how specimens behave in
232 the multivariable space. All statistical tests were carried out using SPSS 22.00 (IBM Corp.,
233 Armonk, New York) with a significance level of $\alpha = 0.05$.

234 RESULTS

235 *Phylogenetic Analysis.*—Each of the five clades of the *O. catherinae* complex *s. l.* was
236 recovered with strong support by the *Cytb* gene dataset, as well as the complex itself,
237 supporting a sister relationship between the western clade and remaining clades of the
238 complex. The remaining four clades of the *O. catherinae* complex *s. l.* were recovered as a
239 strongly supported monophyletic group, with the westernmost clade as the most external
240 lineage (Fig. 2).

241 The *O. catherinae* complex *s. l.* had no statistical support based on the *i7-fgb* gene
242 dataset. The topology differed from that obtained with the mitochondrial marker, with the
243 western clade sister to the eastern clade, followed by westernmost, central, and northern,
244 clades, with no resolution among internal branches (Supplementary Data S2).

245 With the concatenated data, the five clades of the *O. catherinae* complex *s. l.* were
246 recovered, each with strong support. However, the *O. catherinae* complex *s. l.* itself was not
247 supported, because the western clade was recovered outside the complex, as sister to the other
248 four clades of the complex plus all remaining species of *Oecomys* included in the analysis.
249 The westernmost, central, northern, and eastern, clades formed a strongly supported distinct
250 monophyletic group, with the western clade as the most external branch. A group comprising
251 the central and northern clades also had strong support in this analysis (Fig. 3).

252 In the *O. catherinae* complex *s. l.*, the western clade presented the highest genetic
253 divergence in *Cytb*, ranging from 6.97% to the eastern clade, to 8.75% with respect to the
254 westernmost clade. Regarding the other *Oecomys* species, divergence of the western clade
255 ranged from 7.36% to *O. concolor*, to 10.29% to *O. rutilus*. Among the other clades in the *O.*
256 *catherinae* complex *s. l.*, the lowest genetic divergence was 1.38% between the eastern and
257 northern clades, and the highest was 4.66% between the westernmost and northern clades
258 (Table 1).

259 The species delimitation analysis of bPTP from the *Cytb* tree indicated 21 evolutionary
260 lineages, of which 12 corresponded to species recognized in the literature, as well as two
261 independent lineages within the *O. superans* clade and two within the *O. sydandersoni* clade
262 (Fig. 2). The other five evolutionary lineages recognized by bPTP corresponded to the five
263 clades of *O. catherinae* complex *s. l.* (Figure 2). The GMYC analysis of species delimitation
264 based on the *Cytb* indicated the presence of 20 evolutionary lineages, of which 14
265 corresponded to species recognized in the literature and six to the *O. catherinae* complex *s. l.*
266 (Fig. 2). The analysis recognized two independent lineages of individuals from the Atlantic
267 forest. One of these lineages comprises specimens from the states of Rio de Janeiro, São
268 Paulo, and southern Minas Gerais, while the other comprises specimens from the states of
269 Espírito Santo and northern Minas Gerais. Although there is some geographical structure in
270 this arrangement, with the former lineage at north and the latter at south, the low support
271 values (BPP = 0.89) and uncorrected p-distance (1.0%) between them led us to provisionally
272 recognize a single lineage (named eastern clade; Fig. 2). The bPTP analysis from the *Cytb* +
273 *i7-fgb* concatenated tree presented 14 evolutionary lineages, of which seven corresponded to
274 species recognized in the literature, as well as two independent lineages within the *O. cleberi*
275 clade. The remaining five lineages corresponded to the five clades of *O. catherinae* complex

276 *s. l.* (Figure 3). Based on these results, we treated these five clades of the *O. catherinae*
277 complex *s. l.* as independent lineages in our morphological and morphometric analyses.

278 *Morphological and Morphometric Analyses.*—Descriptive statistics of the lineages
279 morphometrically analyzed herein are provided in Table 2. In the Principal Component
280 Analysis (PCA), the first component (PC1) accounted for 54.9% of the total data variation
281 and PC2 for only 8.5% of the variation. The coefficients of all variables showed positive sign
282 in PC1, indicating that this component represents overall size variation. The variables that
283 most contributed to this component were related to the length of the skull (ONL, CIL, and
284 ZL), length of diastema (LD), and height of mandible (MH). With both positive and negative
285 coefficients, PC2 can be associated with skull shape. The variables that contributed most to
286 this component were related to the breadth of first molars (BM1 and Bm1, positive values),
287 length of toothrow (CLM and CLLM, positive values), and bullar breadth (BB, negative
288 value; Supplementary Data S3). The scatter plot of PC1 and PC2 shows specimens of the
289 western lineage overlapping with those of northern and eastern lineages, and slightly
290 overlapping with those of central and westernmost lineages (Fig. 4).

291 The discriminant analysis indicated that the first canonical variate (CV1) is
292 responsible for 62.1% of the total data variation while the second (CV2) is responsible for
293 20.9% of the total variation. Craniodental measurements that most contributed to CV1 are
294 related to the skull length (LR, negative value), zygomatic breadth (ZB, negative value),
295 orbital and diastema length (OL and LD, positive values), and interorbital length (LIB,
296 positive value). In CV2, the most important measurements are related to skull and mandible
297 lengths (CIL positive value; OL and LCBI, negative values), and to the bullar and zygomatic
298 breadth (BB and ZB, positive values; Supplementary Data S3).

299 The scatter plot of CV1 and CV2 shows that the western lineage does not overlap the
300 other four lineages in morphospace (Fig. 4). The discriminant functions generated correctly

301 classified 95.1% of the analyzed specimens (Supplementary Data S3). The western, central,
302 and westernmost, lineages' specimens were correctly classified in 100% of cases, whereas the
303 eastern and northern lineages specimens were correctly classified in 96.3% and 87.5% of
304 cases, respectively.

305 In summary, both morphometric and morphological analyses (as described below)
306 allowed us to discriminate the western clade from all remaining clades of the *O. catherinae*
307 complex *s. l.* This is concordant with the molecular analyses, which revealed high genetic
308 divergence between the western clade and the remaining four clades of the *O. catherinae*
309 complex *s. l.* These results in combination provide sufficient evidence to recognize the
310 western clade as a new species of *Oecomys*, which we describe below, and to restrict the *O.*
311 *catherinae* complex to the eastern, central, northern, and westernmost clades, hereafter
312 referred as *O. catherinae* complex *sensu stricto*.

313 TAXONOMY

314 Family Cricetidae Fischer, 1817

315 Subfamily Sigmodontinae Wagner, 1843

316 Tribe Oryzomyini Vorontsov, 1959

317 Genus *Oecomys* Thomas, 1906

318 ***Oecomys* sp. nov.**

319 Figures 5 – 8; Tables 2 and 3

320 *Oecomys* sp. 1: Di-Nizo et al. 2017:843

321 *Oecomys catherinae* western clade: Suárez-Villota et al. 2018:190.

322 *Oecomys* aff. *catherinae*: Saldanha et al. 2019:44.

323 *Oecomys catherinae* western clade: Brandão et al. 2019:266

324 *Holotype*.—UFMT 4118, Adult, male, preserved in dry skin, skull and complete
 325 postcranial skeleton. Collected by Rogério Vieira Rossi (Field number RVR 89) on 12 May
 326 2014. Hologenotypes *Cytb* and *i7-fgb* are deposited in GenBank (accession number
 327 MK874365 and MT978188, respectively).

328 *Measurements (in mm) and body mass of the holotype*.—TL= 226, HBL= 106, T=
 329 120, E= 17, HFL= 26, ONL= 28.90, CIL= 25.86, BH= 8.36, CZL= 20.51 ZL= 13.35, LD=
 330 6.71, BZP= 2.96, BN= 3.74, LN= 11.15, LR= 9.08, BR= 4.44, LIB= 5.20, OL= 10.39, ZB=
 331 14.98, LIP= 3.81, BIP= 9.58, BIF= 2.12, LIF= 3.94, BRP= 4.58, LPB= 5.95, MB= 10.32,
 332 BOC= 5.99, BB= 4.38, BI= 1.51, BM1= 1.32, CLM= 4.77, Bm1= 1.22, CLLM= 4.97, LLD=
 333 2.89, LCIB= 14.64, MH= 6.67, body mass 33 g.

334 *Paratypes*.—UFMT 1773, adult, female, preserved as skin and skull. Collected by T.
 335 S. Santos-Júnior on 29 October 2009 (Field number UTP 159) from the Teles Pires
 336 Hydroelectric Power Plant, Paranaíta municipality, Mato Grosso state, coordinates: 9°29'06"S,
 337 56°28'19"W, left bank of the Teles Pires River, tributary of the Tapajós River. Measurements:
 338 HBL= 105,82 mm, T= 122,05 mm, E= 15,72 mm, HFL= 25,52 mm, weight 34 g. UFMT
 339 1680, adult, male, preserved in skin and skull. Collected by T. S. Santos-Júnior on 18 April
 340 2009 (Field number UTP 02) at the Teles Pires Hydroelectric Power Plant, Paranaíta
 341 municipality, Mato Grosso state, coordinates: 9°29'10"S, 56°28'19"W, left bank of the Teles
 342 Pires River, tributary of the Tapajós River. Measurements: HBL= 125 mm, T= 132 mm, E=
 343 17 mm, HFL= 24 mm, weight 22 g.

344 *Type locality*.—Estância Santa Clara, Alta Floresta municipality, left bank of the Teles
 345 Pires River, tributary of the Tapajós River, Mato Grosso state, coordinates: 10°00'25"S,
 346 56°02'17"W (GPS coordinates taken at the trap site).

347 *Additional material.*—Twenty specimens from Mato Grosso State, Brazil: skin of
 348 MSF1878, female (9°46'12."S, 56°10'15.6"W, Alta Floresta); skin and skull of
 349 MZUSP29531, female (10°10'01"S, 59°27'W, Aripuanã); skins of MSF1406, female;
 350 MSF1407, 1411, males (11°34'58"S, 55°10'01"W, Cáceres); skin and skull of MZUSP35543,
 351 male (11°34'58"S, 55°10'01"W, Cláudia); skin and skull of MZUSP29516, female
 352 (13°04'58"S, 53°16'58"W, Gaúcha do Norte); skin and skull of MZUSP35537, female
 353 (10°19'01"S, 58°28'58"W, Juruena); skin and skull of UFMT931, female (12°51'S, 58°56'W,
 354 Juruena); skins and skulls of UFMT1772, 1774, 1806, females (9°29'06"S, 56°28'19"W,
 355 Paranaíta); skins and skulls of AC207, 230, males; AC255, 266, females (15°04'45.9"S,
 356 56°33'15.7"W, Rosário Oeste); skins of RFO013, female; RFO027, 029, 040, males
 357 (15°10'33.6"S, 59°59'38.4"W, Vila Bela da Santíssima Trindade). Four specimens from Pará
 358 state, Brazil: skins and skulls of UFMT1775, 1776, males, UFMT1686, UFMT1690, females
 359 (9°18'40"S, 56°46'05"W, Jacareacanga). One specimen from Rondônia state, Brazil: skin and
 360 skull of MPEG34224 (12°43'S, 60°7'W, Vilhena).

361 *Diagnosis.*—Soft, long dark reddish-brown dorsal fur (length: 7 – 11 mm); ventral fur
 362 dark cream, composed of gray-based hairs throughout the venter and self-dark cream hairs on
 363 areas of the throat, neck, forelimbs, and genitalia; caudal tuft absent, but hairs exceed tail tip
 364 (< 1 mm). Rostrum narrow and moderately long; posterior margin of the nasals V- or U-
 365 shaped, surpassing or aligned to the posterior portion of the maxillary-frontal suture, and
 366 premaxillaries terminating anterior to the nasals; supraorbital crest moderately developed,
 367 similar to the temporal crest; parietal slightly expanded below the lateral edges of the dorsum
 368 of the braincase; hamular process narrow; subsquamosal fenestra present; alisphenoid strut
 369 usually absent; complete stapedia circulation (pattern 1, Voss 1988); and anterior cingulum
 370 present on the first upper molar.

371 *Morphological description.*—*Oecomys* sp. nov. is characterized by medium size
372 (HBL: 85–135 mm), tail longer (TL: 106–160 mm) than combined head and body (i.e. tail
373 from 104–148% of HBL). Soft and abundant pelage, with hairs varying from 7 – 11 mm in
374 length. Dorsal hairs gray-based with terminal tips dark reddish-brown, mixed with some gray-
375 based and dark brown-tipped hairs (Figure 5A). Flanks lighter than the dorsum, with poorly
376 marked lateral/ventral transition. Venter dark cream with gray-based hairs throughout the
377 belly, except on the throat, neck, forelimbs, and genitalia, where the hairs are self-dark cream
378 (Figure 5A). Hairs shortest and lightest in the rostrum. Mystacial vibrissae abundant and dark
379 brown, with the longest surpassing the posterior edge of the pinnae. Ears light brown at the
380 base and dark brown at the end, with orange and some brown hairs on the outer and inner
381 pinnae surfaces. Manus and pes dorsally covered with white hairs, mixed with brown hairs in
382 the median portion; on the manus, the brown fur covers the arms towards the body. Ungual
383 hairs white, abundant and long, surpassing the claws, except for digit I. Distal end of digit I
384 surpasses the 2nd interdigital pad. Plantar surface with small scales between pads, four
385 developed interdigital pads equal in size and closely positioned, a hypothenar pad smaller
386 than the interdigital pads, and a developed and long thenar pad that extends proximally. Tail
387 completely brown, but slightly bicolor on the proximal portion. Caudal scales with three hairs,
388 with the longest hair exceeding two scale rows in length. Caudal tuft absent, but hairs exceed
389 tail tip about 1 mm in length. Four mammary pairs distributed as follows: one pectoral, one
390 postaxial, one abdominal, and one inguinal (Voss and Carleton, 1993).

391 Skull small when compared to the other lineages of the *O. catherinae* complex *s. s.*
392 (Table 2), and medium compared to other congeners. Rostrum narrow and moderately long.
393 Anterior margins of the nasal bones rounded, surpassing the anterior portion of premaxillary
394 bones; posterior nasal margins V- or U-shaped, aligned or extending beyond the posterior
395 portion of the maxillary-frontal sutures (Figs. 6, 7A), and premaxillaries terminating anterior

396 to the nasals. Poorly developed zygomatic notch, but dorsally visible. Lacrimal in contact
397 with maxillary and frontal bones. Interorbital region convergent anteriorly, with narrow
398 median region; supraorbital ridges moderately developed, as well as the temporal ridges
399 (Figures 6, 7C). Rounded cranial vault. Interparietal wider than posterior border of frontals,
400 but not contacting the squamosal. Exoccipital crests absent or poorly developed in dorsal view
401 (Fig. 6).

402 Zygomatic plate broad, slightly projected anteriorly to the maxillary root of the
403 zygomatic, and posterior margin positioned anteriorly to M1. Jugals small, their maxillary and
404 squamosal processes not overlapping. Squamosal root of the zygomatic arch expanded
405 laterally. Parietal slightly expanded below the lateral edges of the dorsum of the braincase
406 (greater expansion in UFMT 1680; Fig. 7E). Hamular process narrow; subsquamosal fenestra
407 small or medium, never larger than the postglenoid foramen (Figure 7E). Lambdoidal crests
408 poorly developed. Mastoid with small fenestra that does not contact the edge of the
409 exoccipital, or with a larger fenestra that reaches the exoccipital edge.

410 Incisive foramina small, drop or oval shaped, with posterior margin not reaching the
411 first molars. Palate long and wide (sensu Hershkovitz, 1962) with conspicuous posterolateral
412 palatal pits located in deep palatal depressions. Mesopterygoid fossa U-shaped, aligned with
413 the posterior margin of the maxillary; roof of mesopterygoid fossa fully ossified or with small
414 perforations. Parapterygoid fossa dorsally excavated, but not reaching the mesopterygoid
415 level. Alisphenoid strut absent (except in MPEG 34224 and UNEMAT - AC 266). Primitive
416 pattern of stapedial circulation (pattern 1 of Voss [1988]), with stapedial foramen and
417 posterior opening of the alisphenoid canal developed, and presence of squamosal-alisphenoid
418 groove and sphenofrontal foramen. Tegmen tympani not contacting the squamosal, or
419 contacting the squamosal punctually. Small ectotympanic bulla; periotic slightly exposed and

420 usually reaching the carotid canal. Eustachian tube narrow and short, with edge parallel to the
421 basioccipital suture (Fig. 6).

422 Mandible robust, with mental foramina dorsally located in the diastema, anterior to
423 m1. Upper and lower masseteric ridges converge and fuse only in the anterior portion, below
424 the anterior portion of m1. Capsular process lower incisor small and conspicuous. Coronoid
425 process small and pointed. Angular process short. Condylod process elongated (Fig. 6).

426 Upper incisors opisthodont ungrooved, with yellow-orange anterior enamel surfaces;
427 upper molar rows parallel arranged in opposite labial-lingual pairs. Molars are pentalophodont
428 and brachyodont. Upper first molar (M1): anterior cingulum (i.e. stylar shelf on the anterior
429 border of the procingulum, positioned anteriorly to the anterocone) present (refer to Pires et
430 al. 2016 for description and comments on this structure); procingulum with a central fossete;
431 anterocone not divided by anteromedian flexus (anteromedian flexus present in UFMT 1773,
432 dividing the procingulum into anterolabial and anterolingual conules); anteroloph present and
433 connected to the anterocone and paracone by parastyle; paracone connected to protocone by
434 median mure, with long paraflex; protocone connected to the anterior mure and separated
435 from the anterocone by protoflexus; paralophule present in paracone and connected to the
436 mesoloph; posteroloph fused to metacone, with presence of fossetus derived from the
437 posteroflexus; labial and lingual accessory roots absent; labial and lingual cingula absent (Fig.
438 8). Upper second molar (M2): Anteroloph present; anterolingual cingulum present, but poorly
439 developed in the anterior portion of the protocone; lingual cingulum present; paralophule
440 connecting paracone to mesoloph; posteroloph present (Fig. 8). Upper third molar (M3):
441 smaller than the half of M1 and larger than half of M2; mesoloph and short posteroloph
442 present; hypocone slightly reduced with respect to protocone and separated from the
443 protocone by hypoflexus; reduced metacone (Fig. 8).

444 Lower first molar (m1): anteromedian flexid present, dividing procingulum into
445 anterolabial and anterolingual conulids; procingulum with anteromedian fossetid well-
446 developed. Anterolabial cingulum connected to a well-developed protostylid; ectolophid
447 present; metaconid with metalophulid connected to mesolophid that is fused in its distal
448 portion to the entoconid; posterolophid long and fused by wear to the entoconid; hypolophulid
449 present (Fig. 8). Lower second molar (m2): anterolabial cingulum present and well-
450 developed; entoconid small; small ectolophid and ectostylid present; posterolophid connected
451 to the entoconid (Fig. 8). Lower third molar (m3): smaller than half of m1 and same length as
452 m2; anterolabial cingulum present; small ectolophid and ectostylid present; posterolophid
453 probably present and connected to the entoconid, that is reduced (Fig. 8).

454 *Karyotype*.—Specimens of the western clade exhibited $2n=54$, $FN=54$, with a small
455 submetacentric pair (pair 1) and all the other autosomes acrocentric (pairs 2–26). The X-
456 chromosome is large and submetacentric, with a short heterochromatic arm, and the Y-
457 chromosome is medium sized, metacentric and entirely heterochromatic (see Suárez-Villota et
458 al. 2018).

459 *Etymology*.—The specific name is a geographical reference to the Brazilian state of
460 Mato Grosso, where the holotype was collected and where most of the species distribution is
461 located.

462 *Distribution and sympatry*.—*Oecomys* sp. nov. occurs in southern Amazonia; the
463 species' distributional area extends from Jacareacanga (on the right bank of the Teles Pires
464 river in the extreme southwest of Pará state) southward to Cáceres (in the extreme southwest
465 of Mato Grosso state), and from Vilhena (Rondônia state) and Aripuanã (between the Juruena
466 and Aripuanã rivers, in Mato Grosso state) eastward to Gaúcha do Norte (on the left bank of
467 the Xingu River, Mato Grosso state). The species occurs in sympatry with *O. cleberi* and the

468 westernmost lineage of *O. catherinae* complex *s. s.* on the west margin of the Juruena River,
469 Mato Grosso state; and with *O. bicolor*, *O. paricola*, and *O. roberti*, in the municipality of
470 Cláudia, Mato Grosso state (Suárez-Villota et al. 2018; Saldanha et al. 2019).

471 *Habitat information.*—*Oecomys* sp. nov. was collected in forested habitats from the
472 southern Amazonia, particularly from the Amazonia-Cerrado transition zones, and the edge of
473 the Pantanal biome. Also, two collecting points are located in the Cerrado biome (Localities 6
474 and 9; Fig. 1), but habitat information was not available on the vouchers' labels.

475 *Comparisons.*—*Oecomys* sp. nov. is distinguished from *O. catherinae* complex *s. s.*
476 lineages by exhibiting smaller body size (Tables 2 and 3; Fig. 5) and short dorsal pelage (7 –
477 11 mm) with dark reddish-brown coloration, versus long dorsal pelage (9 – 15 mm) with
478 reddish-brown color. In addition, the new species has a darker cream ventral pelage when
479 compared to the central and eastern lineages (Fig. 5; Table 3).

480 The skull is smaller in *Oecomys* sp. nov. than in *O. catherinae* complex *s. s.* lineages
481 (Table 2). The rostrum is narrow and moderately long in the new species, but is wide and long
482 in eastern and westernmost lineages of *O. catherinae* complex *s. s.*, wide and short in the
483 central lineage, and narrow and short in northern lineage (Table 3). The posterior margin of
484 the nasals extends beyond the posterior portion of the maxillary-frontal suture in *Oecomys* sp.
485 nov. (Fig. 7A), contrasting with the *O. catherinae* complex *s. s.* lineages, whose posterior
486 margin of the nasals does not reach or is aligned to the posterior part of the maxillary-frontal
487 suture (Fig. 7B). In *Oecomys* sp. nov., the interorbital region is narrower compared to the
488 eastern, westernmost, and northern, lineages of *O. catherinae* complex *s. s.* Moreover, the
489 supraorbital and temporal crests are moderately developed in the new species (Fig. 7C),
490 whereas the supraorbital crest is dorsolaterally and distinctly more developed than the
491 temporal crest in the *O. catherinae* complex *s. s.* lineages (Fig. 7D). The subsquamosal

492 fenestra always is present in *Oecomys* sp. nov. (Fig. 7E), while it is reduced in the eastern and
493 westernmost lineages of *O. catherinae* complex *s. s.*, and fully ossified in the central and
494 northern lineages (Fig. 7F). The parietal is slightly expanded below the lateral edges of the
495 dorsum of the braincase in *Oecomys* sp. nov. (Fig. 7E), while it is deeply expanded onto the
496 lateral surface of the braincase in the *O. catherinae* complex *s. s.* lineages (Fig. 7F).

497 Because *O. catherinae* is externally similar to *O. rex* in pelage color and texture, we
498 provide comparisons of *Oecomys* sp. nov. with the latter species. Externally, the new species
499 differs from *O. rex* by exhibiting shorter dorsal fur (7 – 11 mm versus 9 – 14 mm in *O. rex*)
500 and lacking a caudal tuft (versus a small tuft present in *O. rex*). Cranially, the skull is smaller
501 in *Oecomys* sp. nov. (mean 28.9 mm) than in *O. rex* (mean 31.05 ± 3.10 mm; $n = 8$); the
502 supraorbital and temporal crests are moderately developed in the former species (versus
503 strongly developed supraorbital crests, joining in a prominent temporal crest in *O. rex*); and
504 the subsquamosal fenestra always is open in *Oecomys* sp. nov., while it is reduced or absent in
505 *O. rex*.

506 *Oecomys* sp. nov. can be distinguished from other congeneric sympatric species, such
507 as *O. bicolor*, *O. cleberi*, *O. roberti*, and *O. paricola*, by exhibiting medium body and cranial
508 size (versus smaller body and cranial size in *O. bicolor* and *O. cleberi*); dark reddish-brown
509 dorsal coloration (versus orangish-brown in *O. bicolor* and *O. cleberi*; reddish to orangish-
510 brown in *O. roberti*; and reddish-brown in *O. paricola*); dark cream ventral coloration (versus
511 totally white or cream venter in *O. bicolor* and *O. cleberi*; fully white or a white ventral
512 midline with gray-based lateral bands in *O. roberti*); and absence of caudal tuft (versus
513 presence of caudal tuft in *O. bicolor*, *O. cleberi*, and *O. paricola*). Detailed descriptions of the
514 mentioned species can be found in Rocha et al. (2012), Carleton and Musser (2015), and
515 Rocha et al. (2018).

DISCUSSION

516
517 Although *O. catherinae* was recognized as monotypic by Carleton and Musser (2015)
518 and Pardiñas et al. (2017), the species exhibits great genetic diversity and was reported as a
519 species complex by Malcher et al. (2017) and Suárez-Villota et al. (2018). In this study, we
520 analyzed the five clades of the *O. catherinae* complex *s. l.* currently recognized as possible
521 distinct lineages (Suárez-Villota et al. 2018) and found a body of evidence that allowed us to
522 positively recognize the western clade of previous studies as a new species.

523 As noted by Carstens et al. (2013), the appropriate way to conduct a species
524 delimitation is to analyze data with a wide variety of methods and delimit lineages that are
525 consistent across the results. In this report, the western lineage of the *O. catherinae* complex
526 *s. l.* was recovered as monophyletic, with strong support in all the phylogenetic and species
527 delimitation analyses employed herein. In addition, the western lineage was discriminated
528 from remaining lineages of the complex in multivariate space, exhibited several qualitative
529 characters that distinguish it from these latter lineages, and presented the highest interlineage
530 genetic distance values within the complex. Indeed, the genetic distance between *Oecomys* sp.
531 nov. and the westernmost lineage, with which it is sympatric, is high (8.75%) when compared
532 to the distances recorded between the new species and the other *O. catherinae* complex *s. s.*
533 lineages (6.97 – 7.38%). These are higher values compared to those reported for closely
534 related *Oecomys* species in the literature, such as *O. franciscorum* and *O. mamorae* (7.0%;
535 Pardiñas et al. 2016), and *O. tapajinus* and *O. roberti* (5.8%; Rocha et al. 2018).

536 The western lineage also presents an exclusive karyotype within the complex.
537 According to Suárez-Villota et al. (2018), it has a diploid number $2n = 54$ and fundamental
538 number $FN = 54$. In contrast, other lineages of the *O. catherinae* complex *s. l.* present distinct
539 karyotypes, with $2n = 60$ in the central, eastern, and westernmost, lineages, and $2n = 62$ in the
540 northern lineage (Langguth et al. 2005; Di-Nizo et al. 2017; Malcher et al. 2017; Suárez-

541 Villota et al. 2018). Altogether, these results give us strong support to recognize the western
542 lineage as an independent species, herein described as *Oecomys sp. nov.*

543 On the other hand, the remaining four clades of the *O. catherinae* complex *s. l.*
544 (eastern, central, northern, and westernmost) showed low genetic distances among
545 themselves, no exclusive combination of morphological characters, and greatly overlapped in
546 the multivariate space. Moreover, the GMYC analysis recognized two different evolutionary
547 lineages in the central clade, the westernmost clade was not recovered with adequate support,
548 and the central clade was not recovered as a monophyletic group in the BI with *i7-fgb* data
549 (Supplementary Data S2). These results prevent us for now to recognize these four lineages as
550 different species, instead retaining them in the *O. catherinae* complex *s. s.* In this sense, we
551 again follow Carstens et al. (2013), who stated that species delimitation studies should be
552 conservative and, in most contexts, it is better to fail to delimit species than it is to falsely
553 delimit entities that do not represent actual evolutionary lineages.

554 Our phylogenies showed mitonuclear discordance, with the mitochondrial marker
555 recovering the new species as sister to the *O. catherinae* complex *s. s.*, and the nuclear marker
556 recovering *Oecomys sp. nov.* as sister to the eastern lineage of this complex. According to
557 Després (2019), mitonuclear discordance can result from several factors, such as incomplete
558 lineage sorting, asymmetrical introgression, or natural selection. Mitochondrial and nuclear
559 DNA also respond differently to demographic fluctuations, such as during glacial periods, for
560 which mitochondrial DNA will diverge while nuclear genome will retain variability (Després
561 2019). The phylogenies presented by Suárez-Villota et al (2018) also showed mitonuclear
562 discordance for the *O. catherinae* complex *s. l.* clades. The authors discarded the introgressive
563 hybridization hypothesis, because the samples of the eastern clade exhibit $2n = 60$ rather than
564 $2n = 57$ or 58 , which would be expected in hybrids between the western (= *Oecomys sp. nov.* ;
565 $2n = 54$) and the other lineages of the *O. catherinae* complex *s. l.* ($2n = 60$ and 62).

566 The new species is distributed in southern Amazonia and the Amazonia – Cerrado
567 transition areas, where it occurs in sympatry with the westernmost lineage of the *O.*
568 *catherinae* complex *s. s.* and other four species of the genus (*O. bicolor*, *O. cleberi*, *O.*
569 *paricola*, and *O. roberti*). Sympatry among *Oecomys* species in the Amazonian region has
570 been reported by several authors (e.g., Voss and Emmons, 1996; Patton et al. 2000; Voss et al.
571 2001; Rocha et al. 2011; Suárez-Villota et al. 2018; Saldanha et al. 2019). In contrast,
572 sympatry between two different lineages of the same *Oecomys* species complex only has been
573 reported recently by Suárez-Villota et al. (2018), who recorded sympatry for lineages both of
574 the *O. roberti* complex and the *O. catherinae* complex (= *O. catherinae* complex *s. l.* in this
575 report). By using morphological and molecular markers, Rocha et al. (2018) showed that one
576 of the *O. roberti* complex lineages pointed out by Suárez-Villota et al. (2018) actually
577 represents a distinct species, for which the name *O. tapajinus* was available. Similarly, our
578 results based on several kinds of evidences gave us enough support to recognize Suárez-
579 Villota et al.'s (2018) western lineage of the *O. catherinae* complex as *Oecomys* sp. nov. .

580 The description of *Oecomys* sp. nov. in this report increases the richness within the
581 genus from 18 (Pardiñas et al. 2017; Rocha et al. 2018) to 19 species in *Oecomys*. This, allied
582 with the restriction of the *O. catherinae* complex to the eastern, central, northern, and
583 westernmost, lineages, partially reduces the taxonomic intricacies of this complex. Regarding
584 the four lineages of the *O. catherinae* complex *s. s.*, our results showed that they are
585 morphologically similar, and data from the literature show they present low diploid number
586 variation ($2n = 60$ and 62). Among them, the westernmost lineage is that with highest genetic
587 divergence (from 3.99 – 4.66%). Similar results were found by Suárez-Villota et al. (2018) in
588 their analyses using *Cytb* only and a concatenated dataset of *Cytb* and two nuclear markers.

589 Specimens of westernmost lineage are rare in collections (we have examined only
590 eight, some of which are young), and collecting more individuals is important for better

591 evaluating whether this lineage merits consideration as a species. Finally, the relationships
592 among the eastern, central, and northern, lineages still are inconclusive based on our results,
593 corroborating the findings of Suárez-Villota et al. (2018). Further phylogenetic studies with a
594 greater number of genetic markers are required to determine how diversification of these
595 lineages took place.

596 ACKNOWLEDGMENTS

597 We thank the curators, technicians, and staff who gave us access to the specimens in
598 zoological collections and made this study possible, namely: Juliana Gualda and Ismael P. de
599 Jesus from Museu de Zoologia da Universidade de São Paulo; João Alves de Oliveira from
600 Museu Nacional da Universidade Federal do Rio de Janeiro; Alexandra Maria Ramos Bezerra
601 from Museu Paraense Emílio Goeldi; and Manoel Santos-Filho from Universidade do Estado
602 de Mato Grosso. We thank the Fundação de Amparo à Pesquisa do Estado de Mato Grosso
603 (FAPEMAT, processo #477017/2011) and the Programa de Capacitação em Taxonomia
604 (PROTAX II - Edital nº 001/2015) for financial support. This study also was financed in part
605 by the Coordenação de Aperfeiçoamento de Pessoal de Nível Superior - Brasil (CAPES) -
606 Finance Code 001. Finally, we thank Ulyses F.J. Pardiñas and three other referees for
607 improving this manuscript.

608 SUPPLEMENTARY DATA

609 **Supplementary Data SD1.**—List of specimens of *Oecomys* analyzed in the present study.

610 **Supplementary Data SD2.**—Bayesian inference topology based on the nuclear intron 7 β -
611 fibrinogen dataset.

612 **Supplementary Data SD3.**—Quantitative morphological analyses of the *Oecomys*
613 *catherinae* complex *lato sensu*.

LITERATURE CITED

- 614
- 615 BOUCKAERT, R., ET AL. 2014. BEAST 2: A Software Platform for Bayesian Evolutionary
616 Analysis. PLoS Computational Biology 10:e1003537.
- 617 BRANDÃO, M. V., ET AL. 2019. Mammals of Mato Grosso, Brazil: annotated species list and
618 historical review. Mastozoología Neotropical 26:263–307.
- 619 CARLETON, M. D., AND G. G. MUSSER. 1995. Systematic studies of Oryzomyine rodents
620 (Muridae: Sigmodontinae): definition and distribution of *Olygoryzomys vegetus*
621 (Bangs, 1902). Proceedings of the biological society of Washington 108:338–369.
- 622 CARLETON, M. D., AND G. G. MUSSER. 2015. Genus *Oecomys* Thomas, 1906. Pp 393–417 in
623 Mammals of South America. Volume 2. Rodents (J. Patton, U.F.J Pardiñas, and G.
624 D’Elía, eds.). University of Chicago Press. Chicago, Illinois.
- 625 CARLETON, M. D., L. H. EMMONS, AND G. G. MUSSER. 2009. A new species of the rodent
626 genus *Oecomys* (Cricetidae: Sigmodontinae: Oryzomyini) from eastern Bolivia, with
627 emended definitions of *O. concolor* (Wagner) and *O. mamorae* (Thomes). American
628 Museum Novitates 3661:1–32.
- 629 CARSTENS, B. C., T. A. PELLETIER, N. M. REID, AND J. D. SATLER. 2013. How to fail at species
630 delimitation. Molecular Ecology 22:4369–4383.
- 631 D’ELÍA, G., P. H. FABRE, AND E. P. LESSA. 2019. Rodent systematics in an age of discovery:
632 recent advances and prospects. Journal of Mammalogy 100:852–871.
- 633 DARRIBA, D., G. L. TABOADA, R. DOALLO, AND D. POSADA. 2012. jModelTest 2: more
634 models, new heuristics and parallel computing. Nature Methods 9:772.
- 635 DESPRÉS, L. 2019. One, two or more species? Mitonuclear discordance and species
636 delimitation. Molecular Ecology 28:3845–3847.

- 637 DI-NIZO, C. B., K. R. S. BANCI, Y. SATO-KUWABARA, AND M. J. J. SILVA. 2017. Advances in
638 cytogenetics of Brazilian rodents: cytotaxonomy, chromosome evolution and new
639 karyotypic data. *comparative Cytogenetics* 11: 833–892.
- 640 DRUMMOND, A. J., M. A. SUCHARD, D. XIE, AND A. RAMBAUT. 2012. Bayesian phylogenetics
641 with BEAUti and the BEAST 1.7. *Molecular Biology and Evolution* 29:1969–1973.
- 642 FISCHER, G. 1817. *Adversaria zoologica. Fasciculus primus. Quaedam ad Mammalium*
643 *systema et genera illustranda. Mémoires de la Société Impériale des Naturalistes de*
644 *Moscou* 5:357– 446 [error for 428], 2 pls.
- 645 FLORES, T.A. 2010. Diversidade morfológica e molecular do gênero *Oecomys* Thomas, 1906
646 (Rodentia: Cricetidae) na Amazônia oriental brasileira. M.S. dissertation,
647 Universidade Federal do Pará. Belém, Brazil.
- 648 FUJISAWA, T., AND T. G. BARRACLOUGH. 2013. Delimiting species using single-locus data
649 and the generalized mixed yule coalescent approach: a revised method and evaluation
650 on simulated data sets. *Systematic Biology* 62:707–724.
- 651 HALL, T. A. 1999. BioEdit: A user-friendly biological sequence alignment editor and analysis
652 program for Windows 85/98/NT. *Nucleic Acids Symposium Series* 41:95–98.
- 653 HERSHKOVITZ, P. 1962. Evolution of Neotropical cricetine rodents (Muridae) with special
654 reference to the phyllotine group. *Fieldiana: Zoology* 46:1–524.
- 655 IBM CORPORATION. 2013. IBM SPSS statistics for windows, version 22.0. IBM Corporation.
656 Armonk, New York.
- 657 JÚNIOR, R. G., ET AL. 2016. Intense genomic reorganization in the genus *Oecomys* (Rodentia,
658 Sigmodontinae): comparison between DNA barcoding and mapping of repetitive
659 elements in three species of the Brazilian Amazon. *Comparative Cytogenetics*
660 10:401–426.

- 661 KUMAR, S., G. STECHER, AND K. TAMURA. 2016. MEGA7: molecular evolutionary genetics
662 analysis version 7.0 for bigger datasets. *Molecular Biology and Evolution* 33:1870–
663 1874.
- 664 LANGGUTH, A., V. MAIA, AND M. MATTEVI. 2005. Karyology of large size Brazilian species
665 of the genus *Oecomys* Thomas, 1906 (Rodentia, Muridae, Sigmodontinae). *Arquivos*
666 *do Museu Nacional de Rio de Janeiro* 63:183–190.
- 667 MALCHER, M. S., ET AL. 2017. *Oecomys catherinae* (Sigmodontinae, Cricetidae): Evidence for
668 chromosomal speciation? *PLoS ONE* 12: e0181434.
- 669 MILLER, M. A., W. PFEIFFER, AND T. SCHWARTZ. 2010. Creating the CIPRES Science
670 Gateway for inference of large phylogenetic trees. Pp. 1–8 in *Proceedings of the*
671 *Gateway Computing Environments Workshop (GCE)*, New Orleans, Louisiana, 14
672 November 2010. Institute of Electrical and Electronics Engineers. Piscataway, New
673 Jersey.
- 674 MUSSER, G. G., AND M. D. CARLETON. 1993. Superfamily Muroidea. Pp. 501–755. in
675 *Mammal Species of the World: a taxonomic and geographic reference*. 2nd ed. (D.E.
676 Wilson, and D.M. Reeder, eds). Smithsonian Institution Press. Washington, D.C.
- 677 MUSSER, G. G., AND M. D. CARLETON. 2005. Superfamily Muroidea. Pp. 894–1531 in
678 *Mammal Species of the World: a taxonomic and geographic reference*. 3rd ed. (D.E.
679 Wilson and D.M. Reeder, eds). Johns Hopkins University Press. Baltimore,
680 Maryland.
- 681 PARDIÑAS, U. F. J., P. TETA, J. SALAZAR–BRAVO, P. MYERS, AND C. A. GALLIARI. 2016. A
682 new species of arboreal rat, genus *Oecomys* (Rodentia, Cricetidae) from Chaco.
683 *Journal of Mammalogy* 97:1177–1196.

- 684 PARDIÑAS, U., ET AL. 2017. Species Accounts of Cricetidae. Pp. 281–535 in Handbook of
685 mammals of the world, Vol.7, Rodents II (D.E. Wilson, T.E. Lacher, R.A.
686 Mittermeier eds.). Lynx Edicions. Barcelona, Spain.
- 687 PATTON, J. L., M. N. F. DA SILVA, AND J. R. MALCOLM. 2000. Mammals of the rio Juruá and
688 the evolutionary and ecological diversification of Amazonia. Bulletin of the
689 American Museum of Natural History 244:1–306.
- 690 PERCEQUILLO, A. R. 1998. Sistemática de *Oryzomys* Baird, 1858 do leste do Brazil
691 (Muroidea: Sigmodontinae). Volume II – Tabelas e Figuras. M.S. thesis,
692 Universidade Federal de São Paulo. São Paulo, Brazil.
- 693 PIRES, C., F. GUDINHO, AND M. WEKSLER. 2016. Morfologia dentária de gêneros de
694 Sigmodontinae (Rodentia: Cricetidae) com ocorrência no Cerrado brasileiro. Boletim
695 da Sociedade Brasileira de Mastozoologia 75:1–32.
- 696 RAMBAUT, A. 2016. Tree figure drawing Tool. v1.4.3. Institute of Evolutionary Biology,
697 University of Edinburgh: <http://tree.bio.ed.ac.uk/software/figtree>.
- 698 RAMBAUT, A., M. SUCHARD, AND A. J. DRUMMOND. 2014. Tracer v1.6: MCMC Trace
699 Analysis Package. Institute of Evolutionary Biology, University of Edinburgh:
700 <http://tree.bio.ed.ac.uk/software/tracer>.
- 701 REIG, O. A. 1977. A proposed unified nomenclature for the enamelled components of the
702 molar teeth of the Cricetidae (Rodentia). Journal of Zoology (London) 181:227–241.
- 703 ROCHA, R. G., C. FONSECA, Z. ZHOU, Y. L. R. LEITE, AND L. P. COSTA. 2012. Taxonomic and
704 conservation status of the elusive *Oecomys cleberi* (Rodentia, Sigmodontinae) from
705 central Brazil. Mammalian Biology 77:414–419.
- 706 ROCHA, R. G., ET AL. 2011. Small mammals of the mid–Araguaia River in central Brazil, with
707 the description of a new species of climbing rat. Zootaxa 2789:1–34.

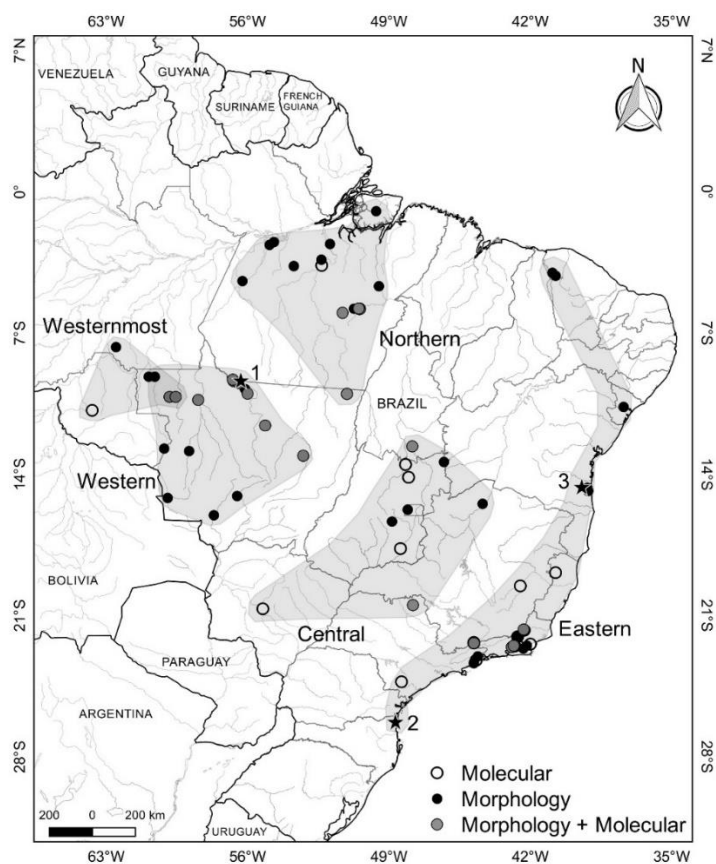
- 708 ROCHA, R. G., ET AL. 2018. Cryptic diversity in the *Oecomys roberti* complex: revalidation of
709 *Oecomys tapajinus* (Rodentia, Cricetidae). *Journal of Mammalogy* 99:174–186.
- 710 RONQUIST, F., ET AL. 2012. MrBayes 3.2: efficient Bayesian phylogenetic inference and
711 model choice across a large model space. *Systematic Biology* 61:539–542.
- 712 SALDANHA, J., D. C. FERREIRA, V. F. DA SILVA, M. SANTOS–FILHO, A. C. MENDES–OLIVEIRA,
713 AND R. V. ROSSI. 2019. Genetic diversity of *Oecomys* (Rodentia, Sigmodontinae)
714 from the Tapajós River basin and the role of rivers as barriers for the genus in the
715 region. *Mammalian Biology* 97:41–49.
- 716 SIKES, R. S., W. L. GANNON, AND THE ANIMAL CARE AND USE COMMITTEE OF THE AMERICAN
717 SOCIETY OF MAMMALOGISTS. 2011. Guidelines of the American Society of
718 Mammalogists for the use of wild mammals in research. *Journal of Mammalogy*
719 92:235–253.
- 720 SOKAL, R. L., AND F. J. ROHLF. 1981. *Biometry*. 2nd ed. W. H. Freeman and Company. New
721 York, New York.
- 722 SUÁREZ-VILLOTA, E. Y., A. P. CARMIGNOTTO, M. V. BRANDÃO, A. R. PERCEQUILLO, AND M.
723 J. J. SILVA. 2018. Systematics of the genus *Oecomys* (Sigmodontinae: Oryzomyini):
724 molecular phylogenetic, cytogenetic and morphological approaches reveal cryptic
725 species. *Zoological Journal of The Linnean Society* 184:182–210.
- 726 SUKUMARAN, J., AND M. T. HOLDER. 2010. DendroPy: a Python library for phylogenetic
727 computing. *Bioinformatics* 26:1569–1571.
- 728 THOMAS, O. 1906. Notes on South-American rodents. *Annals and Magazine of Natural*
729 *History*, 7th Series 18:442–48.
- 730 THOMAS, O. 1909. New species of *Oecomys* and *Marmosa* of Amazonia. *Annals and*
731 *Magazine of Natural History*, 8th Series 3:378–380.

- 732 VORONTSOV, N. N. 1959. The system of hamster (Cricetinae) in the sphere of the world fauna
733 and their phylogenetic relations. The system of hamster (Cricetinae) in the sphere of
734 the world fauna and their phylogenetic relations. Byulleten' Moskovskogo
735 Obshchestva Ispytatelei Prirody. Otdel Biologicheskii, Moscow 64:134–37. [In
736 Russian].
- 737 VOSS, R. S., AND L. H. EMMONS. 1996. Mammalian diversity in neotropical lowland
738 rainforests: a preliminary assessment. Bulletin of the American Museum of Natural
739 History 215: 1–115.
- 740 VOSS, R. S. 1988. Systematics and ecology of ichthyomyine rodents (Muroidea): patterns of
741 morphological evolution in a small adaptive radiation. Bulletin of the American
742 Museum of Natural History 188:259–493.
- 743 VOSS, R. S., AND M. D. CARLETON. 1993. New genus for *Hesperomys molitor* Winge and
744 *Holochilus magnus* Hershkovitz (Mammalia, Muridae) with an analysis of its
745 phylogenetic relationships. American Museum Novitates 3085:1–39.
- 746 VOSS, R. S., D. P. LUNDE, AND N. B. SIMMONS. 2001. The mammals of Paracou, French
747 Guiana: a Neotropical lowland rainforest fauna, part 2. Nonvolant species. Bulletin of
748 the American Museum of Natural History 263:1–236.
- 749 WAGNER, J. A. 1843. Die Säugthiere in Abbildungen nach der Natur mit Beschreibungen von
750 Dr. Johann Christian Daniel von Schreber. Supplementband. Vol. 3: Die Beutelhthiere
751 und Nager (erster Abschnitt). Expedition das Schreber'schen Säugthier und des
752 Esper'schen Schmetterlingswerkes, und in Commission der Voß'schen
753 Buchhandlung in Leipzig. Erlangen, Germany.

- 754 WEKSLER, M. 2006. Phylogenetic relationships of Oryzomine rodents (Muroidea:
 755 Sigmodontinae): separate and combined analyses of morphological and molecular
 756 data. *Bulletin of the American Museum of Natural History* 296:1–149.
- 757 ZHANG, J., P. KAPLI, P. PAVLIDIS, AND A. STAMATAKIS. 2013. A general species delimitation
 758 method with applications to phylogenetic placements. *Bioinformatics* 29:2869–2876.
- 759 ZWICKL, D. J. 2006. Genetic algorithm approaches for the phylogenetic analysis of large
 760 biological sequence datasets under the maximum likelihood criterion. Ph.D.
 761 dissertation, The University of Texas at Austin. Austin, Texas.

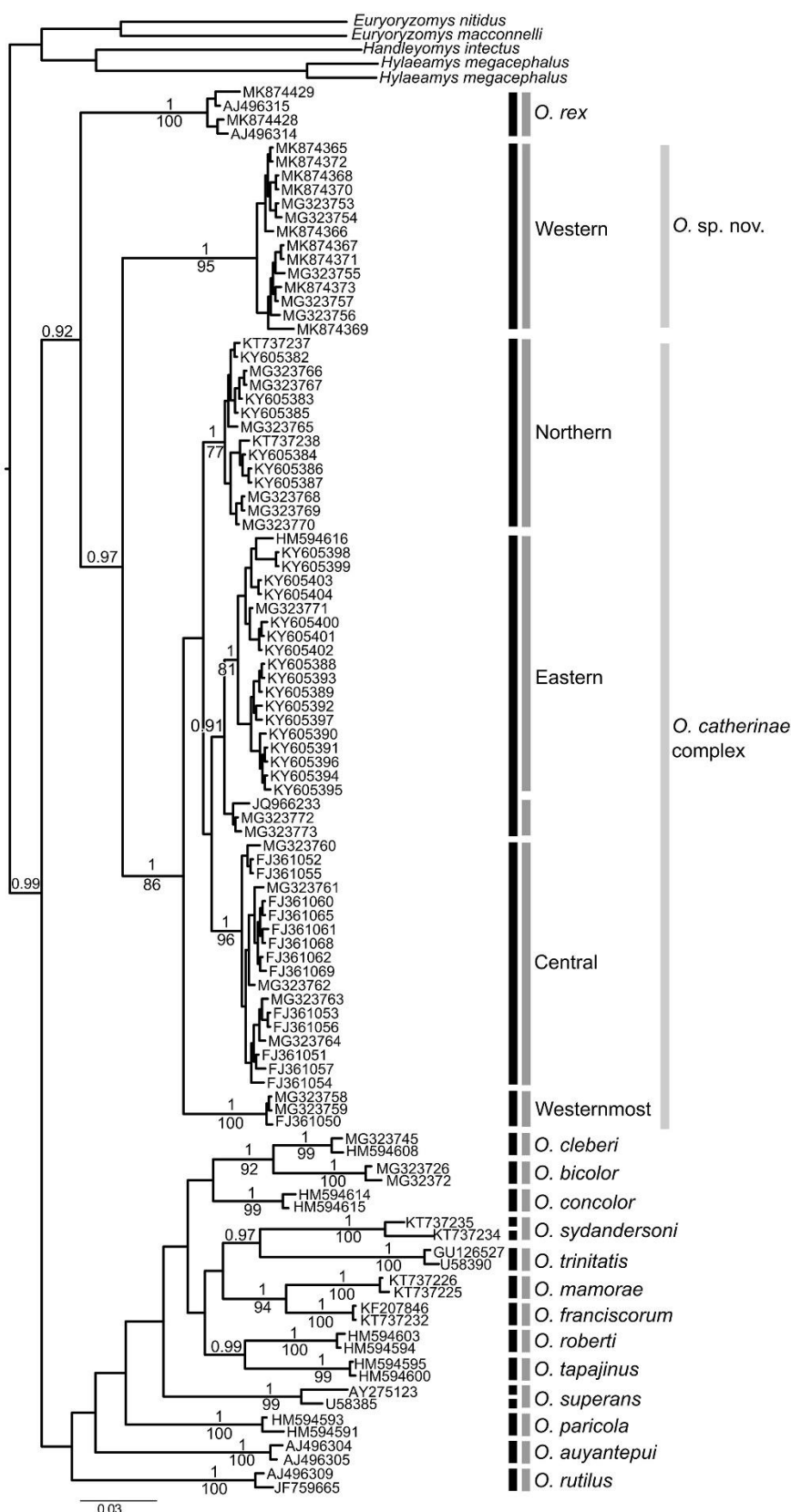
762

FIGURES



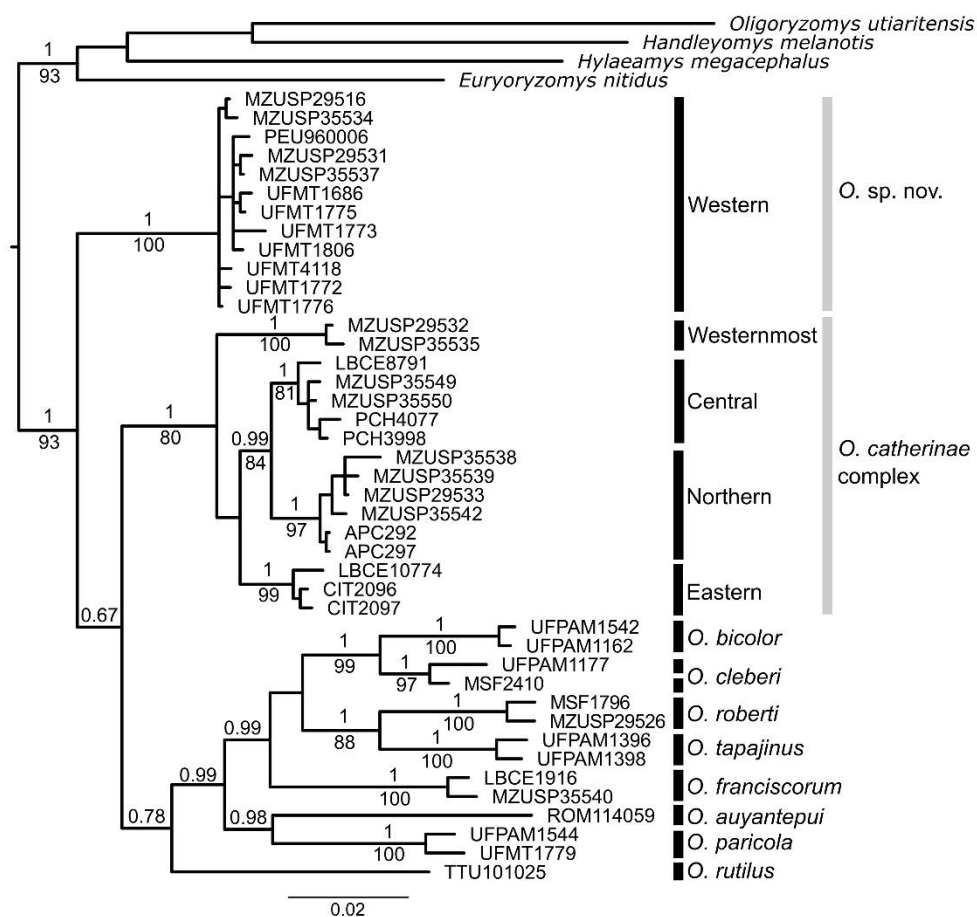
763

- 764 **Fig. 1.**—Map of samples of the *Oecomys catherinae* complex *s. l.* included in this study, with
 765 discrimination of the lineages recognized for the complex. Stars indicate the type localities of
 766 *Oecomys* sp. nov. (1; western lineage), *Oecomys catherinae* (51), and *Oryzomys concolor*
 767 *bahiensis* (39).



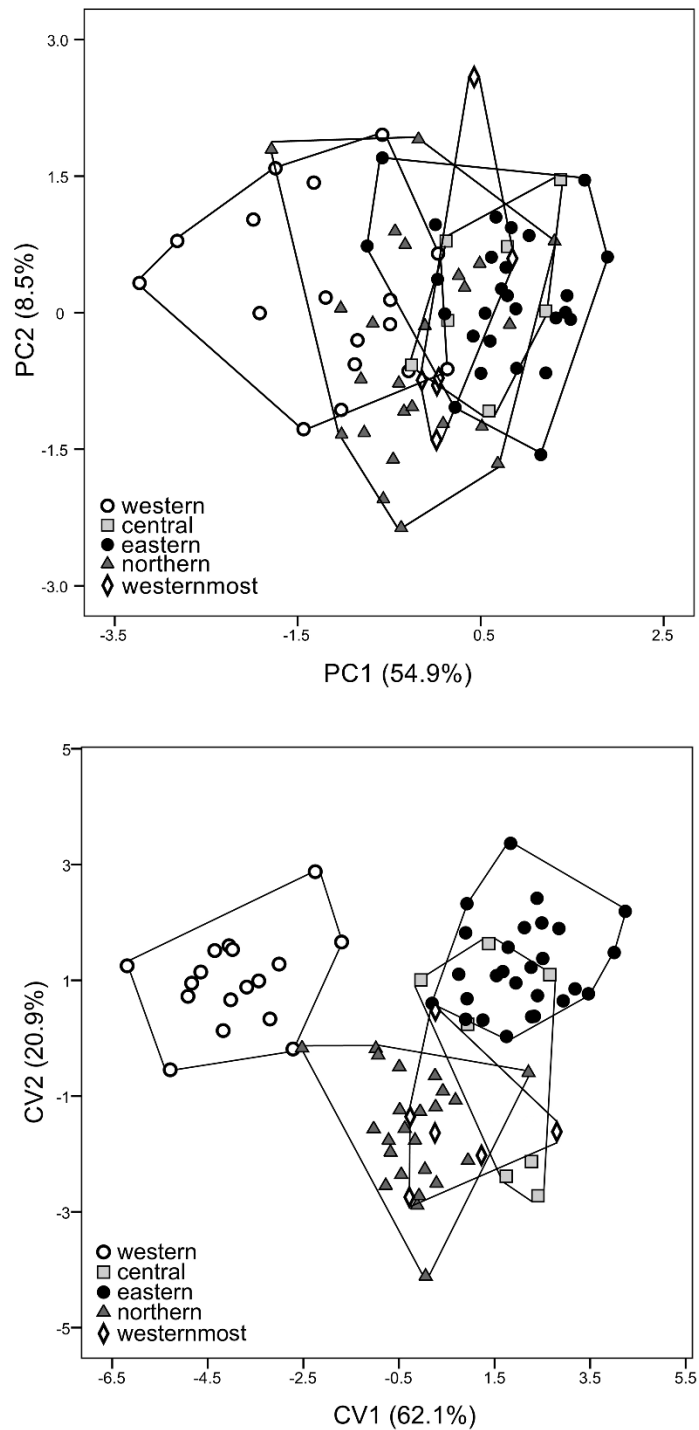
768
769 **Fig. 2.**—Bayesian Inference topology based on mitochondrial Cytochrome b gene. Numbers
770 above the branches indicate bayesian posterior probabilities and below the branches indicate

771 maximum likelihood bootstrap values. Side bars indicate evolutionary lineages recognized in
 772 bPTP (black) and GMYC (medium gray) analyses. The light gray side bars indicate *Oecomys*
 773 sp. nov. and the *Oecomys catherinae* complex s.s. recognized in this study. The sample data
 774 are presented in Supplementary Data S1.



775
 776 **Fig. 3.**—Bayesian Inference topology based on the mitochondrial Cytochrome b gene and
 777 nuclear intron 7 β -fibrinogen concatenated. Numbers above the branches indicate bayesian
 778 posterior probabilities and below the branches indicate maximum likelihood bootstrap values.
 779 The black side bars indicate evolutionary lineages recognized in the analysis of bPTP and the
 780 light gray bars indicate *Oecomys* sp. nov. and the *Oecomys catherinae* complex recognized in
 781 this study. Sample data is provided in Supplementary Data S1.

782



783

784 **Fig. 4.**—Scatterplot of principal components 1 and 2 of Principal Component Analysis (top)

785 and of canonical variate 1 and 2 of Discriminant Analysis (bottom) of 31 craniodental

786 measurements of the *Oecomys catherinae* complex *s. l.* The western lineage corresponds to787 *Oecomys* sp. nov. described in this study.



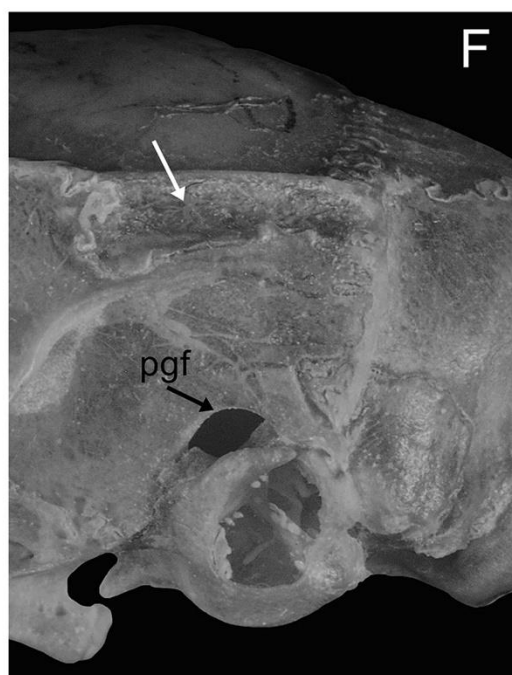
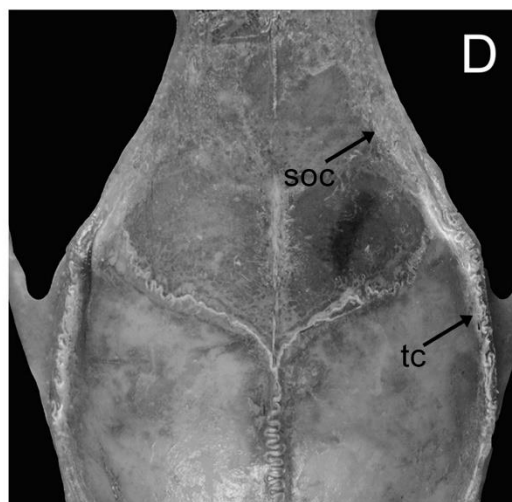
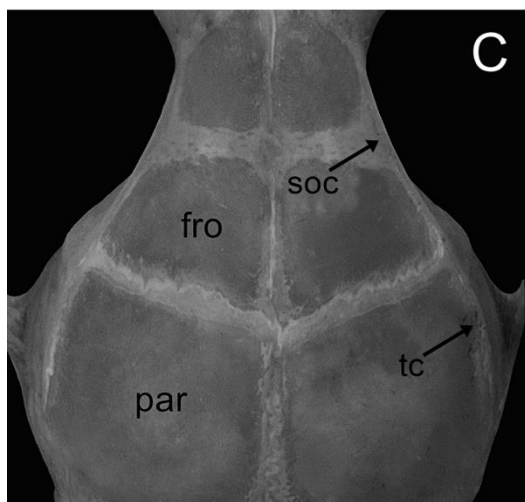
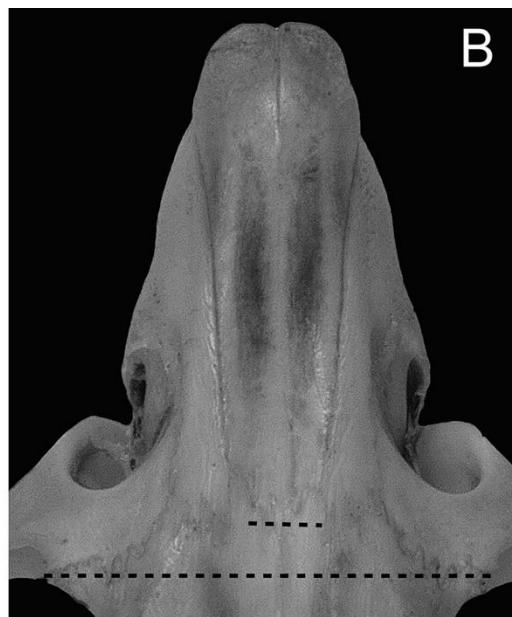
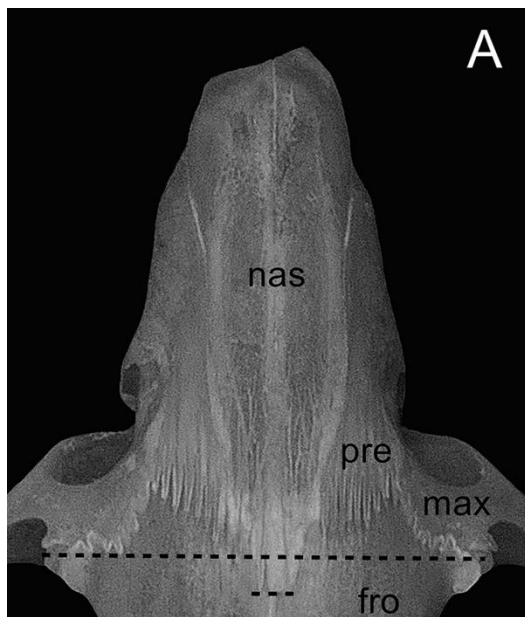
788

789 **Fig. 5.**—Dorsal view (above) and ventral view (below) of: A) the holotype of *Oecomys* sp.
 790 nov. (UFMT 4118), and specimens of the *Oecomys catherinae* complex lineages: B) eastern
 791 (MN 10748), C) central (PCH 4077), D) westernmost (APC 292), and E) northern (MZUSP
 792 35535 above, and MZUSP 29532 below).



793

794 **Fig. 6.**—Dorsal, ventral and lateral views of skull and lateral view of mandible of the
795 holotype (UFMT 4118) of *Oecomys* sp. nov. from Estância Santa Clara, Alta Floresta, Mato
796 Grosso state, Brazil. Scale: 5 mm.



798 **Fig. 7.**—Anatomical traits that differentiate *Oecomys* sp. nov. (UFMT 4118) from the *O.*
799 *catherinae* complex lineages: A) posterior nasal terminus (shorter dashed line) surpassing the
800 maxillary-frontal suture (longer dashed line) and the premaxillaries terminating anterior to the
801 nasal in *Oecomys* sp. nov. ; B) posterior nasal terminus (shorter dashed line) anterior to the
802 maxillary-frontal suture (longer dashed line) and the premaxillaries aligned to the posterior
803 margin of the nasals in *O. catherinae* (BNMH 9.11.19.24); C) supraorbital and temporal
804 crests poorly developed in *Oecomys* sp. nov. ; D) supraorbital crest dorsolaterally expanded in
805 *O. catherinae* northern lineage (MPEG 39899), being more developed than temporal crest; E)
806 subsquamosal fenestra present, always smaller than postglenoid foramen, and parietal slightly
807 expanded below the lateral edges of the dorsum of the braincase (white arrow) in *Oecomys* sp.
808 nov. ; F) subsquamosal fenestra ossified and parietal deeply expanded onto the lateral surface
809 of the braincase (white arrow) in *O. catherinae* northern lineage (MPEG 39899).
810 Abbreviations: exo, exoccipital; fro, frontal; ip, interparietal; mas, mastoid; max, maxillary;
811 nas, nasal; par, parietal; pgf, postglenoid foramen; pre, premaxillary; soc, supraorbital crest;
812 sq, squamosal; ssf, subsquamosal fenestra; tc, temporal crest.



813
814 **Fig. 8.**—Paratype of *Oecomys* sp. nov. from Teles Pires Hydroelectric Power Plant, Paranaíta
815 municipality, Mato Grosso state, Brazil (UFMT 1680): upper molar series (left) and lower
816 molar series (right). Abbreviation: ac, anterior cingulum.

817

TABLES

818

Table 1.—Uncorrected p-distances of the Cytochrome b within and among *Oecomys* species. Eastern, central, northern, western, and

819

westernmost, correspond to lineages in the *Oecomys catherinae* complex *sensu lato*. Values above diagonal correspond to standard deviation and

820

bold numbers to genetic distance within clades. Values in percentage.

		1	2	3	4	5	6	7	8	9	10	11	12	13	14	15	16	17	18	19
1	Western*	0.77	1.27	1.22	1.25	1.47	1.46	1.42	1.34	1.29	1.38	1.50	1.48	1.43	1.50	1.34	1.41	1.38	1.38	1.41
2	Central	7.38	0.24	0.57	0.66	1.04	1.42	1.41	1.48	1.45	1.58	1.64	1.53	1.55	1.58	1.47	1.53	1.52	1.51	1.42
3	Eastern	6.97	1.76	0.88	0.49	1.05	1.34	1.37	1.43	1.39	1.51	1.55	1.51	1.49	1.53	1.43	1.46	1.48	1.47	1.34
4	Northern	7.16	1.85	1.38	0.34	1.15	1.36	1.41	1.47	1.44	1.56	1.56	1.52	1.56	1.60	1.48	1.49	1.54	1.51	1.38
5	Westernmost	8.75	3.99	4.14	4.66	0	1.42	1.67	1.57	1.58	1.66	1.68	1.67	1.56	1.50	1.62	1.55	1.70	1.64	1.39
6	<i>O. auyantepui</i>	9.37	8.48	7.59	7.87	8.08	0.6	1.51	1.46	1.42	1.49	1.49	1.47	1.43	1.55	1.46	1.54	1.59	1.54	1.36
7	<i>O. bicolor</i>	8.30	8.97	8.83	8.92	11.53	9.43	0.3	1.01	1.35	1.36	1.34	1.53	1.48	1.52	1.34	1.60	1.32	1.33	1.60
8	<i>O. cleberi</i>	7.89	9.41	9.00	9.37	10.18	8.08	4.34	0.6	1.28	1.29	1.44	1.50	1.35	1.52	1.27	1.57	1.27	1.42	1.60
9	<i>O. concolor</i>	7.36	8.53	8.11	8.19	9.43	7.93	6.89	6.44	0.3	1.15	1.41	1.43	1.24	1.53	1.34	1.38	1.39	1.35	1.51
10	<i>O. franciscorum</i>	8.08	10.31	9.62	9.75	10.78	9.88	7.34	6.89	5.24	0	1.26	1.43	1.35	1.57	1.41	1.40	1.40	1.51	1.61
11	<i>O. mamorae</i>	9.56	11.44	10.41	10.35	11.98	9.88	7.63	8.68	7.63	5.69	0	1.56	1.45	1.55	1.38	1.53	1.51	1.47	1.63
12	<i>O. paricola</i>	9.64	9.71	9.77	9.67	11.08	8.98	9.43	8.68	8.83	8.08	10.48	1.2	1.41	1.66	1.32	1.38	1.49	1.52	1.62
13	<i>O. roberti</i>	8.79	9.12	9.09	9.24	9.28	8.23	8.53	7.56	5.99	6.74	8.23	7.78	0.3	1.45	1.41	1.36	1.36	1.39	1.63
14	<i>O. rutilus</i>	10.29	10.84	10.45	10.86	9.58	9.88	9.43	9.13	9.88	10.78	11.08	11.38	9.13	1.2	1.50	1.62	1.61	1.69	1.55
15	<i>O. superans</i>	8.02	9.55	9.32	9.39	10.93	9.13	8.08	7.49	7.78	8.23	8.08	7.19	7.49	9.88	1.5	1.45	1.38	1.31	1.43
16	<i>O. sydandersoni</i>	8.90	9.86	9.35	9.39	10.03	9.43	9.88	9.73	7.49	6.74	9.13	7.86	7.04	11.83	8.68	0.3	1.54	1.46	1.67
17	<i>O. tapajinus</i>	7.78	9.68	9.59	9.75	11.98	10.78	6.74	6.89	7.34	6.89	8.38	9.43	6.74	11.38	7.78	8.83	0	1.48	1.63
18	<i>O. trinitatis</i>	7.87	8.98	9.09	9.24	10.48	9.58	7.34	8.38	7.34	9.58	8.98	9.43	7.49	12.28	7.34	8.83	8.98	0	1.66
19	<i>O. rex</i>	8.19	7.55	7.23	7.06	7.63	7.63	10.63	10.18	8.38	10.63	11.08	10.33	9.58	9.96	8.23	11.08	10.48	10.03	0.5
20	Outgroup	12.45	14.17	13.60	13.67	14.13	12.66	13.62	13.14	13.14	13.53	13.23	14.31	12.66	14.55	13.98	13.98	13.29	14.19	14.07

821

* Referred as *Oecomys* aff. *catherinae* by Saldanha et al. (2019). Named as *Oecomys* sp. nov. in this report.

822 **Table 2.**—External, cranial and dental measurements (in mm) and weight (in grams) of adult specimens of *Oecomys* sp. nov. and lineages of the
 823 *Oecomys catherinae* complex *stricto sensu*. See “Material and Methods” section for abbreviations.

	<i>Oecomys</i> sp. nov.	<i>Oecomys catherinae</i> complex <i>stricto sensu</i>				<i>Oecomys catherinae</i>
		Eastern	Central	Northern	Westernmost	
		Mean \pm SD Min.–Max. (N)	Mean \pm SD Min.–Max. (N)	Mean \pm SD Min.–Max. (N)	Mean \pm SD Min.–Max. (N)	
HBL	111.46 \pm 14.84 85–135 (23)	131.69 \pm 11.16 105–151 (26)	129 \pm 13.65 112–150 (6)	123.64 \pm 12.08 103–146 (18)	126.43 \pm 6.9 120–140 (7)	132
TL	130.27 \pm 15.68 106–160 (23)	157.08 \pm 10.73 138–180 (25)	144.67 \pm 8.36 131–155 (6)	138.89 \pm 10.36 121–154 (18)	141.57 \pm 16.45 115–161 (7)	166
HFL	25.19 \pm 1.52 21–27.04 (23)	28.46 \pm 3.61 23–38 (25)	26.33 \pm 3.78 20–31 (6)	26.47 \pm 1.72 22–30 (18)	27.86 \pm 1.21 26–29 (7)	30
Ear	16.64 \pm 2.32 12–21 (23)	18.29 \pm 2.89 12–24 (26)	16.67 \pm 3.39 11–20 (6)	17.65 \pm 1.5 15–20 (17)	18.36 \pm 1.55 15–19.5 (7)	20
Weight	40.37 \pm 12.37 22–63 (23)	73.63 \pm 19.55 33–110.7 (23)	51.67 \pm 2.89 50–55 (3)	58.69 \pm 14.11 35–90 (16)	72.2 \pm 13.79 54–90 (5)	-
BB	4.69 \pm 0.25 4.35–5.05 (15)	5.26 \pm 0.29 4.52–5.68 (27)	5.20 \pm 0.20 4.96–5.46 (7)	4.98 \pm 0.30 4.33–5.62 (24)	4.93 \pm 0.15 4.70–5.18 (6)	4.52
BH	8.44 \pm 0.53 7.62–9.61 (15)	9.07 \pm 0.37 8.53–9.89 (28)	9.33 \pm 0.32 8.89–9.81 (7)	8.71 \pm 0.34 7.97–9.49 (24)	8.86 \pm 0.17 8.60–9.10 (7)	8.84
BI	1.59 \pm 0.16 1.30–1.86 (16)	1.91 \pm 0.21 1.63–2.74 (27)	1.83 \pm 0.15 1.62–2.07 (7)	1.80 \pm 0.17 1.47–2.28 (24)	1.81 \pm 0.09 1.72–1.98 (7)	2.74
BIF	2.30 \pm 0.26 1.94–2.70 (16)	2.54 \pm 0.20 2.04–2.94 (28)	2.47 \pm 0.16 2.19–2.65 (7)	2.27 \pm 0.21 1.74–2.77 (24)	2.46 \pm 0.17 2.34–2.83 (7)	2.65
BIP	9.45 \pm 0.59 8.08–10.17 (16)	10.11 \pm 0.52 8.62–10.89 (27)	10.03 \pm 0.36 9.47–10.56 (7)	9.79 \pm 0.35 9.27–10.42 (24)	9.98 \pm 0.63 9.20–10.92 (7)	8.62

	<i>Oecomys</i> sp. nov.	<i>Oecomys catherinae</i> complex <i>stricto sensu</i>				<i>Oecomys catherinae</i>
		Eastern	Central	Northern	Westernmost	
		Mean \pm SD Min.–Max. (N)	Mean \pm SD Min.–Max. (N)	Mean \pm SD Min.–Max. (N)	Mean \pm SD Min.–Max. (N)	
BM1	1.44 \pm 0.14 1.32–1.76 (16)	1.47 \pm 0.06 1.36–1.61 (28)	1.46 \pm 0.10 1.34–1.61 (7)	1.43 \pm 0.11 1.21–1.72 (24)	1.45 \pm 0.11 1.32–1.66 (7)	1.46
Bm1	1.27 \pm 0.07 1.18–1.42 (16)	1.35 \pm 0.08 1.12–1.52 (28)	1.37 \pm 0.09 1.24–1.53 (7)	1.27 \pm 0.08 1.12–1.40 (24)	1.32 \pm 0.08 1.23–1.46 (7)	1.28
BN	3.63 \pm 0.33 2.83–4.32 (16)	4.02 \pm 0.31 3.42–4.61 (27)	3.96 \pm 0.23 3.60–4.26 (7)	3.74 \pm 0.25 3.36–4.29 (24)	3.80 \pm 0.22 3.50–4.02 (7)	-
BOC	6.46 \pm 0.24 5.99–6.97 (15)	7.12 \pm 0.28 6.47–7.58 (28)	7.13 \pm 0.21 6.70–7.40 (7)	6.89 \pm 0.23 6.50–7.31 (23)	6.89 \pm 0.28 6.50–7.25 (7)	7.43
BRP	4.79 \pm 0.29 4.40–5.52 (16)	5.46 \pm 0.41 4.61–6.19 (28)	5.00 \pm 0.38 4.30–5.50 (7)	5.16 \pm 0.28 4.72–5.67 (24)	5.34 \pm 0.30 4.95–5.83 (7)	6.13
BR	4.70 \pm 0.25 4.18–5.00 (16)	5.07 \pm 0.40 4.00–5.67 (28)	5.13 \pm 0.32 4.65–5.47 (7)	4.93 \pm 0.30 4.20–5.54 (24)	5.25 \pm 0.32 4.93–5.85 (7)	5.18
BZP	3.07 \pm 0.36 2.45–3.70 (16)	3.66 \pm 0.23 3.21–4.21 (27)	3.64 \pm 0.20 3.37–3.87 (7)	3.42 \pm 0.27 2.85–3.93 (24)	3.40 \pm 0.51 2.80–4.35 (7)	3.95
CIL	26.82 \pm 1.76 23.49–29.74 (15)	30.19 \pm 1.42 27.07–32.62 (28)	29.94 \pm 0.97 28.80–31.09 (7)	28.54 \pm 1.46 25.73–32.16 (24)	28.94 \pm 0.98 27.35–30.55 (7)	31.04
CLM	4.94 \pm 0.25 4.68–5.46 (16)	5.17 \pm 0.17 4.86–5.57 (28)	5.14 \pm 0.16 4.90–5.33 (7)	4.95 \pm 0.21 4.64–5.34 (24)	5.04 \pm 0.31 4.73–5.62 (7)	5.26
CLLM	5.04 \pm 0.18 4.78–5.50 (16)	5.24 \pm 0.14 4.98–5.52 (28)	5.20 \pm 0.19 5.04–5.48 (7)	5.02 \pm 0.19 4.64–5.37 (24)	5.12 \pm 0.38 4.75–5.91 (7)	5.46
CZL	21.18 \pm 1.46 18.18–23.40 (15)	23.92 \pm 1.04 21.86–25.57 (27)	23.81 \pm 0.78 22.90–24.96 (7)	23.09 \pm 2.24 20.50–32.28 (24)	22.87 \pm 0.81 21.72–24.32 (7)	25.14
LCIB	15.32 \pm 1.06 13.31–17.08 (16)	16.77 \pm 1.15 12.85–18.27 (28)	16.98 \pm 0.35 16.35–17.47 (7)	16.39 \pm 0.87 14.68–18.55 (24)	16.57 \pm 0.62 15.35–17.25 (7)	12.85

	<i>Oecomys</i> sp. nov.	<i>Oecomys catherinae</i> complex <i>stricto sensu</i>				<i>Oecomys catherinae</i>
		Eastern	Central	Northern	Westernmost	
		Mean \pm SD Min.–Max. (N)	Mean \pm SD Min.–Max. (N)	Mean \pm SD Min.–Max. (N)	Mean \pm SD Min.–Max. (N)	
LD	7.25 \pm 0.59 6.24–8.23 (16)	8.21 \pm 0.54 7.00–8.92 (28)	8.13 \pm 0.42 7.48–8.56 (7)	7.73 \pm 0.49 6.58–8.95 (24)	7.95 \pm 0.36 7.44–8.47 (7)	8.50
LIB	5.14 \pm 0.18 4.64–5.34 (16)	5.90 \pm 0.34 5.23–6.52 (28)	5.80 \pm 0.38 5.37–6.35 (7)	5.54 \pm 0.38 5.07–6.54 (24)	5.56 \pm 0.44 4.90–6.04 (7)	6.16
LIF	4.83 \pm 0.445 3.94–5.54 (16)	5.45 \pm 0.44 3.96–6.14 (28)	5.68 \pm 0.34 5.11–6.03 (7)	5.07 \pm 0.34 4.47–5.71 (24)	5.22 \pm 0.22 4.79–5.50 (7)	5.54
LIP	4.13 \pm 0.41 3.54–4.72 (16)	4.77 \pm 0.39 3.78–5.34 (28)	4.71 \pm 0.40 4.26–5.18 (7)	4.30 \pm 0.37 3.45–5.06 (24)	4.36 \pm 0.42 3.97–5.24 (7)	3.78
LLD	3.36 \pm 0.25 2.89–3.70 (16)	3.75 \pm 0.37 3.03–4.43 (27)	3.65 \pm 0.28 3.24–4.03 (7)	3.67 \pm 0.36 2.81–4.36 (24)	3.58 \pm 0.20 3.27–3.80 (7)	4.43
LN	10.67 \pm 1.06 8.29–12.41 (16)	11.39 \pm 0.68 9.93–12.66 (28)	11.21 \pm 0.43 10.51–11.80 (7)	11.23 \pm 0.81 9.41–13.39 (24)	11.47 \pm 0.63 10.60–12.20 (7)	10.91
LPB	6.22 \pm 0.37 5.29–6.83 (16)	6.78 \pm 0.50 5.94–8.01 (28)	6.39 \pm 0.35 5.94–6.89 (7)	6.42 \pm 0.45 5.59–7.81 (24)	6.50 \pm 0.19 6.30–6.88 (7)	7.18
LR	9.46 \pm 0.79 7.77–10.58 (16)	10.32 \pm 0.66 8.54–11.62 (28)	10.39 \pm 0.57 9.68–11.12 (7)	9.90 \pm 0.48 8.74–10.52 (24)	10.16 \pm 0.34 9.86–10.87 (7)	10.80
MB	10.50 \pm 0.41 9.91–11.50 (15)	11.22 \pm 0.37 10.44–11.88 (27)	11.27 \pm 0.38 10.83–11.74 (7)	10.85 \pm 0.39 10.12–11.79 (24)	10.85 \pm 0.22 10.45–11.05 (6)	11.30
MH	7.40 \pm 0.68 6.40–8.60 (16)	8.63 \pm 0.59 7.38–10.06 (28)	8.57 \pm 0.55 7.55–9.34 (7)	8.16 \pm 0.64 6.89–9.53 (24)	8.07 \pm 0.38 7.60–8.74 (7)	8.35
OL	10.54 \pm 0.61 9.50–11.47 (16)	11.61 \pm 0.54 10.00–12.32 (28)	11.63 \pm 0.20 11.42–11.90 (7)	11.31 \pm 0.48 10.32–12.34 (24)	11.45 \pm 0.39 10.82–12.02 (7)	11.66
ONL	29.89 \pm 1.88 26.06–32.21 (15)	33.30 \pm 1.36 30.21–35.77 (27)	33.33 \pm 1.00 32.25–34.67 (7)	31.77 \pm 1.41 28.47–34.90 (24)	32.17 \pm 1.06 30.74–34.22 (7)	-

	<i>Oecomys</i> sp. nov.	<i>Oecomys catherinae</i> complex <i>stricto sensu</i>				<i>Oecomys catherinae</i>
		Eastern	Central	Northern	Westernmost	
	Mean \pm SD	Mean \pm SD	Mean \pm SD	Mean \pm SD	Mean \pm SD	
	Min.–Max. (N)	Min.–Max. (N)	Min.–Max. (N)	Min.–Max. (N)	Min.–Max. (N)	Holotype ^a
ZB	15.48 \pm 0.96 13.70–16.80 (16)	16.94 \pm 0.84 14.93–18.61 (28)	16.79 \pm 0.81 15.85–18.10 (7)	15.97 \pm 1.07 14.29–18.05 (24)	16.34 \pm 0.39 15.84–16.83 (7)	16.41
ZL	13.36 \pm 0.86 11.47–14.59 (16)	15.06 \pm 0.63 13.67–15.88 (27)	15.01 \pm 0.40 14.60–15.60 (7)	14.52 \pm 0.74 12.85–15.77 (24)	14.45 \pm 0.74 13.34–15.46 (7)	-

824 ^aExternal measurements were transcribed from original skin labels.

825 **Table 3.**—External and craniodental character comparisons among *Oecomys* sp. nov. and lineages of the *Oecomys catherinae* complex *stricto*
 826 *sensu* (central, eastern, northern, and westernmost). HBL, head and body length; M1, upper first molar; TL, tail length. See the “Comparisons”
 827 section for comparisons of *Oecomys* sp. nov. with other congeneric species.

	<i>Oecomys</i> sp. nov.	<i>O. catherinae</i> eastern	<i>O. catherinae</i> central	<i>O. catherinae</i> westernmost	<i>O. catherinae</i> northern
TL in relation to HBL	118.28% 103.8–147.62 (23)	119.69% 101.33–132.74 (25)	113.08% 96.67–131.25 (6)	112.21% 88.46–128.8 (7)	113.08% 84.93–136.36 (18)
Dorsal fur color	Gray-based, terminal tips dark reddish-brown, mixed with dark brown	Gray-based, terminal tips reddish-brown, mixed with dark brown	Gray-based, terminal tips reddish-brown, mixed with dark brown	Gray-based, terminal tips reddish-brown, mixed with dark brown	Gray-based, terminal tips reddish-brown, mixed with dark brown
Dorsal body fur length	7–11 mm	12–15 mm	12–14 mm	9–12 mm	9–12 mm
Ventral fur color	Dark cream, gray-based except on throat, neck, forelimbs, and genitalia (self-dark cream)	Cream, gray-based except on ventral midline, throat, neck, and genitalia (self-cream)	Cream, gray-based except ventral midline, throat, neck, and genitalia (self-cream)	Dark cream, inconspicuously gray-based except on throat and neck (self-dark cream)	Dark cream, gray-based except on throat and neck (self-dark cream)
Tail color	Brown, slightly bicolored at the base	Brown	Brown, bicolored at the base	Brown	Brown, slightly bicolored at the base
Tail apical tuft	Absent or poorly developed (< 1 mm)	Poorly developed (< 1 mm)	Absent or poorly developed (< 1 mm)	Absent or poorly developed (< 1 mm)	Poorly developed (< 1 mm)
Rostrum	Narrow and moderately long	Wide and long	Wide and short	Wide and long	Narrow and short

	<i>Oecomys sp. nov.</i>	<i>O. catherinae</i> eastern	<i>O. catherinae</i> central	<i>O. catherinae</i> westernmost	<i>O. catherinae</i> northern
Posterior margin of nasals	Surpassing or aligned to the maxillary-frontal suture	Aligned to the maxillary-frontal suture	Aligned to the maxillary-frontal suture	Aligned to the maxillary-frontal suture	Aligned to the maxillary-frontal suture
Zygomatic plate	Slightly projected previously to the maxillary root	Projected previously to the maxillary root	Projected previously or the same level to the maxillary root	Projected previously to the maxillary root	Projected previously to the maxillary root
Interorbital region	Narrow, anteriorly convergent	Moderate, anteriorly convergent	Narrow, anteriorly convergent	Moderate, anteriorly convergent	Moderate, anteriorly convergent
Supraorbital and temporal crests	Both present and moderately developed	Supraorbital crests dorsolaterally expanded, more developed than temporal crests	Supraorbital crests dorsolaterally expanded, more developed than temporal crests	Supraorbital crests dorsolaterally expanded, more developed than temporal crests	Supraorbital crests dorsolaterally expanded, more developed than temporal crests
Lateral expansion of parietals	Slightly expanded bellow the lateral edges of the dorsum of the braincase	Deeply expanded onto the lateral surface of the braincase	Deeply expanded onto the lateral surface of the braincase	Deeply expanded onto the lateral surface of the braincase	Deeply expanded onto the lateral surface of the braincase
Alisphenoid strut	Usually absent	Usually absent	Absent	Usually absent	Usually absent
Subsquamosal fenestra	Present, smaller than postglenoid foramen	Reduced	Ossified	Reduced	Ossified
Incisive foramina	Oval or drop shaped	Anteriorly convergent	Oval or drop shaped	Parallel or anteriorly convergent	Anteriorly convergent

	<i>Oecomys sp. nov.</i>	<i>O. catherinae</i> eastern	<i>O. catherinae</i> central	<i>O. catherinae</i> westernmost	<i>O. catherinae</i> northern
Posterolateral palatal pits	Conspicuous perforations in deeply depression	Small perforations	Large, in palatal depression	Large, in small palatal depression	Large, in palatal depression
Anterior cingulum of M1	Present	Usually absent	Present	Absent	Absent
Diploid chromosome number (2n) *	54	60	60	60	62

828 * (Suárez-Villota et al. 2018).

829 **APPENDIX I: Specimens examined**

830 Specimens examined are deposited in the following institutions: Museu Nacional
 831 (MN), Rio de Janeiro; Museu de Zoologia da Universidade de São Paulo (MZUSP), São
 832 Paulo; Museu Paraense Emílio Goeldi (MPEG), Belém; Universidade do Estado de Mato
 833 Grosso (Unemat), Cáceres; Universidade Federal de Mato Grosso (UFMT), Cuiabá; and The
 834 Natural Natural History Museum (BNMH), London. The material examined also includes
 835 uncatalogued specimens, such as those collected by Manoel dos Santos Filho (MSF), Robson
 836 Oliveira (RFO), and A. Casagrande (AC), which will be deposited at Unemat. Specimens
 837 collected by Ana Paula Carmignoto (APC) and by several biologists in the Pequena central
 838 Hidrelétrica de São Joaquim da Barra (PCH) will be deposited at MZUSP. Finally, specimens
 839 collected by the Serviço Nacional da Peste (IP) will be deposited at the MN.

840 *Oecomys* sp. nov. (n = 28): Brazil: Mato Grosso: Alta Floresta (1): UFMT 4118 (10°00'25"S,
 841 56°02'17"W); Unemat–MSF 1878 (9°54'12"S, 56°10'15.6"W), Aripuanã (12): MZUSP 29531
 842 (10°10'01"S, 59°27'W); Cáceres (7): Unemat–MSF 1406, 1407, 1411 (16°01'55"S
 843 57°42'24"W); Campos de Julho (9): UFMT 931 (12°51'00"S, 58°56'00"W); Cláudia (4):
 844 MZUSP 35543 (11°34'58"S, 55°10'01"W); Gaúcha do Norte (5): MZUSP 29516 (13°04'58"S,
 845 53°16'58"W); Juruena (11): MZUSP 35537 (10°19'01"S, 58°28'58"W); Paranaíta (2): UFMT
 846 1772, 1773, 1774, 1806 (9°29'06"S, 56°28'19"W); Rosário Oeste (6): Unemat–AC 207, 230,
 847 255, 266 (15°04'45.9"S, 56°33'15.7"W); Vila Bela da Santíssima Trindade (8): Unemat–RFO
 848 013, 027, 029, 040 (15°10'33.6"S, 59°59'38.4"W). Pará: Jacareacanga (3): UFMT 1680
 849 (9°29'06"S, 56°28'19"W), UFMT 1775, 1776, 1686, 1690 (9°18'40"S, 56°46'05"W).
 850 Rondônia: Vilhena (10): MPEG 34224 (12°43'S, 60°7'W).

851 *Oecomys catherinae* complex s.s. (n = 89): Central lineage (n = 11): Brazil: Distrito Federal:
 852 Brasília (31): MN 21996, 22013 (15°45'21"S, 48°06'28"W); Goiás: Anápolis (32): MN4346,
 853 4348 (16°20'37"S 48°53'08"W); São Domingos (28): MZUSP 4012, 4020, MPEG 10901

854 (13°23'36"S 46°18'55"W); São Paulo: São Joaquim da Barra (34): MZUSP-PCH 3998, 4077
855 (20°28'58"S, 47°51'W); Tocantins: Paranã (27): MZUSP 35549, 35550 (12°37'01"S,
856 47°52'58"W). Eastern lineage (n = 41): Brazil: Bahia: Ilhéus (39): MN 9340, 10648, 10691,
857 10724, 10748, 10761, 10792, 10812, 10854, 10882, 10940, 10951, 11212, 11561
858 (14°40'15"S, 39°12'46"W); Ceará: Guaraciaba do norte (37): MN-IP 738 (4°10'04"S,
859 40°46'58"W); São Benedito (36): MN-IP 804, 806, 820, 831 (4°01'19"S, 40°56'31"W); Minas
860 Gerais: Pirapitinga (42): MN 72737 (21°41'28"S, 42°22'05"W); Rio de Janeiro: Cachoeira de
861 Macacu (46): MN 74364, MN 74367 (22°31'S, 42°48'W), MN 74370, 74374 (22°30'S,
862 42°45'W), MN 74371 (22°28'58"S, 42°51'W); Casimiro de Abreu (44): MN 44805
863 (22°29'32"S, 42°12'43"W); Guapimirim (47): MN 74359 (22°34'58"S, 42°57'W), MN 74360
864 (22°33'00"S 42°57'00"W), MN 74369 (22°34'S, 42°54'W); Paraty (48): MN 75261
865 (23°01'30"S, 44°38'13"W); Silva Jardim (45): MN 66137 (22°38'09"S, 42°23'13"W);
866 Sumidouro (43): MN 53616 (22°03'14"S, 42°40'04"W); Santa Catarina: Joinville (51):
867 BMNH 9.11.19.24; Sergipe: Areia Branca (38): MPEG 24553, 24554, 24561, 24562, 24563
868 (10°40'S, 37°25'W); São Paulo: Ubatuba (49): MN 74375, 74376, 74378 (23°19'58"S,
869 44°49'58"W). Northern lineage (n = 29): Brazil: Mato Grosso: Vila Rica (16): MZUSP-APC
870 292, 297, MZUSP 29533, 35538, 35539, 35542 (10°01'01"S, 51°07'01"W); Pará: Altamira
871 (23): MPEG 10913 (3°22'01"S, 52°22'58"W), Altamira (24): MPEG 10251, 10911, 10912
872 (3°41'S, 53°45'W); Belterra: MPEG 15293, 15294 (2°38'S, 54°57'W); Ilha de Marajó (21):
873 MN 2000 (0°57'58"S, 49°40'16"W); Itaituba (26): MN 2001 (4°25.5'S, 56°17.5'W); Marabá
874 (17): MPEG 38898, 38976 (6°S, 51°19'58"W), Marabá (18): UFMT 1294 (5°47'51.8"S
875 50°46'15.3"W), Marabá (19) MPEG 39899, 39900 (5°49'01"S, 50°28'58"W), MPEG 39901,
876 39903, 39909 (5°46'58"S, 50°31'58"W); Novo Repartimento (20): MPEG 10924 (4°41'S,
877 49°32'W); Santarém (25): MPEG 8229, 15094, 15099, 15120, 15121 (2°29'34"S,
878 54°44'06"W); Senador José Porfírio (22): MPEG 42454 (2°35'59"S, 51°56'42"W).

- 879 Westernmost lineage (n = 8): Brazil: Amazonas (15): Humaitá: MPEG 13171 (7°41'53"S,
880 62°33'11"W); Mato Grosso: Aripuanã (12): MZUSP 29532, 35535 (10°10'01"S, 59°27'W);
881 Colniza (13): MPEG 12652, 12654, 12691, 13172, 13173 (9°10'S, 60°38'W).
- 882 *Oecomys rex* (n = 09): Brazil: Amazonas: Manaus: MN 19617, 19618 (2°57'32"S,
883 59°56'49"W); Amapá: rio Amapari: MN 20646 (1°05'42.3"N 52°11'49.1"W); rio Maracá: MN
884 20688 (0°11'00.4"S 51°43'56.0"W); Serra do Navio: MZUSP 20517, 20518 (1°04'58"N,
885 52°14'10"W); Vila Velha do Cassiporé: MPEG 8044, 8047 (3°13'N, 51°13'W); Guiana:
886 BMNH 1910.9.29.17 (6°58'58"N, 58°31'01"W).

887

SUPPLEMENTARY DATA SD1

888 **Supplementary Data S1.**—Field number, voucher, Genbank accession number (Cytochrome b and intron 7 β -fibrinogen), specimen includes in
 889 morphological analyses (Morphology), country, division/state, locality and coordinates of samples analyzed in the present study. Lineages of the
 890 *Oecomys catherinae* complex: eastern, central, western, westernmost, and northern.

Species/Lineage	Field number	Voucher number	GenBank <i>Cytb</i>	GenBank <i>i7-fgb</i>	Morphology	Country: Division	Locality	Map	Lat.	Long.	Source
Western *	RVR 89	UFMT4118	MK874365	MT978188	Skin/skull	Brazil: Mato Grosso	Alta Floresta	1	-10.007	-56.038	1
Western *	UTP02	UFMT1680	MK874366	-	Skin/skull	Brazil: Mato Grosso	Paranaíta	2	-9.485	-56.472	1
Western *	UTP132	UFMT1686	MK874367	MK874449	Skin/skull	Brazil: Pará	Jacareacanga	3	-9.311	-56.768	1
Western *	UTP158	UFMT1772	MK874368	MK874450	Skin/skull	Brazil: Mato Grosso	Paranaíta	2	-9.485	-56.472	1
Western *	UTP159	UFMT1773	MK874369	MK874451	Skin/skull	Brazil: Mato Grosso	Paranaíta	2	-9.485	-56.472	1
Western *	UTP162	UFMT1774	MK874370	-	Skin/skull	Brazil: Mato Grosso	Paranaíta	2	-9.485	-56.472	1
Western *	UTP176	UFMT1775	MK874371	MK874452	Skin/skull	Brazil: Pará	Jacareacanga	3	-9.311	-56.768	1
Western *	UTP177	UFMT1776	MK874372	MK874453	Skin/skull	Brazil: Pará	Jacareacanga	3	-9.311	-56.768	1
Western *	UTP181	UFMT1806	MK874373	MK874454	Skin/skull	Brazil: Mato Grosso	Paranaíta	2	-9.485	-56.472	1
Western *	M000029	MZUSP29516	MG323753	MG323837	Skin/skull	Brazil: Mato Grosso	Gaúcha do Norte	5	-13.083	-53.283	2
Western *	M97055	MZUSP35543	MG323754	MG323838	Skin/skull	Brazil: Mato Grosso	Cláudia	4	-11.583	-55.167	2
Western *	PEU960006	-	MG323755	MG323839	-	Brazil: Mato Grosso	Aripuanã	12	-10.167	-59.450	2
Western *	APC244	MZUSP29531	MG323756	MG323777	Skin/skull	Brazil: Mato Grosso	Aripuanã	12	-10.167	-59.450	2
Western *	APC145	MZUSP35537	MG323757	MG323779	Skin/skull	Brazil: Mato Grosso	Juruena	11	-10.317	-58.483	2
Eastern	CIT2096	CIT2096	MG323772	MG323774	-	Brazil: Minas Gerais	Parque Estadual rio Doce	41	-19.533	-42.533	2
Eastern	CIT2097	CIT2097	MG323773	MG323775	-	Brazil: Minas Gerais	Parque Estadual rio Doce	41	-19.533	-42.533	2
Eastern	-	LBCE10774	MG323771	MG323852	-	Brazil: Rio de Janeiro	Paraty	48	-23.217	-44.717	2
Eastern	FS4-1	MN74359	KY605388	-	Skin/skull	Brazil: Rio de Janeiro	Guapimirim	47	-22.583	-42.950	3
Eastern	FS4-35	MN74360	KY605389	-	Skin/skull	Brazil: Rio de Janeiro	Guapimirim	47	-22.550	-42.950	3
Eastern	FS4-38	MN74361	KY605390	-	-	Brazil: Rio de Janeiro	Guapimirim	47	-22.550	-42.950	3
Eastern	FS08-21	MN74366	KY605391	-	-	Brazil: Rio de Janeiro	Guapimirim	47	-22.517	-42.800	3

Eastern	FS08-55	MN74368	KY605392	-	-	Brazil: Rio de Janeiro	Guapimirim	47	-22.517	-42.800	3
Eastern	FS14-20	MN74371	KY605393	-	Skin/skull	Brazil: Rio de Janeiro	Cachoeiras de Macacu	46	-22.492	-42.860	3
Eastern	FS14-35	NM74372	KY605394	-	-	Brazil: Rio de Janeiro	Cachoeiras de Macacu	46	-22.446	-42.686	3
Eastern	FU16	-	KY605396	-	-	Brazil: Rio de Janeiro	Casimiro de Abreu	44	-22.475	-42.210	3
Eastern	FU17	-	KY605397	-	-	Brazil: Rio de Janeiro	Casimiro de Abreu	44	-22.475	-42.210	3
Eastern	ITA30	MN72737	KY605398	-	Skin/skull	Brazil: Minas Gerais	Pirapitinga	42	-21.691	-42.368	3
Eastern	ITA31	MN72738	KY605399	-	-	Brazil: Minas Gerais	Pirapitinga	42	-21.691	-42.368	3
Eastern	PSP12	MN74377	KY605400	-	-	Brazil: São Paulo	Ubatuba	49	-23.333	-44.833	3
Eastern	PSP19	MN74378	KY605401	-	Skin/skull	Brazil: São Paulo	Ubatuba	49	-23.333	-44.833	3
Eastern	PSP38	MN74379	KY605402	-	-	Brazil: São Paulo	Ubatuba	49	-23.333	-44.833	3
Eastern	SU63	-	KY605403	-	-	Brazil: Rio de Janeiro	Sumidouro	43	-22.054	-42.668	3
Eastern	SU86	-	KY605404	-	-	Brazil: Rio de Janeiro	Sumidouro	43	-22.054	-42.668	3
Eastern	FS14-40	MN74373	KY605395	-	-	Brazil: Rio de Janeiro	Cachoeiras de Macacu	46	-22.492	-42.860	3
Eastern	-	MVZ200982	HM594616	-	-	Brazil: São Paulo	Capão Bonito	51	-24.283	-48.417	4
Eastern	-	UFES247	JQ966233	-	-	Brazil: Espírito Santo	Águia Branca	40	-18.875	-40.786	5
Central	-	MN36231	FJ361060	-	-	Brazil: Goiás	Colinas do Sul	30	-14.150	-48.067	14
Central	-	MN36273	FJ361061	-	-	Brazil: Goiás	Colinas do Sul	30	-14.150	-48.067	14
Central	-	MN36301	FJ361062	-	-	Brazil: Goiás	Colinas do Sul	30	-14.150	-48.067	14
Central	-	MN36350	FJ361065	-	-	Brazil: Goiás	Colinas do Sul	30	-14.150	-48.067	14
Central	-	MN36747	FJ361068	-	-	Brazil: Goiás	Minaçu	29	-13.517	-48.217	14
Central	-	MN36791	FJ361069	-	-	Brazil: Goiás	Minaçu	29	-13.517	-48.217	14
Central	-	MN37763	FJ361051	-	-	Brazil: Goiás	Caldas Novas	33	-17.683	-48.467	14
Central	-	MN37764	FJ361052	-	-	Brazil: Goiás	Caldas Novas	33	-17.683	-48.467	14
Central	-	MN37765	FJ361053	-	-	Brazil: Goiás	Caldas Novas	33	-17.683	-48.467	14
Central	-	MN37766	FJ361054	-	-	Brazil: Goiás	Caldas Novas	33	-17.683	-48.467	14
Central	-	MN37767	FJ361055	-	-	Brazil: Goiás	Caldas Novas	33	-17.683	-48.467	14
Central	-	MN37768	FJ361056	-	-	Brazil: Goiás	Caldas Novas	33	-17.683	-48.467	14
Central	-	MN37769	FJ361057	-	-	Brazil: Goiás	Caldas Novas	33	-17.683	-48.467	14
Central	-	LBCE8791	MG323760	MG323842	-	Brazil: Mato Grosso do Sul	Dois Irmãos de Buriti	35	-20.667	-55.283	2
Central	MRT3875	MZUSP35549	MG323761	MG323843	Skin/skull	Brazil: Tocantins	Paraná	27	-12.617	-47.883	2
Central	MRT3897	MZUSP35550	MG323762	MG323844	Skin/skull	Brazil: Tocantins	Paraná	27	-12.617	-47.883	2

Central	PCH4077	-	MG323763	MG323845	Skin	Brazil: São Paulo	São Joaquim da Barra	34	-20.483	-47.850	2
Central	PCH3998	-	MG323764	MG323846	Skin/skull	Brazil: São Paulo	São Joaquim da Barra	34	-20.483	-47.850	2
Westernmost	-	MN37776	FJ361050	-	-	Brazil: Rondônia	Guajará-Mirim	15	-10.833	-63.733	14
Westernmost	APC249	MZUSP29532	MG323758	MG323840	Skin/skull	Brazil: Mato Grosso	Aripuanã	12	-10.167	-59.450	2
Westernmost	APC243	MZUSP35535	MG323759	MG323841	Skin/skull	Brazil: Mato Grosso	Aripuanã	12	-10.167	-59.450	2
Northern	APC288	MZUSP35538	MG323765	MG323847	Skin/skull	Brazil: Mato Grosso	Vila Rica	16	-10.017	-51.117	2
Northern	APC289	MZUSP35539	MG323766	MG323848	Skin/skull	Brazil: Mato Grosso	Vila Rica	16	-10.017	-51.117	2
Northern	APC304	MZUSP29533	MG323767	MG323849	Skin	Brazil: Mato Grosso	Vila Rica	16	-10.017	-51.117	2
Northern	-	MZUSP29533	KY605382	-	Skin/skull	Brazil: Mato Grosso	Vila Rica	-	-	-	3
Northern	APC292	-	MG323768	MG323850	Skin/skull	Brazil: Mato Grosso	Vila Rica	16	-10.017	-51.117	2
Northern	APC297	-	MG323769	MG323784	Skin	Brazil: Mato Grosso	Vila Rica	16	-10.017	-51.117	2
Northern	APC310	MZUSP35542	MG323770	MG323851	Skin/skull	Brazil: Mato Grosso	Vila Rica	16	-10.017	-51.117	2
Northern	CS26	-	KT737237	-	-	Brazil: Pará	Flona Tapirape-Aquiri	19	-5.800	-50.500	6
Northern	-	USNM549530	KT737238	-	-	Brazil: Pará	East bank rio Xingu	23	-3.650	-52.367	6
Northern	IAVRD330	MPEG38898	KY605383	-	Skin/skull	Brazil: Pará	Marabá	17	-6.000	-51.333	3
Northern	PSA128	MPEG39899	KY605384	-	Skin/skull	Brazil: Pará	Marabá	19	-5.817	-50.483	3
Northern	PSA139	MPEG39900	KY605385	-	Skin/skull	Brazil: Pará	Marabá	19	-5.817	-50.483	3
Northern	PSA164	MPEG39901	KY605386	-	Skin/skull	Brazil: Pará	Marabá	19	-5.783	-50.533	3
Northern	PSA176	MPEG39903	KY605387	-	Skin/skull	Brazil: Pará	Marabá	19	-5.783	-50.533	3
<i>O. rex</i>	CSA22	IEPA2410	MK874428	-	-	Brazil: Amapá	Laranjal do Jari, Iratapuru	-	0.1472	-52.520	1
<i>O. rex</i>	RC01	IEPA2038	MK874429	-	-	Brazil: Amapá	Laranjal do Jari, Reserva extrativista do rio Cajari	-	-0.7261	-52.008	1
<i>O. rex</i>	V-1102	-	AJ496314	-	-	French Guiana	Sauel	-	-3.617	-53.200	14
<i>O. rex</i>	V-1099	-	AJ496315	-	-	French Guiana	Sauel	-	-3.617	-53.200	14
<i>O. auyantepui</i>	V-971	-	AJ496304	-	-	French Guiana	Les Nouragues	-	4.083	-52.683	14
<i>O. auyantepui</i>	V-1001	-	AJ496305	-	-	French Guiana	Les Nouragues	-	4.083	-52.683	14
<i>O. auyantepui</i>	ROM114059	-	KP778302	KP778670	-	Suriname: Brokopondo	Brownsberg Nature Park	-	-	-	14
<i>O. bicolor</i>	M97074	MZUSP29528	MG323726	-	-	Brazil: Mato Grosso	Cláudia	-	-11.583	-55.167	2
<i>O. bicolor</i>	M97107	MZUSP35544	MG323725	-	-	Brazil: Mato Grosso	Cláudia	-	-11.583	-55.167	2
<i>O. bicolor</i>	JL26	UFPAM1542	MK874348	MK874445	-	Brazil: Pará	Itaituba	-	-5.376	-56.923	1
<i>O. bicolor</i>	JMIJ40	UFPAM1162	MK874350	MK874447	-	Brazil: Pará	Jacareacanga	-	-6.127	-57.588	1
<i>O. cleberi</i>	APC210	MZUSP35534	MG323745	-	-	Brazil: Mato Grosso	Aripuanã	-	-10.167	-59.450	1

<i>O. cleberi</i>	-	UFMG2802	HM594608	-	-	Brazil: Mato Grosso	Barra do Garças	-	-15.633	-52.350	4
<i>O. cleberi</i>	JMIG01	UFPAM1177	MK874381	MK874459	-	Brazil: Pará	Jacareacanga	-	-5.722	-57.366	1
<i>O. cleberi</i>	MSF2410	-	MK874389	MK874466	-	Brazil: Mato Grosso	Alta Floresta	-	-9.798	-55.926	1
<i>O. concolor</i>	JLP16728	-	HM594614	-	-	Brazil: Amazonas	rio Jau	-	-2.217	-62.383	4
<i>O. concolor</i>	JLP16806	-	HM594615	-	-	Brazil: Amazonas	rio Jau	-	-2.217	-62.383	4
<i>O. franciscorum</i>	roe224	-	KF207846	-	-	Argentina: Chaco	Pampa del Indio	-	-25.917	-58.933	7
<i>O. franciscorum</i>	-	MACN26663	KT737232	-	-	Argentina: Formosa	Estacion Guaycolec	-	-25.967	-58.167	6
<i>O. franciscorum</i>	LBCE1916	-	MG323715	MG323804	-	Brazil: Mato Grosso do Sul	Corumbá	-	-19.000	-57.650	2
<i>O. franciscorum</i>	PNPA300	MZUSP35540	MG323716	MG323786	-	Brazil: Mato Grosso	Parque Nacional do Pantanal	-	-17.000	-57.433	2
<i>O. mamorae</i>	PZ94	-	KT737226	-	-	Bolivia: La Paz	Tumupasa	-	-14.150	-67.917	6
<i>O. mamorae</i>	PZ316	-	KT737225	-	-	Bolivia: La Paz	Buena Vista	-	-15.283	-68.383	6
<i>O. paricola</i>	LPC570	MVZ197507	HM594593	-	-	Brazil: Mato Grosso	Alta Floresta	-	-9.583	-55.917	4
<i>O. paricola</i>	LPC525	UFMG2841	HM594591	-	-	Brazil: Mato Grosso	Alta Floresta	-	-9.583	-55.917	4
<i>O. paricola</i>	JL28	UFPAM1544	MK874410	MK874480	-	Brazil: Pará	Itaituba	-	-5.376	-56.923	1
<i>O. paricola</i>	UTP668	UFMT1779	MK874425	MK874488	-	Brazil: Pará	Jacareacanga	-	-9.311	-56.768	1
<i>O. roberti</i>	-	UFES1370	HM594603	-	-	Brazil: Pará	Santana do Araguaia	-	-9.630	-50.144	4
<i>O. roberti</i>	-	MVZ197619	HM594594	-	-	Brazil: Mato Grosso	Chapada dos Guimarães	-	-15.194	-55.950	4
<i>O. roberti</i>	MSF1796	-	MK874430	MK874489	-	Brazil: Mato Grosso	Alta Floresta	-	-9.840	-56.005	1
<i>O. roberti</i>	M97060	MZUSP29526	MG323720	MG323807	-	Brazil: Mato Grosso	Cláudia	-	-11.583	-55.166	2
<i>O. rutilus</i>	CN123	-	JF759665	-	-	Brazil: Pará	Floresta Trombetas	-	-1.167	-55.650	8
<i>O. rutilus</i>	-	MNHN1995.3236	AJ496309	-	-	French Guiana	Saint-Eugene	-	-	-	14
<i>O. rutilus</i>	TTU101025	-	KP778344	KP778659	-	Peru: Loreto	Maynas	-	-	-	14
<i>O. superans</i>	JLP15517	MVZ200944	U58385	-	-	Brazil: Amazonas	Right bank rio Juruá	-	-6.833	-70.750	9
<i>O. superans</i>	-	MVZ155006	AY275123	-	-	Peru: Amazonas	Huampami, rio Cenepa	-	-5.517	-79.817	10
<i>O. sydandersoni</i>	-	USNM584557	KT737234	-	-	Bolivia: Santa Cruz	Parque Kempff mercado	-	-15.250	-61.017	6
<i>O. sydandersoni</i>	-	USNM588189	KT737235	-	-	Bolivia: Santa Cruz	rio Paraguay	-	-14.767	-61.033	6
<i>O. tapajinus</i>	-	MVZ197511	HM594595	-	-	Brazil: Tocantins	Peixe, rio Santa tereza	-	-11.833	-48.633	4
<i>O. tapajinus</i>	-	UFES1359	HM594600	-	-	Brazil: Tocantins	Lagoa da Confusão	-	-10.861	-49.713	4
<i>O. tapajinus</i>	JB11	UFPAM1396	MK874439	MK874491	-	Brazil: Pará	Itaituba	-	-5.227	-56.929	1
<i>O. tapajinus</i>	JB13	UFPAM1398	MK874440	MK874492	-	Brazil: Pará	Itaituba	-	-5.227	-56.929	1
<i>O. trinitatis</i>	-	MUSM13320	GU126527	-	-	Peru: Loreto	rio Galvez	-	-5.200	-72.883	11

<i>O. trinitatis</i>	-	MVZ200948	U58390	-	-	Brazil: Acre	-	-	-8.667	-72.783	9
<i>Euryoryzomys nitidus</i>	-	MZUSP29524	MG323695	MG323787	-	Brazil: Mato Grosso	Apiacás	-	-	-	2
<i>Hylaeamys megacephalus</i>	-	M968452	MG323696	MG323788	-	Brazil: Mato Grosso	Apiacás	-	-	-	2
<i>Euryoryzomys macconnelli</i>	-	AMNH272669	GU126538	-	-	Peru: Loreto	rio Galvez	-	-	-	11
<i>Hylaeamys megacephalus</i>	GD463	-	AY275124	-	-	-	-	-	-	-	10
<i>Handleyomys intectus</i>	-	CADV088	EU579490	-	-	Colombia: Antioquia	4 km S El Tetiro	-	-	-	14
<i>Oligoryzomys utiaritensis</i>	-	MN75625	JQ013752	JQ282893	-	Brazil: Mato Grosso	Campo Novo do Parecis	-	-	-	12
<i>Handleyomys melanotis</i>	-	ASNHC3419	KF658409	KF658415	-	Mexico: Nayarit	8 KM E of San Blas	-	-	-	13

891 * Referred as *Oecomys* aff. *catherinae* by Saldanha et al. (2019). Named as *Oecomys* sp. nov. in this report.

892 1 - Saldanha, J., D. C. Ferreira, V. F. da Silva, M. Santos-Filho, A. C. Mendes-Oliveira, and R. V. Rossi. 2019. Genetic diversity of *Oecomys*
893 (Rodentia, Sigmodontinae) from the Tapajós River basin and the role of rivers as barriers for the genus in the region. *Mammalian Biology* 97:41–
894 49.

895 2 - Suárez-Villota, E. Y., A. P. Carmignotto, M. V. Brandão, A. R. Percequillo, and M. J. J. Silva. 2018. Systematics of the genus *Oecomys*
896 (Sigmodontinae: Oryzomyini): molecular phylogenetic, cytogenetic and morphological approaches reveal cryptic species. *Zoological Journal of*
897 *the Linnean Society* 184:182–210.

898 3 - Malcher, M. S., J. C. Pieczarka, L. Geise, R. V. Rossi, A. L. Pereira, P. C. M. O'brien, P. H. Asfora, V. F. Silva, M. I Sampaio, M. A. Ferguson–
899 Smith, and C. Y. Nagamachi. 2017. *Oecomys catherinae* (Sigmodontinae, Cricetidae): Evidence for chromosomal speciation? *PLoS ONE*
900 12:e0181434.

901 4 - Rocha, R. G., E. Ferreira, B. M. A. Costa, I. C. M. Martins, Y. L. R. Leite, L. P. Costa, and C. Fonseca. 2011. Small mammals of the mid–
902 Araguaia River in central Brazil, with the description of a new species of climbing rat. *Zootaxa* 2789:1–34.

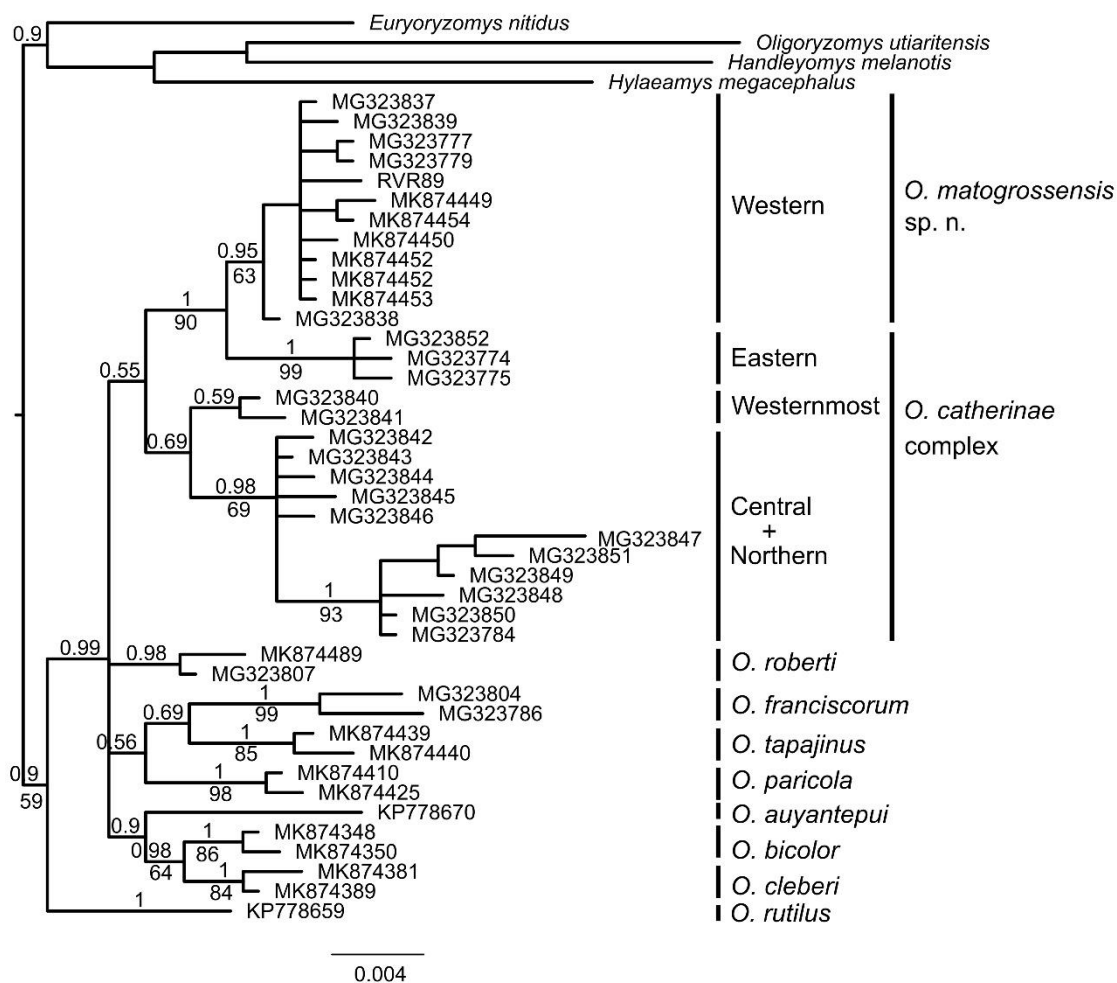
903 5 - Machado, L. F., Y. L. R. Leite, A. U. Christoff, and L. G. Giugliano. 2014. Phylogeny and biogeography of tetralophodont rodents of the tribe
904 Oryzomyini (Cricetidae: Sigmodontinae). *Zoologica Scripta* 43(2):119-130.

- 905 6 - Pardiñas, U. F. J., P. Teta, J. Salazar–Bravo, P. Myers, and C. A. Galliari. 2016. A new species of arboreal rat, genus *Oecomys* (Rodentia,
906 Cricetidae) from Chaco. *Journal of Mammalogy* 97:1177–1196.
- 907 7 - Orozco, M. M., R. V. Piccinali, M. S. Mora, G. F. Enriquez, M. V. Cardinal and R. E. Gürtler. 2014. The role of sigmodontine rodents as
908 sylvatic hosts of *Trypanosoma cruzi* in the Argentinean Chaco. *Infection, Genetics and Evolution* 22: 12-22.
- 909 8 - Rosa, C.C., T. Flores, J. C. Pieczarka, R. V. Rossi, M. I. C. Sampaio, J. D. Rissino, P. J. S. Amaral, and C. Y. Nagamachi. 2012. Genetic and
910 morphological variability in South American rodent *Oecomys* (Sigmodontinae, Rodentia): evidence for a complex of species. *Journal of Genetics*
911 91(3):265-277.
- 912 9 - Patton, J. L., and M. N. F. Da Silva. 1995. A review of the spiny mouse genus *Scolomys* (Rodentia: Muridae: Sigmodontinae) with the description
913 of a new species from the western Amazon of Brazil. *Proceedings of the Biological Society of Washington* 108:319-337.
- 914 10 - D'Elia, G. 2003. Phylogenetics of Sigmodontinae (Rodentia, Muroidea, Cricetidae), with special reference to the akodont group, and with
915 additional comments on historical biogeography. *Cladistics* 19:307-323.
- 916 11 - Percequillo, A. R., M. Weksler, and L. P. Costa. 2011. A new genus and species of rodent from the Brazilian Atlantic Forest (Rodentia:
917 Cricetidae: Sigmodontinae), with comments on the Oryzomyine biogeography *Zoological Journal of the Linnean Society* 161:357-390.
- 918 12 - Agrellos, R., C. R. Bonvicino, E. S. T. Rosa, A. A. R. Marques, P. S. D'Andrea, and M. Weksler. 2012. The taxonomic status of the Castelo
919 dos Sonhos Hantavirus reservoir, *Oligoryzomys utiaritensis* Allen 1916 (Rodentia: Cricetidae: Sigmodontinae). *Zootaxa* 3220:1-28.
920 <http://dx.doi.org/10.11646/zootaxa.3220.1.1>
- 921 13 - Almendra, A. L., D. S. Rogers, and F. X. González-Cózatl. 2014. Molecular phylogenetics of the *Handleyomys chapmani* complex in
922 Mesoamerica. *Journal of Mammalogy* 95(1):26-40.
- 923 14 - unpublished

924

925

SUPPLEMENTARY DATA S2



926

927 **Supplementary Data S2.**—Bayesian Inference topology of *Oecomys*, based on the nuclear
 928 intron 7 β -fibrinogen dataset. Numbers above branches indicate Bayesian posterior
 929 probabilities and below branches indicate maximum likelihood bootstrap values. The black
 930 side bars indicate lineages and species recognized in this study.

931

SUPPLEMENTARY DATA S3

932 **Table S3.1.**—Results of the Principal Component Analysis of adult specimens of *Oecomys*933 sp. nov. and lineages of the *Oecomys catherinae* complex *stricto sensu* based on 31

934 craniodental variables. See “Materials and Methods” section for abbreviations. PC = principal

935 component. Bold numbers correspond to the five most contributive variables for each PC.

Variables	PC1	PC2	PC3
ONL	0.959	-0.064	-0.071
CIL	0.964	-0.025	-0.097
BH	0.736	-0.136	0.156
CZL	0.845	0.032	-0.064
ZL	0.922	-0.001	-0.104
LD	0.901	-0.213	-0.159
BZP	0.785	0.007	-0.068
BN	0.791	0.145	-0.012
LN	0.675	-0.215	-0.214
LR	0.844	-0.056	-0.070
BR	0.421	-0.077	0.576
LIB	0.800	0.084	-0.043
OL	0.883	-0.083	-0.096
ZB	0.889	0.002	-0.136
LIP	0.567	0.221	0.541
BIP	0.532	-0.026	0.431
BIF	0.611	-0.202	0.056
LIF	0.788	-0.088	-0.040
BRP	0.744	-0.084	-0.055
LPB	0.734	0.103	-0.223
MB	0.820	-0.008	0.021
BOC	0.743	-0.127	0.226
BB	0.589	-0.283	0.551
BI	0.775	-0.068	-0.233
BM1	0.277	0.759	-0.023
CLM	0.550	0.696	0.056
Bm1	0.382	0.698	0.042
CLLM	0.462	0.789	-0.036
LLD	0.591	-0.198	-0.298
LCIB	0.820	-0.205	0.086
MH	0.910	-0.097	0.026
% Variance	54.9	8.5	5.0

936

937 **Table S3.2.**—Results of the Discriminant Function Analysis of adult specimens of *Oecomys*
 938 sp. nov. and lineages of the *Oecomys catherinae* complex *stricto sensu* based on 31
 939 craniodental variables. See “Materials and Methods” section for abbreviations. CV =
 940 canonical variate. Bold numbers correspond to the five most contributive variables for each
 941 CV.

Variables	CV1	CV2	CV3
ONL	0.579	0.086	-0.139
CIL	0.066	1.102	-0.512
BH	-0.073	-0.511	0.761
CZL	-0.484	-0.675	0.083
ZL	0.063	0.168	0.292
LD	0.755	-0.296	0.117
BZP	0.394	0.316	0.214
BN	-0.533	0.516	0.168
LN	0.403	-0.322	-0.445
LR	-1.413	0.259	0.861
BR	0.134	-0.743	0.409
LIB	0.701	-0.085	-0.175
OL	0.871	-1.143	-0.069
ZB	-0.799	0.965	-0.043
LIP	0.521	0.341	-0.288
BIP	0.214	0.043	-0.395
BIF	0.090	0.924	-0.077
LIF	-0.374	0.085	0.721
BRP	-0.001	0.071	-0.764
LPB	-0.516	0.523	-0.529
MB	0.083	-0.239	0.338
BOC	0.423	-0.172	0.016
BB	0.233	0.943	-0.212
BI	0.312	-0.187	-0.391
BM1	-0.265	-0.062	0.007
CLM	0.465	-0.059	0.187
Bm1	0.535	0.101	0.310
CLLM	-0.154	0.066	-0.152
LLD	0.203	-0.371	-0.125
LCIB	-0.352	-1.164	0.090
MH	-0.023	-0.313	-0.167
Eigenvalue	5.226	1.761	0.868
% Variance	62.1	20.9	10.3

943 **Table S3.3.**—Classification matrix determined by the Discriminant Function Analysis of
 944 *Oecomys* sp. nov. and the *Oecomys catherinae* complex *stricto sensu* lineages (central,
 945 eastern, northern and westernmost).

Group	Group classification					Total	% correct classification
	<i>Oecomys</i> sp. nov.	Central	Eastern	Northern	Westernmost		
<i>Oecomys</i> sp. nov.	17	0	0	0	0	17	100
Central	0	7	0	0	0	7	100
Eastern	0	1	26	0	0	27	96.3
Northern	1	1	0	21	1	24	87.5
Westernmost	0	0	0	0	6	6	100
Total							95.1

946

CAPÍTULO III

Diversificação do complexo *Oecomys catherinae* Thomas, 1909 (Rodentia, Sigmodontinae): quantas espécies existem?

RESUMO

A espécie *Oecomys catherinae* foi apontada como um complexo de espécies em vários estudos, com linhagens amplamente distribuídas em território brasileiro. Destas linhagens, apenas uma foi reconhecida como distinta do complexo e descrita como uma nova espécie, enquanto as demais linhagens apresentam relações de parentesco e diversificação ainda confusas, principalmente em relação as possíveis linhagens da Mata Atlântica. Neste estudo, investigamos a diversificação e relações entre as linhagens de *O. catherinae* e da nova espécie. Para isso, realizamos análises moleculares com Citocromo b, uma representação do genoma (ddRADseq) e análises morfométricas, de representantes de todas as linhagens mencionadas na literatura. Nossas análises moleculares indicaram a ocorrência de outra possível linhagem com ocorrência no nordeste do Brasil. Recuperamos o monofiletismo com a linhagem extremo oeste como irmã das demais, seguida da linhagem norte, central, nordeste e leste, esta última com dois subclados, denominados leste A e leste B. Apesar disso, apenas três grupos biológicos foram recuperados, sendo um com a linhagem extremo oeste, outro com a linhagem norte e o terceiro grupo com central, nordeste e leste juntos. Estimamos os eventos de diversificação do complexo para o Pleistoceno em concordância com os refúgios da Amazônia e as glaciações na Mata Atlântica. Em contrapartida das diferenciações moleculares, as análises morfométricas indicam ampla sobreposição entre as linhagens, principalmente as do Cerrado e Mata Atlântica. Com isso, consideramos como espécies distintas apenas as linhagens extremo oeste e norte. Consideramos as linhagens central, leste e nordeste como espécies crípticas, visto que ainda é necessária uma ampla amostragem das lacunas de distribuição da Mata Atlântica para confirmar se estas linhagens estão evoluindo separadamente.

Palavras-chave: Espécies crípticas, ddRADseq, Mata Atlântica, Pleistoceno.

ABSTRACT

Oecomys catherinae was indicated as a species complex in several studies, with lineages widely distributed in Brazilian territory. With five lineages in the complex, only one was recognized as distinct and described as a new species, while the other lineages relationship and diversification still uncertain. In this study, we investigate the divergence and relationships between the *O. catherinae* lineages and the new species. For this, we used molecular analysis with Cytochrome b, a genome representation (ddRADseq), and morphometric analysis, of all the lineages mentioned on literature. Our molecular analyses recovered another probable lineage with occurrence in the northeastern of Brazil, and the group monophyly, with the westernmost lineage as sister of the others, followed by the northern, central, northeastern and eastern lineage, the last one with two subclades (eastern A and eastern B). However, only three biological groups were recovered, one with the westernmost lineage, the second with the northern lineage and the third group with the central, northeastern and eastern together. The diversification events of the complex were estimated to the Pleistocene in agreement with the refuges on Amazonia and glaciation periods in the Atlantic Forest. Besides the molecular differentiations, the morphometric analyses indicate a wide overlap between the lineages. With this, we consider as distinct species only the westernmost and northern lineages. We consider the central, eastern and northeastern as cryptic species, since a large number of samples of the Atlantic Forest gaps distribution are necessary to confirm if these lineages are evolving separately.

Keywords: Cryptic species, ddRADseq, Atlantic Forest, Pleistocene.

1. INTRODUÇÃO

Quando descrita, a espécie *Oecomys catherinae* Thomas, 1909 apresentava distribuição conhecida ao sul da Mata Atlântica, com localidade tipo no município de Joinville, Santa Catarina, Brasil. Outros dois nomes provenientes do estado da Bahia foram associados a *O. catherinae*. O primeiro foi *Mus cinnamomeus* Pictet & Pictet, 1844, porém este estava pré-ocupado por *Mus cinnamomeus* Lichtenstein, 1830, associado a um *Proechimys*. Outro nome foi *Oryzomys concolor bahiensis* Hershkovitz 1960 descrita em substituição a *Mus cinnamomeus*, com localidade tipo Ilhéus, Bahia. Atualmente, ambos são considerados sinônimos de *O. catherinae*, cuja distribuição estende-se até o sul do estado da Bahia (Carleton & Musser 2015; Musser & Carleton 2005). Mais recentemente, em análises de registros de ocorrência de *O. catherinae*, Asfora et al. (2011) confirmaram a presença de representantes da espécie no estado da Paraíba, Brasil, estendendo mais ao norte os limites da distribuição geográfica da espécie. Além disso, os autores apontaram a existência de duas populações aparentemente disjuntas: uma abrangendo as regiões sul, sudeste e central do Brasil e outra restrita à região nordeste ao norte do rio São Francisco.

Além da ocorrência *O. catherinae* confirmada ao norte da Mata Atlântica e em florestas de galeria do Cerrado (Asfora et al. 2011, Carleton & Musser 2015), recentes estudos comprovaram a ocorrência desta espécie também na Amazônia (Malcher et al. 2017; Suárez-Villota et al. 2018; Saldanha et al. 2019, Saldanha & Rossi, no prelo). Segundo Asfora et al. (2011), estes relatos de ocorrência disjunta da espécie podem ser artefatos de amostragem ou indicam que *O. catherinae*, como atualmente reconhecido, pode ser composto por mais de uma espécie.

O primeiro indício da existência de espécies crípticas em *O. catherinae* foi indicada por Malcher et al. (2017), que revelaram ausência de diferenciação molecular (marcador Citocromo b) e morfológica significativa entre populações de *O. catherinae* da Mata Atlântica e Amazônia, porém indicaram a presença de variações cromossômicas entre estas duas populações. Na última revisão sistemática do gênero *Oecomys*, Suárez-Villota et al. (2018), usando dados moleculares (marcador mitocondrial Citocromo b e marcadores nucleares proteína ligante do fotoreceptor retinóide e íntron 7 Beta-fibrinogênio), afirmam que este grupo é, de fato, um complexo de espécies amplamente distribuído, composto por cinco linhagens. Além disso, os autores afirmam que o nome *O. catherinae* estaria restrito a indivíduos distribuídos na Mata Atlântica (leste do território brasileiro) e que as demais

linhagens representam supostas novas espécies dentro do complexo, distribuídas na região central, norte, oeste e extremo oeste do território brasileiro.

Recentemente, a linhagem oeste do complexo *O. catherinae* (senso Suárez-Villota et al. 2018), com ocorrência na Amazônia, foi descrita como uma nova espécie – *Oecomys* sp. nov. – por Saldanha & Rossi (no prelo) com base em dados morfológicos, moleculares e citogenéticos. Com isso, devido as semelhanças morfológicas, baixa distância genética e escassa divergência no número diploide, os autores restringiram o complexo *O. catherinae* às linhagens leste, central, norte e extremo oeste de Suárez-Villota et al. (2018).

Saldanha & Rossi (no prelo) também indicaram a existência de dois grupos de *O. catherinae* na Mata Atlântica, um ao norte e outro ao sul, mas devido ao baixo suporte filogenético e baixas distâncias genéticas, os autores consideraram uma única linhagem para esta região (linhagem leste). A ocorrência de linhagens distintas ao norte e sul da Mata Atlântica já foi mencionada para outros grupos, cuja origem é geralmente associada às mudanças climáticas do Pleistoceno e mudanças vegetacionais a elas associadas (Costa & Leite 2012). Na Mata Atlântica, também existem registros de ocorrência da espécie *O. catherinae* ao norte do rio São Francisco (Asfora et al. 2011), porém, amostras desta região não foram incluídas em estudos filogenéticos anteriores, sendo os registros de quebras filogenéticas para este complexo apenas ao sul deste rio (Saldanha & Rossi, no prelo).

Os recentes estudos com o complexo *O. catherinae* indicaram discordância nas topologias entre hipóteses filogenéticas obtidas a partir do marcador mitocondrial Citocromo b e de marcadores nucleares, principalmente relacionadas às relações de parentesco entre as linhagens (Suárez-Villota et al. 2018; Saldanha & Rossi, no prelo). Com essas descobertas sobre a problemática do complexo *O. catherinae* quanto aos baixos suportes nos nós nas relações de parentesco, diversificação e evolução entre as linhagens que constituem o grupo, o presente estudo tem como objetivo esclarecer estas relações filogenéticas e inferir sobre a diversificação de linhagens evolutivas dentro do complexo *O. catherinae*. Assim como investigar as possíveis origens da diversificação entre as linhagens, principalmente na problemática da Mata Atlântica, incluindo o norte do rio São Francisco, onde são registradas populações disjuntas para o complexo. Para isso, além do marcador mitocondrial (Citb), utilizamos novas abordagens com fragmentos de DNA associados a sítios de restrição produzidos pela técnica de ddRADseq, e dados morfométricos, a fim de verificar a congruência entre as inferências filogenéticas e inferir a diversidade e diversificação de linhagens e espécies do complexo.

2. MATERIAL E MÉTODOS

Dados moleculares

Empregamos análises moleculares com o gene mitocondrial Citocromo b (Citb) e com fragmentos de DNA associados a sítios de restrição (*double digest restriction site-associated DNA sequencing* - ddRADseq), obtidos com sequenciamento de nova geração. Para isso, utilizamos alíquotas de tecidos de exemplares do acervo de mamíferos (Anexo 02) da Universidade Federal de Mato Grosso, do laboratório de Ecologia e Evolução do Instituto Butantan, do laboratório de Mastozoologia da Universidade do Estado do Rio de Janeiro e do acervo de mamíferos da universidade Federal de Pernambuco, permitindo a reunião de amostras de representantes de todas as linhagens mencionadas na literatura.

Os procedimentos laboratoriais de extração do DNA total foram realizados no Laboratório de Citogenética e Genética Animal (LabGen) da Universidade Federal de Mato Grosso (UFMT), campus Cuiabá, Mato Grosso, através dos protocolos de extração salina de Aljanabi & Martinez (1997) e no Laboratório de Evolução e Genética Animal (LEGAL) na Universidade Federal do Amazonas (UFAM), campus Manaus, Amazonas, através dos protocolos de extração CTAB 2% (Doyle & Doyle 1987).

Obtenção de dados mitocondriais

A amplificação do gene citocromo b (Citb) do DNA mitocondrial (mtDNA) foi obtida através da reação em cadeia da polimerase (PCR) para dez amostras sem sequências disponíveis no GenBank (Anexo 01, Tabela 1). As reações de amplificação, purificação e sequenciamento foram realizadas no LEGAL/UFAM. A amplificação foi obtida com os *primers forward* L14725 (5'-CGAAGCTTGATATGAAAAACCATCGTTG-3') (Kocher et al. 1989) e *reverse* MVZ16 (5'-AAATAGGAARTATCAYTCTGGTTTRAT-3') (Smith & Patton 1993).

A PCR foi realizada com volume final de 15 µL contendo 6,8 µL de H₂O, 1,5 µL de tampão 10X, 1,5 µL do primer L14725 (2 pmol), 1,5 µL do primer MVZ16 (2 pmol), 1,2 µL de dNTPs (2 mM), 1,2 µL MgCl₂ (25 mM), 0,3 µL da taq (0,02 U) e 1 µL de DNA. A PCR foi realizada em termociclador, com um ciclo inicial a 94° C por 2 minutos, seguido por 35 ciclos de desnaturação a 94° C por 15 segundos, anelamento a 55° C por 35 segundos e extensão a 68° C por 1 minuto e 30 segundos, seguido de um ciclo de extensão final de 68° C por 5 minutos.

As amostras de PCR foram purificadas com ExoSap-IT® e posteriormente sequenciadas utilizando-se os mesmos primers da PCR, em uma reação com 4,5 µl de H₂O, 1,45 µl de tampão de sequenciamento 5X, 2 µl do *primer forward* ou *reverse*, 0,3 µl de BigDye Terminator v 3.1 (Applied Biosystems®) e 2 µl do PCR purificado. As reações de sequenciamento seguiram as recomendações indicadas pelo fabricante. Posteriormente, os produtos foram purificados com a adição de 2,5 µL de Acetato e 30 µL de álcool 70% e então ressuspensos em 10 µl de formamida e injetado em sequenciador automático ABI 3500 (Applied Biosystems®). As sequências obtidas foram visualizadas e alinhadas para montagem da fita consenso no programa Geneious®.

Análise de dados mitocondriais

Além das 10 sequências obtidas neste estudo, utilizamos mais 63 sequências de *Citb* das linhagens do complexo *O. catherinae*, 15 sequências de *Oecomys* sp. nov., espécie irmã do complexo e até recentemente incluída nele (= linhagem oeste de Suarez-Villota et al. 2018), e mais 23 sequências do grupo externo depositadas no Genbank, que inclui as espécies *Oecomys auyantepui*, *O. bicolor*, *O. concolor*, *O. franciscorum*, *O. mamorae*, *O. paricola*, *O. rex*, *O. roberti*, *O. rutilus*, *O. superans*, *O. sydandersoni*, *O. tapajinus*, *O. trinitatis*, *Holoclitus brasiliensis*, *H. chacarius*, *H. sciureus*, *Hylaeamys megacephalus*, *Oligoryzomys destructor*, *O. flavescens*, *O. fulvencens*, *O. microtis* e *O. nigripes* (Anexo 01: tabela 1). Posteriormente, todas as sequências foram editadas e alinhadas no programa BioEdit 7.0.5.2 (Hall 1999).

Para a análise filogenética utilizamos os métodos de Inferência Bayesiana (IB), realizada no programa MrBayes 3.2.7a (Ronquist et al. 2012), com quatro cadeias, 50 milhões de gerações e uma amostragem de árvore a cada 1.000 gerações. O modelo evolutivo que melhor representa a matriz de dados foi o *Transition model* com proporção de sítios invariáveis e distribuição gama (TIM2 + I + G) gerado através do programa JModeltest2 (Darriba et al. 2012). As árvores obtidas foram visualizadas e editadas no programa Figtree 1.4.3 (Rambaut 2016). As relações entre os haplótipos foi avaliada através da rede haplotípica com o método *Median-Joining* (Bandelt et al. 1999) no programa PopArt (<http://popart.otago.ac.nz>).

Obtenção de dados genômicos

Para a representação parcial do genoma utilizamos a técnica de ddRADseq de Peterson et al. (2012), com modificações para a plataforma *Ion Torrent*. A técnica

ddRADseq foi aplicada em 43 amostras, sendo 21 espécimes da linhagem leste, quatro da linhagem central, seis da linhagem norte, duas da linhagem extremo oeste, uma amostra do nordeste e nove amostras da espécie *Oecomys* sp. nov. (= linhagem oeste de Suarez-Villota et al. 2018; Anexo 01: tabela 1). Além destes, utilizamos a biblioteca genômica de indivíduos de *O. auyantepui*, *O. bicolor*, *O. paricola*, *Hylaeamys megacephalus* e *Sooretamys angouya* como grupo externo.

A integridade e concentração do DNA foram checadas em Nanodrop 2000 (Thermo Scientific, USA) para posterior diluição e obtenção da concentração de 50 ng/ul. Para a digestão do DNA de cada amostra utilizamos a enzima de restrição de corte frequente SdaI e a enzima de corte raro Csp6I. Essas enzimas cortam as moléculas de DNA, criando pontas livres em ambas as extremidades para a ligação dos adaptadores. Utilizamos dois adaptadores, sendo o adaptador P1 comum a todas as amostras, que se liga à ponta gerada pela enzima SdaI, e o adaptador AY, no qual o Y representa um barcode único para cada amostra e se liga à ponta gerada pela enzima Csp6I. O processo de digestão e ligação ocorre de forma simultânea.

A reação de digestão/ligação foi realizada com volume final de 50 µL, sendo 4,0 µL de DNA (200 ng), 0,1 µL (1 U) da enzima SdaI, 0,1 µL (1 U) da enzima Csp6I, 2,0 µl (0,1 µM) do adaptador P1, 2,0 µl (5 uM) do adaptador AY (individual), 0,5 µl (5 U) da enzima T4 ligase, 0,5 µl de ATP (5 mmol) e 5 µl Tampão Tango 10X. A reação ocorreu em termociclador com um ciclo de 37° C durante 3 horas para a digestão do DNA pelas enzimas e ligação dos adaptadores, seguido de um ciclo de 68° C durante 15 minutos para desnaturação das enzimas.

Em seguida, realizamos uma PCR teste para a verificação da reação de digestão, com volume final de 15 µL contendo 4,25 µL de H₂O, 1,5 µL de tampão 10X, 1,5 µL do primer P1 (2 mM), 1,5 µL do primer AY-individual (2 mM), 1,5 µL de BSA, 1,2 µL dNTPs (10 mM), 1,2 µl MgCl₂ (25 mM), 0,35 µl da taq (1 U) e 2 µL de DNA digerido. A PCR foi realizada com um ciclo inicial a 94° C por 2 minutos, seguido por 35 ciclos de 94° C por 15 segundos, 55° C por 35 segundos e 68° C por 1 minuto e 30 segundos, seguido de um ciclo de final de 68° C por 1 minutos e 30 segundos. As amplificações testes foram checadas via eletroforese em gel de agarose a 1%.

Posteriormente, realizamos a etapa de enriquecimento com quatro réplicas de PCR para cada amostra, para aumentar o número dos fragmentos de DNA que realizaram a ligação com os adaptadores P1 e AY. Cada uma das quatro PCR de cada amostra ocorreram em volume final de 25 µL, sendo 11,45 µL de H₂O, 2,0 µL MgCl₂ (25 mM), 2,0 µL dNTPs

(10 mM), 2,5 µL de tampão 10X, 2,5 µL de primer P1 (2 mM), 2,5 µL de primer AY-individual (2 mM), 0,05 µL de Taq (Klentaq) e 2 µL do DNA digerido. As PCR foram realizadas em termociclador, com um ciclo inicial de 68° C por 1 minuto seguido por 18 ciclos de 93° C por 10 segundos, 52° C por 35 segundos, 68° C por 1 min e 30 segundos e um ciclo final de 68° C por 7 minutos. Em seguida, as cinco PCR foram agrupadas em um único tubo por amostra, totalizando um volume final de 100 µL.

As amplificações foram quantificadas no Qubit 2.0 (Thermo Fisher Scientific), seguindo o protocolo do fabricante. Estas amostras foram unidas em um único tubo, de maneira equimolar (200 ng/ul de cada amostra), e posteriormente foram concentradas em Speedvac até atingir aproximadamente 100 ul. Em seguida, realizamos a purificação com AMPure Beads (Beckman Coulter Inc), seguindo o protocolo dos fabricantes.

Após a purificação, selecionados fragmentos variando entre 350 – 450 pb através do Pippin Prep em gel de agarose 2 % Pippin Prep (Sage Science). Após a construção da biblioteca, realizamos o sequenciamento no sequenciador Ion Torrent (PGM, Life Technologies) com a utilização do kit de sequenciamento 318 Ion PGM chip de 400 pb, seguindo as recomendações dos fabricantes.

Análise de dados genômicos

As leituras da biblioteca genômica obtidas no Ion Torrent foram processadas no programa pyRAD 3.0.66 (Eaton 2014), onde separamos as sequências de cada indivíduo por barcode (AY-individual) e posteriormente os barcodes e adaptadores foram removidos. Em seguida, foi realizado o alinhamento destas sequências com a ferramenta Vsearch (Rognes et. al. 2016) com similaridade de 88% e os alinhamentos finais foram obtidos com a ferramenta MUSCLE. Os arquivos de saída (output) foram gerados a partir de uma matriz de dados para análises populacionais, somente com o complexo *O. catherinae* e a espécie *Oecomys* sp. nov., e uma matriz de dados para análises filogenéticas com a inclusão do grupo externo (*O. auyantepui*, *O. bicolor*, *O. paricola*, *Hylaeamys megacephalus* e *Sooretamys angouya*).

As árvores filogenéticas foram estimadas através do método de Máxima verossimilhança (MV) no programa RAxML versão 8 (Stamatakis 2014) e do método de Inferência Bayesiana (IB) no programa MrBayes 3.2.7a (Ronquist et al. 2012). Para a análise de MV, utilizamos o modelo GTR+GAMMA com 1.000 réplicas de bootstrap. Para a IB, utilizamos 50 milhões de gerações amostradas a cada 1.000 gerações e 25% de *burnin*.

Para a inferência da árvore de espécies, utilizamos a matriz de SNP (*Single Nucleotide Polimorphism*) não ligados, convertida pelo pacote Phrynomics do R. A ferramenta utilizada para gerar a árvore de espécies foi o pacote SNAPP 1.3.0 implementado no Beauti e Beast 2.4.7 (Bouckaert et al. 2014), com as taxas de mutação U e V = 1 e lambda *prior* com distribuição gamma estimada pelo programa. A cadeia de MCMC teve o comprimento de um milhão de gerações, amostrados a cada 1.000 e 10% de *burnin*. A convergência entre as cadeias foi observada através dos valores de ESS no programa Tracer 1.6 (Rambaut et al. 2014).

Para a delimitação das linhagens do complexo *O. catherinae*, obtidos com os resultados das análises de MV e IB dos ddRADseq, utilizamos o *Bayes factor delimitation* (BFD*). Testamos seis modelos com distintos números e arranjos de linhagens, cada um deles com *path sampling* de 48 *steps*, com 1.000 gerações por *step*, 10% de *burnin* e alpha de 0,3. A avaliação dos modelos com delimitações de linhagens alternativas foi realizada com o ranqueamento conforme o marginal *likelihood*, seguindo o *Bayes Factor* de Kass & Raftery (1995) para comparação de modelos.

Para estimar o tempo de divergência entre as linhagens, utilizamos como ponto de calibração a diversificação estimada entre *Oecomys* e *Hylaeamys* em 3,5 M.a (Leite et al. 2014), com desvio padrão de 0,5 M.a. Além disso, utilizamos a taxa de mutação estimada com base em Kimura (1980). Considerando a distância genética média (*p-distance*) de 4,289% entre *Oecomys* e *Hyaleamys* para o conjunto de dados com 612854 loci e o tempo de divergência entre as duas espécies, estimada em 3,5 M.a., a taxa de mutação foi de 0,0062 substituições por sítio por milhão de ano. A análise foi realizada no programa Beast 1.8.0 através do Relógio Relaxado Lognormal não Correlacionado e Yule Process como prior, com 50 milhões de gerações, uma amostragem de árvore a cada 1.000 gerações, e *burnin* de 10%. Posteriormente, as árvores foram sumarizadas no programa TreeAnnotator 1.7.1 (Drummond et al. 2012) e visualizadas no FigTree 1.4.3 (Rambaut 2016).

A verificação da estrutura populacional e grupos biológicos foi realizada através do programa FastSTRUCTURE (Raj et al. 2014), com os agrupamentos estimados com o *prior simple*. Realizamos interações com K= 1-10, sendo o modelo K que melhor explica a estrutura do conjunto de dados estimado pela ferramenta chooseK.py. Posteriormente, utilizamos o distruct.py para visualização gráfica dos agrupamentos do melhor K.

Dados morfométricos

Para as análises morfométricas, utilizamos as informações de linhagens obtidas nas análises genéticas. Ademais, como não foi possível distinguir morfologicamente os exemplares pertencentes aos subclados leste A e leste B através de caracteres morfológicos qualitativos, alocamos exemplares sem dados moleculares a estes subclados com base na distribuição geográfica. Assim, exemplares entre o sul do rio Jequitinhonha e norte do rio Paraíba do Sul foram alocados ao subclado leste B, e os exemplares ao sul deste último rio, ao subclado leste A (Figura 2). A linhagem nordeste, localizada ao norte do rio São Francisco, está representada em nossas amostras apenas por um exemplar, sem dados morfométricos, não sendo possível incluí-la nas análises morfométricas. Com isso, restringimos a análise morfométrica a cinco supostas linhagens/subclados de *O. catherinae* (extremo oeste, norte, central, leste A e leste B) e à espécie *Oecomys* sp. nov. .

Examinamos o crânio de 77 exemplares do complexo *O. catherinae* e 14 exemplares da espécie *Oecomys* sp. nov. (Anexo 02), estes adicionados na análise devido a estreita relação desta espécie com o complexo, visto que foi recentemente descrita como distinta de *O. catherinae*. Extraímos 17 medidas craniodentárias utilizando paquímetro digital com precisão de duas casas decimais enquanto os espécimes eram examinados em estereomicroscópio. Seguimos Voss (1988) para 13 dimensões craniodentárias: largura entre os côndilos occipitais (LCO), largura através do forame incisivo (LFI), largura do dente incisivo (LI), largura do primeiro molar superior (LM1), largura do nasal (LNA), largura da placa zigomática (LZP), comprimento côndilo–incisivo (CCI), comprimento coronal dos molares superiores (CCM), largura do zigomático (LZI), menor largura interorbital (LIO), comprimento do forame incisivo (CFI), comprimento do nasal (CN) e comprimento do diastema superior (CDI). Além destas, seguimos Carleton & Musser (1995) para as dimensões craniodentárias largura da bula auditiva (LBU), comprimento da ponte palatina (CPP), comprimento do rostro (CR) e comprimento occipto-nasal (CON).

Os exemplares foram agrupados em classes etárias de acordo com a eclosão e desgaste dos dentes seguindo Reig (1977). Utilizamos somente dados morfométricos de exemplares adultos como variáveis nos testes estatísticos. O dimorfismo sexual foi testado através do teste t de Student aplicado a exemplares pertencentes a uma mesma linhagem. Os dados foram transformados em logaritmos na base 10 para a realização de Análise de Componentes Principais (CP) e Análise Discriminante (AD), com o intuito de testar possíveis diferenças morfométricas para os agrupamentos identificados a partir das análises

moleculares. Todos os testes estatísticos foram realizados no programa SPSS 20 com nível de significância de 5%.

3. RESULTADOS

Dados mitocondriais

A análise de inferência Bayesiana com o banco de dados com o marcador mtDNA *Citb* recuperou a espécie *Oecomys* sp. nov. com alto suporte (PP = 1), irmã (PP = 0,9) do complexo *O. catherinae* (PP= 1), este último formado por cinco linhagens, cada uma com suporte $\geq 0,99$ (o suporte para a linhagem nordeste, constituída por um único exemplar, não foi calculado). Com alto suporte, a linhagem extremo oeste (PP = 1), composta por exemplares da região oeste da Amazônia brasileira e Amazônia do Peru, aparece como irmã das demais. Também com alto suporte, as linhagens nordeste, com o exemplar da região ao norte da Mata Atlântica, linhagem norte, com exemplares do norte da Amazônia, linhagem central, com exemplares do cerrado (PP = 1) e linhagem leste com exemplares da Mata Atlântica (PP = 0,99) formam um grupo monofilético, porém as relações entre elas não estão bem resolvidas, sustentadas por baixo suporte (Figuras 1 e 2). Dentro da linhagem leste verificamos a ocorrência de dois subclados com alto suporte filogenético (PP \geq 0,99), aqui denominados subclados leste A e leste B (Figuras 1 e 2).

A rede de haplótipos obtida com os dados de *Citb* (Figura 3) apontou uma clara separação para a maioria das linhagens recuperadas na análise filogenética. O haplogrupo de *Oecomys* sp. nov. aparece mais distante, separado por 45 passos mutacionais do haplogrupo mais próximo (extremo oeste). O haplogrupo extremo oeste separa-se do haplogrupo nordeste por 34 passos mutacionais e dos demais haplogrupos por 21 (norte), 25 (leste) e 28 (central) passos mutacionais. No haplogrupo leste não recuperamos o compartilhamento de haplótipos entre os subclados A e B, mas o número de passos mutacionais que separa estes subclados é de apenas dois. O haplogrupo central separa-se dos haplogrupos norte e leste por 13 passos mutacionais, e o haplogrupo norte e leste estão separados por 10 passos mutacionais (Figura 3).

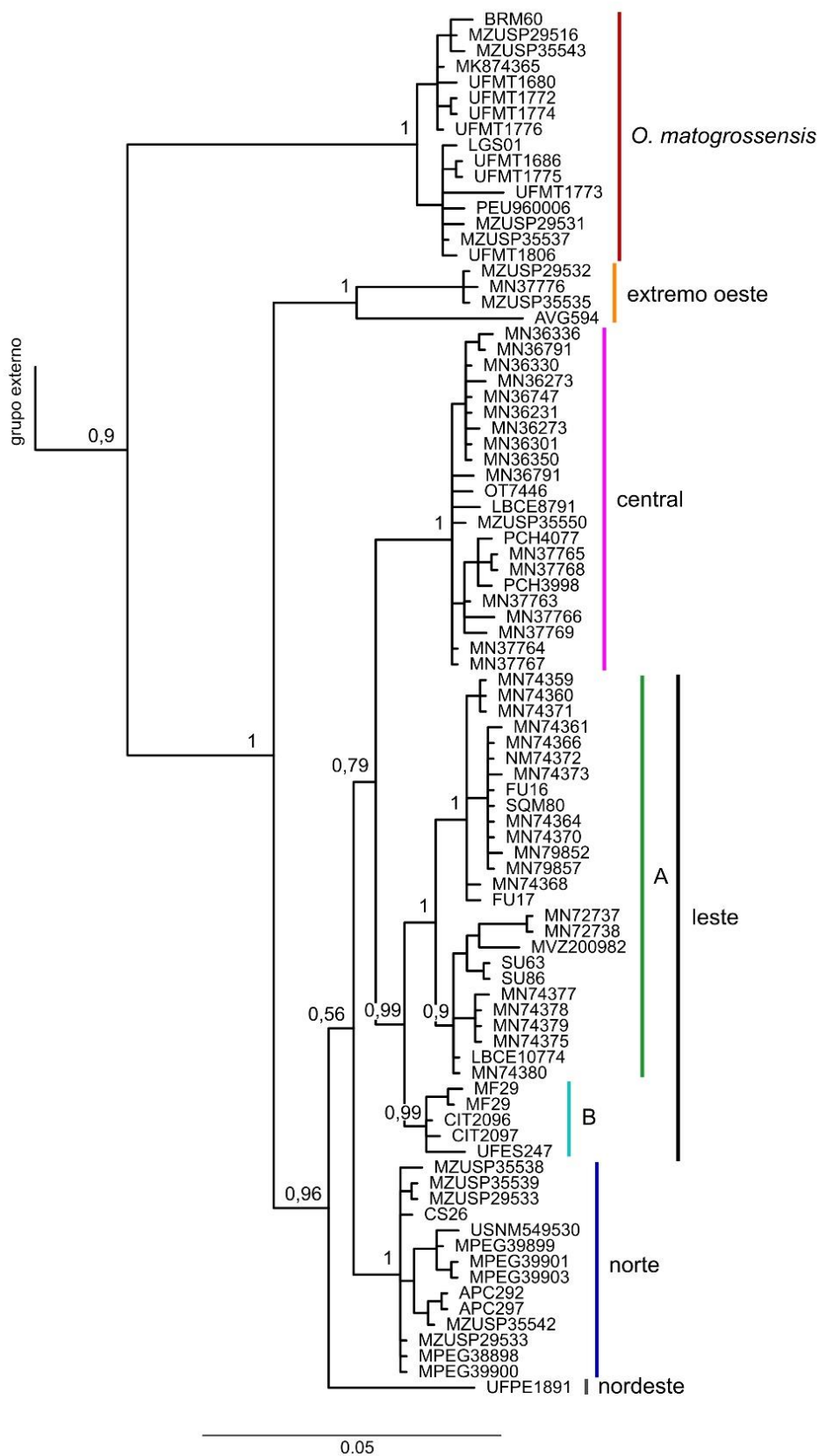


Figura 1. Topologia de inferência Bayesiana com o marcador mitocondrial Citocromo b de *Oecomys* sp. nov. e do complexo *O. catherinae* (senso Saldanha & Rossi, no prelo). Números próximos aos ramos indicam a probabilidade posterior (PP). Os dados das amostras e grupo externo utilizados são apresentados no Anexo 01: tabela 1.

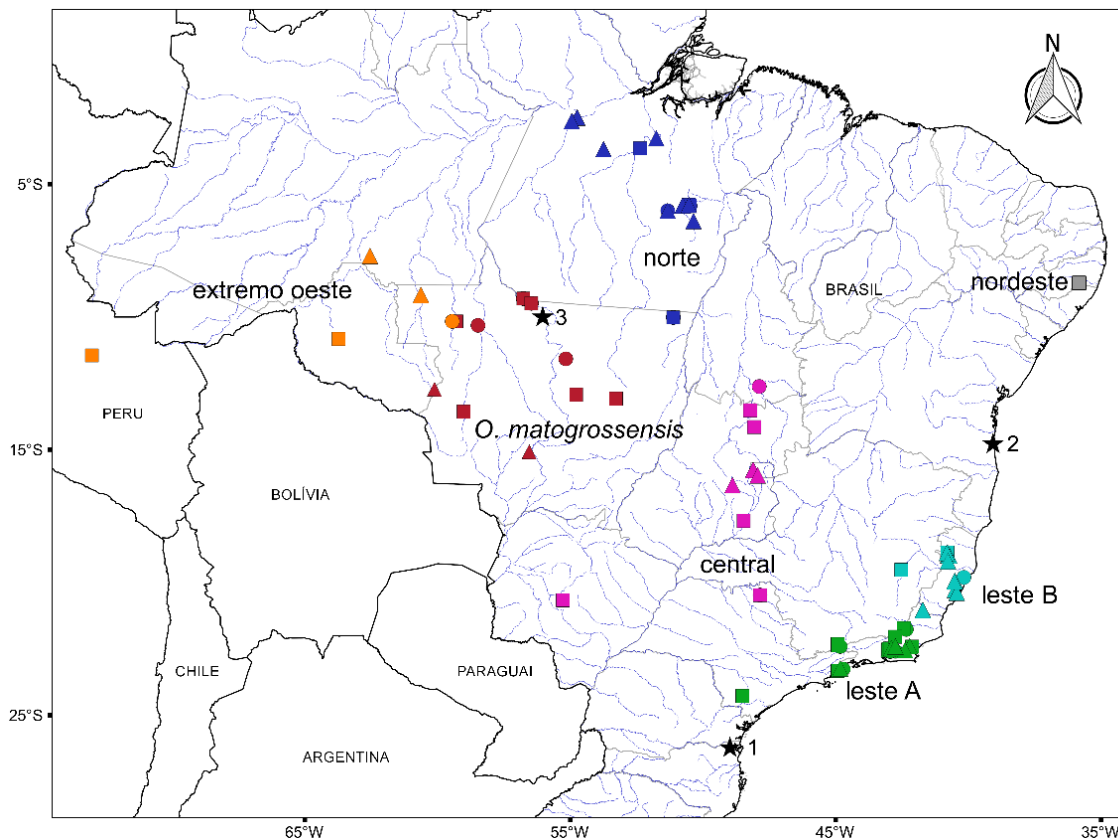


Figura 2. Mapa com as localidades das amostras de *Oecomys* sp. nov. e do complexo *O. catherinae* (senso Saldanha & Rossi, no prelo). As cores representam as espécies e linhagens obtidas nas análises filogenéticas. Triângulos representam exemplares com dados morfológicos, quadrados com dados moleculares, e círculos com ambos os dados. As estrelas pretas representam a localidade tipo de *O. catherinae* (1), *O. bahiensis* (2) e *Oecomys* sp. nov. (3).

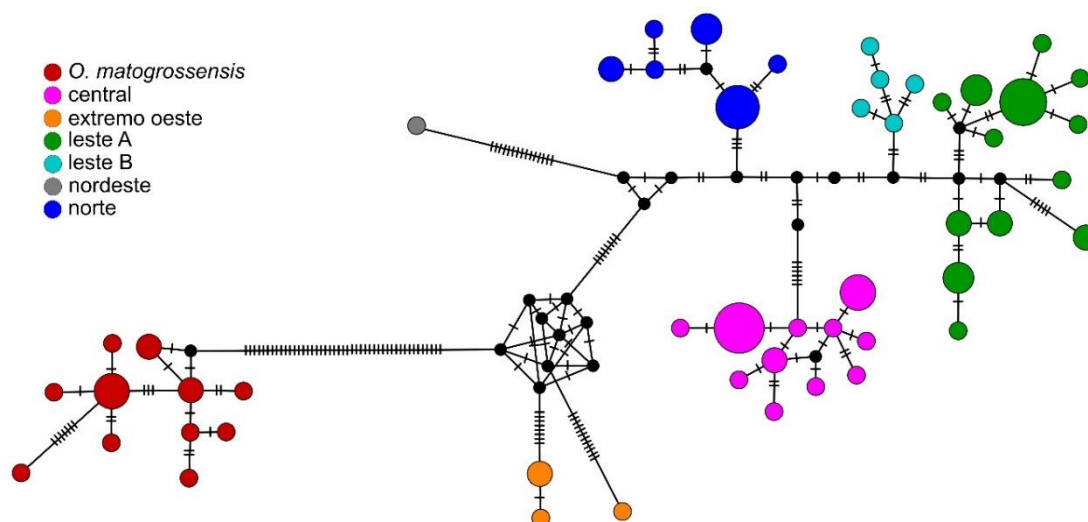


Figura 3. Rede haplotípica com o marcador mitocondrial Citocromo b de *Oecomys* sp. nov. e do complexo *O. catherinae* (senso Saldanha & Rossi, no prelo). As cores representam as espécies e linhagens obtidas nas análises filogenéticas, e o tamanho das amostras (círculos) representa o número de haplótipos. Círculos pretos representam haplótipos não amostrados e as barras representam eventos de passos mutacionais.

Dados genômicos

As análises moleculares com ddRADseq resultaram em hipóteses filogenéticas com alto suporte, confirmando o monofiletismo de *Oecomys* sp. nov. e do complexo *O. catherinae* (senso Saldanha & Rossi, no prelo), assim como a relação entre estes clados, sendo congruente com a maior parte dos resultados obtidos pelos dados de Citb, exceto pela posição da linhagem nordeste que aparece nitidamente relacionada à linhagem leste (Figura 4), porém, na filogenia com Citb a linhagem nordeste aparece agrupada com as linhagens norte, central e leste, com a posição dentro do grupo não definida (Figura 1).

No complexo *O. catherinae* recuperamos quatro linhagens com alto valor de suporte (PP = 1 e bootstrap = 100): norte, central, leste e extremo oeste. Dentro da linhagem leste recuperamos os subclados A e B com alto suporte (leste A: PP = 1 e bootstrap = 100; leste B: PP = 1 e bootstrap = 90), assim como a amostra do nordeste, esta última como irmã dos subclados leste A e B (Figura 4).

A estimativa de tempo de divergência molecular apontou que os eventos de diversificação relacionados a *Oecomys* sp. nov. e *O. catherinae* ocorreram durante o Pleistoceno. O surgimento do clado composto por *Oecomys* sp. nov. e as linhagens do complexo *O. catherinae* ocorreu há cerca de 2,35 M.a. (95% HPD = 2,02–2,77), e a diversificação entre estes dois grupos foi estimada para 1,53 M.a. (95% HPD = 1,29–1,8). Dentro do complexo, o ancestral da linhagem do extremo oeste diversificou há cerca de 1,05 M.a. (95% HPD = 0,89–1,23). O ancestral da linhagem norte diversificou há 0,85 M.a. (95% HPD = 0,73–1,01), e as linhagens central e leste se diversificaram há cerca de 0,58 M.a. (95% HPD = 0,5–0,68). Dentro da linhagem leste, a amostra do nordeste divergiu das demais há cerca de 0,47 M.a. (95% HPD = 0,41–0,54), e os subclados A e B divergiram entre si há cerca de 0,4 M.a. (95% HPD = 0,35–0,46) (Figura 5).

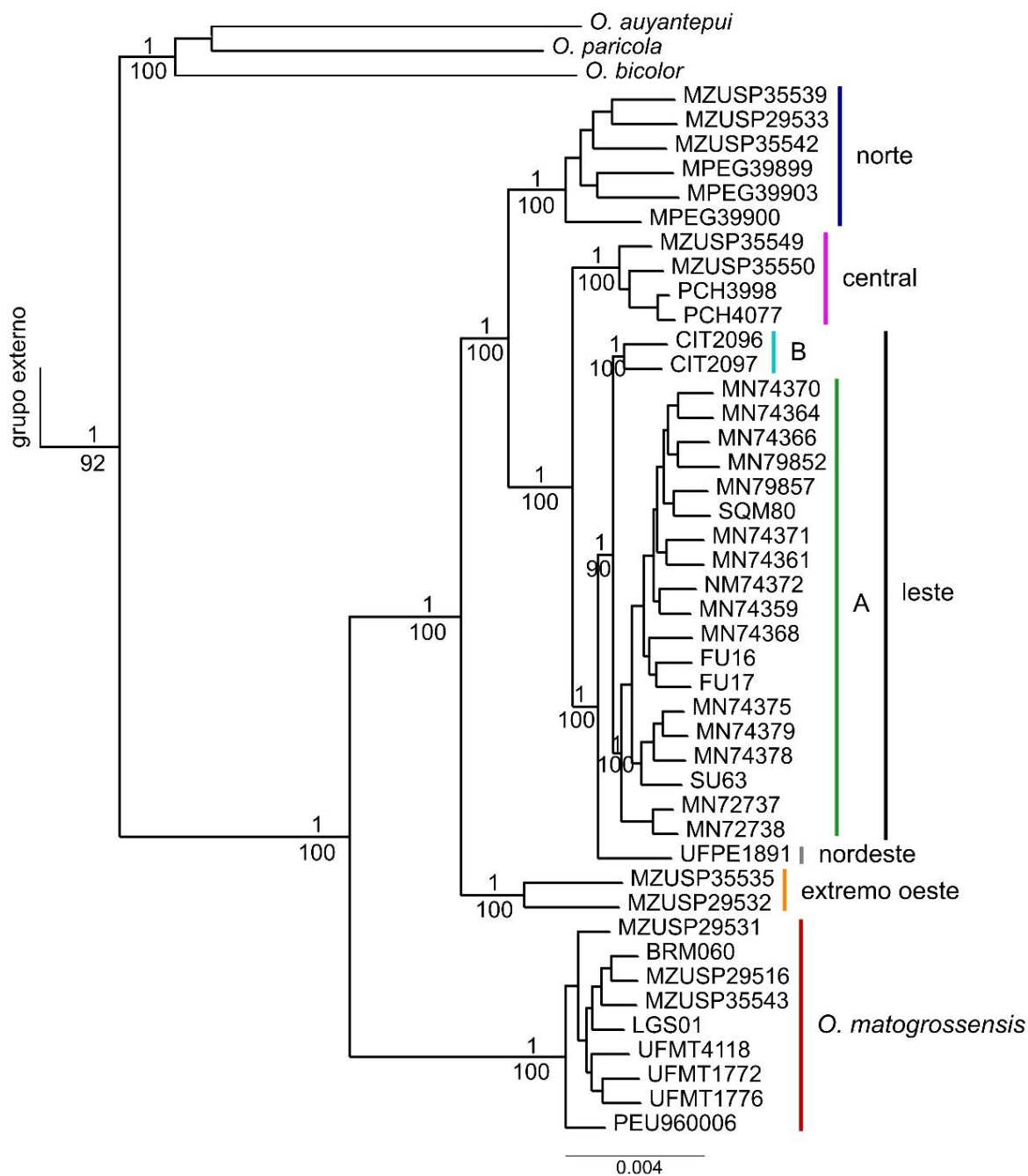


Figura 4. Topologia de inferência Bayesiana com matriz de dados de ddRADseq de *Oecomys* sp. nov. e do complexo *O. catherinae* (senso Saldanha & Rossi, no prelo). Valores acima dos ramos indicam a probabilidade posterior (PP) e, abaixo dos ramos, o valor de bootstrap. Os dados das amostras são apresentados no Anexo 01: tabela 1.

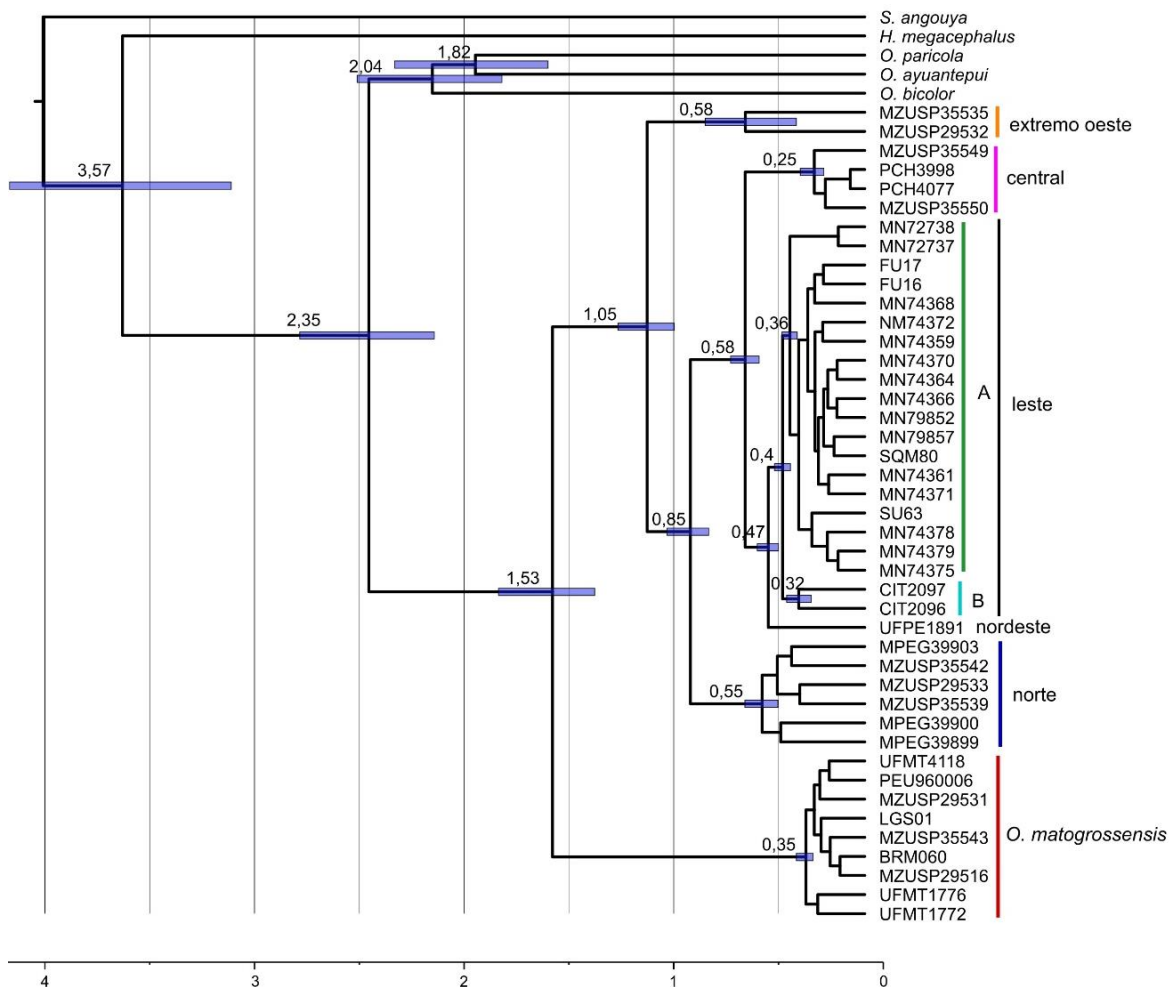


Figura 5. Árvore datada de *Oecomys* sp. nov. e do complexo *O. catherinae* (senso Saldanha & Rossi, no prelo). Os valores acima dos nós se referem às datas de divergência estimadas em milhões de anos pelo BEAST, e as barras correspondem aos intervalos de confiança de 95% das datas estimadas. Os dados das amostras são apresentados no Anexo 01: tabela 1.

Entre os seis modelos de delimitação das linhagens testadas, o BFD* selecionou como o melhor modelo a topologia com *Oecomys* sp. nov. irmão do complexo *O. catherinae*, este último composto por seis linhagens (Marginal Likelihood = -2976,7, Tabela 1). Estas linhagens são coincidentes com as encontradas nas análises de IB e MV com RADseq e também com aqueles presentes nas análises com Citb. O SNAPP recuperou alto suporte para a relação entre a maioria das linhagens (Figura 6), exceto para as relações entre leste A e B (0,5) e destas com a linhagem nordeste (0,81).

Tabela 1. Modelos de linhagens testadas pela *Bayes Factor Delimitation* (BFD*) para os dados se SNPs. ML: marginal likelihood, BF= Bayes Factor.

Modelo testado	linhagens	ML	BF	classificação
<i>Oecomys</i> sp. nov. / complexo <i>O. catherinae</i> (taxonomia atual)	2	-7306,8	-	-
<i>Oecomys</i> sp. nov. / extremo oeste / norte+central+leste	3	-6242,1	-2129,5	5
<i>Oecomys</i> sp. nov. / extremo oeste / norte / central / leste	5	-4836,1	-4941,4	4
<i>Oecomys</i> sp. nov. / extremo oeste / norte / central / leste A+B / nordeste	6	-3271,3	-8071,1	2
<i>Oecomys</i> sp. nov. / extremo oeste / norte / central / leste A / nordeste+leste B	6	-4603,6	-5406,4	3
<i>Oecomys</i> sp. nov. / extremo oeste / norte / central / leste A / leste B / nordeste	7	-2976,7	-11637,0	1

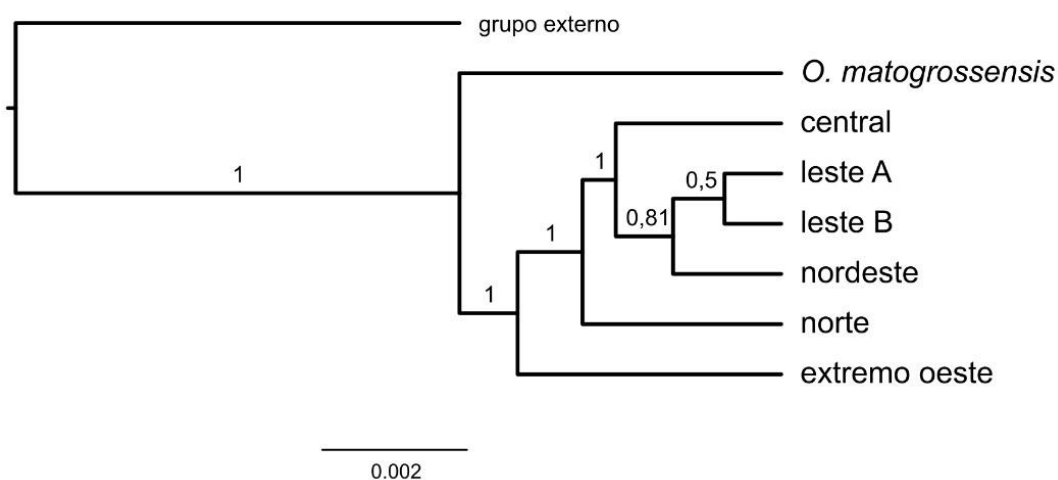


Figura 6. Árvore de espécie obtida no programa SNAPP para o modelo com *Oecomys* sp. nov. mais seis linhagens/subclados de *O. catherinae* (extremo oeste, norte, central, nordeste, leste A e leste B).

A análise realizada no FastSTRUCTURE apontou o $K = 4$ (Figura 7) como o mais provável para explicar a estrutura do banco de dados testado. Esta análise identificou agrupamentos biológicos com nenhum admixture e distintos daqueles apontados pelas análises filogenéticas de RADseq e mtDNA. Esses agrupamentos incluem na mesma população os subclados leste A, leste B, linhagens nordeste e central, as demais populações com linhagens isoladas (extremo oeste, norte e *Oecomys* sp. nov.).

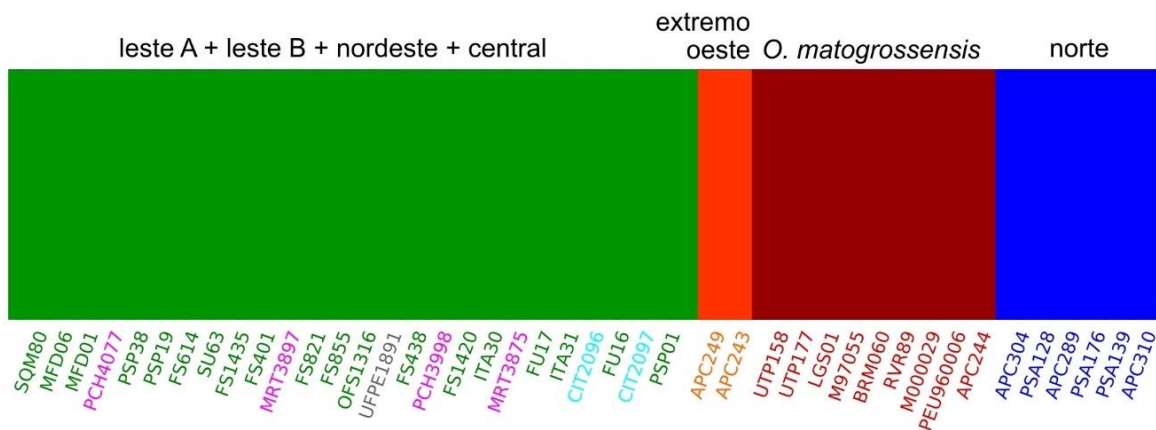


Figura 7. Grupos biológicos apontados pelo FastSTRUCTURE com K=4 para *Oecomys* sp. nov., e as linhagens do complexo *O. catherinae*. As cores aplicadas aos exemplares indicam as espécies e linhagens reconhecidas nas análises filogenéticas.

Dados morfométricos

A Análise de Componentes Principais indica que o primeiro componente principal (CP 1) explica 57,75% da variação total e o segundo componente principal (CP 2), 9,24% da variação total. As medidas que mais contribuíram para o CP 1 foram comprimento occipito-nasal (CON) e comprimento côndilo-incisivo (CCI). Já no CP 2, as principais medidas foram largura do primeiro molar superior (LM1) e comprimento coronal dos molares superiores (CCM; Tabela 2). O gráfico dos escores do primeiro e segundo componentes mostrou que exemplares de *Oecomys* sp. nov. separam-se completamente dos exemplares da linhagem central e leste A de *O. catherinae* ao longo do eixo do CP1 e tendem a se separar das demais linhagens do complexo ao longo deste mesmo eixo (Figura 8A), que expressa o tamanho geral dos exemplares uma vez que os coeficientes são todos positivos neste componente principal (Tabela 2). Ademais, a linhagem leste A sobrepõe parcialmente com a linhagem norte e extremo oeste ao longo do eixo da CP1, e há ampla sobreposição entre as linhagens leste A, leste B e central ao longo do mesmo eixo. Não há separação de nenhuma das amostras ao longo do eixo da CP2.

Tabela 2. Resultado da Análise de Componentes Principais de espécimes de *Oecomys* sp. nov. e linhagens do complexo *Oecomys catherinae* com base em 17 medidas crânio-dentárias. As descrições das medidas são apresentadas na seção Material e Métodos.

	Componente		
	1	2	3
CON	0,97	-0,04	-0,05
CCI	0,96	0,01	-0,02
CDI	0,92	-0,13	-0,12
LPZ	0,78	0,00	0,01
LNA	0,75	0,13	0,01
CN	0,65	-0,05	-0,63
CR	0,88	-0,04	-0,18
LIO	0,77	-0,01	0,38
LZI	0,88	0,08	-0,11
LFI	0,66	-0,15	-0,04
CFI	0,84	-0,10	0,15
CPP	0,70	0,24	-0,13
LCO	0,71	-0,27	0,50
LBU	0,54	-0,45	0,24
LI	0,80	-0,07	-0,06
LM1	0,25	0,83	0,24
CCM	0,49	0,69	0,04
% da variação	57,75	9,24	6,00

A Análise de Função Discriminante indica que a primeira função é responsável por 69,5% da variação, enquanto a segunda função responde por 18,8% da variação. As medidas que mais contribuíram para a função 1 foram o comprimento do rostro (CR, coeficiente negativo) e a largura do zigomático (LZI, coeficiente negativo). Para a função 2, as medidas que mais contribuíram foram a largura do incisivo (LI, coeficiente negativo) e forame incisivo (LFI, coeficiente positivo; Tabela 3).

O gráfico com as funções discriminantes 1 e 2 confirma a clara separação da espécie *Oecomys* sp. nov. em relação ao complexo *O. catherinae* ao longo do eixo da primeira função. No complexo *O. catherinae*, a linhagem extremo oeste não se sobrepõe às linhagens leste A e central, e a linhagem norte tende a se separar das demais linhagens ao longo do eixo da função 2. Em contrapartida, as linhagens central, leste A e leste B estão amplamente sobrepostas entre si (Figura 8B).

Tabela 3. Resultado da análise de Função Discriminante de espécimes de *Oecomys* sp. nov. e linhagens do complexo *Oecomys catherinae* com base em 17 medidas crânio-dentárias. As descrições das medidas são apresentadas na seção Material e Métodos.

	Função				
	1	2	3	4	5
CON	0,31	0,23	-2,18	-0,56	-0,48
CCI	0,42	-0,47	0,94	-0,24	-0,11
CDI	0,27	-0,67	0,62	0,31	0,52
LPZ	0,25	-0,24	0,16	-0,50	-0,08
LNA	-0,05	0,19	0,28	-0,05	-0,14
CN	0,12	-0,68	0,32	0,28	0,23
CR	-0,78	0,49	0,40	-0,15	0,37
LIO	0,38	-0,05	-0,28	0,50	0,05
LZI	-0,64	0,57	0,87	-0,42	-0,44
LFI	0,13	0,71	-0,13	0,34	0,35
CFI	0,10	0,67	-0,23	-0,22	0,03
CPP	-0,15	0,44	-0,24	1,05	-0,37
LCO	0,56	-0,12	-0,08	-0,04	0,25
LBU	0,41	0,03	0,44	0,01	-0,71
LI	0,08	-0,76	-0,34	0,30	0,23
LM1	-0,10	0,28	-0,34	-0,17	-0,29
CCM	0,16	-0,21	0,56	-0,08	0,73
% da variação	69,5	18,8	6,4	4,3	1,1
Autovalor	3,88	1,05	0,36	0,24	0,06

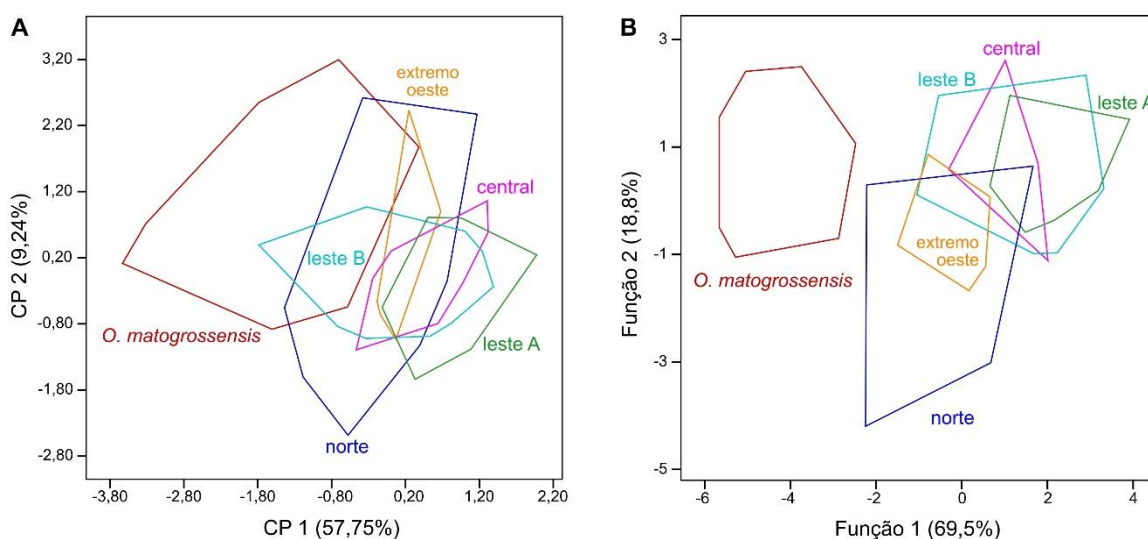


Figura 8. Gráfico de dispersão dos componentes principais 1 e 2 (A) e funções discriminantes 1 e 2 (B), de espécimes de *Oecomys* sp. nov. e linhagens do complexo *Oecomys catherinae* com base em 17 medidas crânio-dentárias.

4. DISCUSSÃO

Os recentes estudos envolvendo sistemática e diversidade genética do gênero *Oecomys* proporcionaram uma nova visão sobre *Oecomys catherinae*. Apontado como um complexo de espécies por diversos autores, o grupo apresenta ampla distribuição geográfica e considerável divergência genética, em contraste com a escassez ou ausência de variação morfológica (Suárez-Villota et al. 2018; Saldanha & Rossi, no prelo). Apenas uma das linhagens deste complexo pôde ser distinguida morfológicamente, descrita como uma nova espécie por Saldanha & Rossi (no prelo). Com os nossos dados, corroboramos a distinção de *Oecomys* sp. nov. do complexo *O. catherinae* em todas as análises realizadas com mtDNA e RADseq. Recuperamos a ocorrência de dois subclados na linhagem leste, como mencionado por Saldanha & Rossi (no prelo). Ademais, esclarecemos as relações entre as linhagens, recuperando a linhagem extremo oeste como irmã das demais, seguida da linhagem norte, central e leste, discordando da topologia apresentada por Suárez-Villota et al. (2018). Por fim, recuperamos outra possível linhagem para o complexo (aqui denominada linhagem nordeste), além das linhagens já citadas, localizada ao norte do rio São Francisco.

Na filogenia com mtDNA, evidenciamos a incerteza no posicionamento da linhagem nordeste, em contraste com resultados de RADseq onde a linhagem nordeste aparece nitidamente relacionada à linhagem leste (Figuras 1 e 4, respectivamente). Incongruências entre topologias de hipóteses filogenéticas em *Oecomys* já foram relatadas na literatura (Rocha et al. 2018; Suárez-Villota et al. 2018; Saldanha et al. 2019; Saldanha & Rossi, no prelo). Por isso, o uso de marcador mitocondrial como única ferramenta para estudos de delimitação de espécies e populações é amplamente questionada, pois pode limitar a compreensão da evolução e histórico populacional (Galtier et al. 2009).

Na abordagem multilocus com RADseq, o BFD* apontou como melhor modelo para o conjunto de dados o modelo com maior número de espécies (Tabela 1). Estudos com outros grupos também verificaram que o BFD tende a apontar como melhor modelo aquele com o maior número de espécies (ver Villamil et al. 2019). Além disso, este método não considera explicitamente o fluxo gênico, isolamento por distância, seleção ou vários outros processos biológicos importantes, e os resultados devem considerar outros aspectos como a geografia das possíveis espécies antes de concluir as delimitações (Leaché & Bouckaert 2018).

Em contraposição aos métodos filogenéticos, que buscam reconstruir o passado evolutivo das espécies, as análises de estrutura populacional visam detectar padrões de fluxo gênico atuais, que permitem a delimitação geográfica das populações (Cunha &

Solé-Cava 2012). Com isso, a relação de maior proximidade da linhagem nordeste com os subclados leste A e leste B fica evidente nas análises populacionais, corroborando a topologia obtida com matriz de dados de ddRADseq. Ademais, os agrupamentos biológicos obtidos indicam a ausência de compartilhamento de haplótipos entre as espécies e linhagens analisadas (Figura 3).

Assim, nossos resultados sugerem a ocorrência de dois grupos biológicos com populações distintas (linhagens norte e extremo oeste), sem fluxo gênico, na Amazônia, e um grupo biológico com populações nas regiões de Mata Atlântica (subclados leste A, leste B e linhagem nordeste) e Cerrado (linhagem central) (Figuras 2 e 7). A ocorrência de um único grupo biológico composto por linhagens do Cerrado e Mata Atlântica vai ao encontro ao proposto por Costa (2003), ao afirmar que a região central do Brasil não se comporta como uma região separada, mas sim complementar à Amazônia ou à Mata Atlântica, a depender do táxon em questão. Em particular, no caso do grupo denominado como *Oecomys trinitatis* por Costa (2003), a autora confirma a relação do Cerrado e Caatinga como áreas irmãs da Mata Atlântica, e não da Amazônia, assim como a linhagem central do complexo *O. catherinae*.

Com a árvore datada, nossos dados apontam a divergência estimada entre *Oecomys* e *Hylaeamys* para cerca de 3,57 M.a., durante o Plioceno, semelhante aos 4,4 M.a. propostos por Parada et al. (2013). Segundo os autores, a maioria das tribos de Sigmodontinae, incluindo Oryzomyini, diversificou-se no Mioceno Superior (7,72 M.a.), com distribuição do ancestral mais recente para a região sul-americana antes do fechamento do Istmo do Panamá. A divergência entre o complexo *O. catherinae* e a espécie *Oecomys* sp. nov. foi estimada para o Pleistoceno Calabriano (cerca de 1,53 M.a.), na região amazônica. Posteriormente, ainda na região amazônica, divergiu a extremo oeste seguida da linhagem norte ainda no pleistoceno.

A diversificação da espécie *Oecomys* sp. nov. das linhagens da Amazônia podem estar associados à hipótese dos refúgios (Haffer 1969), que relaciona mudanças climáticas durante o Pleistoceno com ciclos de fragmentação e reconexão de florestas, que formavam refúgios, isolando populações e promovendo a especiação. Apesar do número, tamanho e localização destes refúgios ainda serem incertos, a distribuição de *Oecomys* sp. nov. e da linhagem extremo oeste coincidem com possíveis refúgios nas florestas úmidas adjacentes do Planalto dos Parecís (Haffer 2008). Similarmente, a área de distribuição da linhagem norte pode ter surgido na Serra do Cachimbo, cujos arredores constituídos por

terras baixas foram cobertos por camadas de areia no Pleistoceno tardio (Haffer 2008; Haffer & Prance 2002), promovendo o isolamento de populações nas partes mais altas da Serra.

A linhagem central, que ocupa o Cerrado, divergiu das linhagens da Mata Atlântica no Pleistoceno médio (cerca de 0,58 M.a.), mesmo período estimado para a divergência das linhagens e clados dentro da Mata Atlântica (0,47 e 0,4 M.a). Costa et al. (2000), em análise parcimoniosa de endemismo, identificou a ocorrência de duas regiões (norte e sul) na Mata Atlântica e propôs que a Serra da Mantiqueira seria o local da divisão entre essas regiões. Outros estudos na Mata Atlântica também identificaram uma lacuna entre os táxons do norte e sul, que coincide com a Depressão do rio Paraíba do Sul, localizado entre duas principais montanhas do sudeste do Brasil, a Serra da Mantiqueira e a Serra do Mar (Silva & Straube 1996). Entretanto, para *O. catherinae*, as divergências entre as linhagens da Mata Atlântica não são compatíveis com a formação da Serra do Mar e Serra da Mantiqueira, estimadas durante o Plioceno-Pleistoceno (ver Silva & Straube 1996).

Na Mata Atlântica, a estrutura genética de alguns táxons coincide com a presença de sistemas fluviais, sendo a quebra filogeográfica mais profunda coincidente com o sistema do rio Doce (Costa & Leite 2012). Apesar disso, para os subclados A e B da linhagem leste, o rio Doce não atua como um divisor, visto que exemplares do subclado leste B estão presentes ao norte (UFES247) e ao sul (MF29) deste rio. Além disso, para o roedor *Akodon cursor*, o rio Doce não constitui uma barreira efetiva ao fluxo gênico entre populações (Colombi et al. 2010). Estudos sobre o papel dos rios da Mata Atlântica como barreiras ainda são negligentes, porém, entre as teorias mais citadas como possíveis explicações para a quebras populacionais da Mata Atlântica, estão as mudanças climáticas e vegetais que ocorreram no Plioceno e Quaternário (Costa & Leite 2012). Resultado semelhante foi encontrado por Nascimento et al. (2013), onde a diversificação de *Thrichomys* não foi associada ao rio São Francisco como barreira, devido à idade mais avançada do rio em relação à origem de *Thrichomys*. Segundo os autores é mais provável que o padrão de diversificação observado seja consequência de mudanças climáticas e períodos áridos.

Distintos componentes nas regiões norte e sul da Mata Atlântica foram relatados por Costa (2003). Para o roedor *Rhipidomys* e o marsupial *Micoureus*, por exemplo, os clados recuperados pela autora correspondem a espécies distintas; já para o marsupial *Metachirus nudicaudatus*, Costa (2003) recuperou dois clados estruturados geograficamente. Segundo a autora, essa quebra entre espécies e clados ao norte e sul da Mata Atlântica é coincidente e as flutuações climáticas são uma explicação plausível para

este padrão coincidente no espaço, mas não no tempo. Apesar disso, para a diversificação entre as linhagens nordeste, que ocorre ao norte do rio São Francisco, e entre os subclados leste A e leste B, entre distintas regiões do rio Paraíba do Sul, as divergências estimadas são compatíveis com as mudanças climáticas ocasionadas pela glaciação Mindel estimada em 0,45 M.a. (Nascimento et al. 2013).

Nossos resultados morfométricos indicam a sobreposição entre as linhagens analisadas, principalmente as procedentes da Mata Atlântica (consideramos as amostras ao sul do rio Paraíba do Sul como pertencentes ao subclado leste A e ao norte do subclado leste B) e Cerrado (Figura 8B). Apesar de todas as hipóteses filogenéticas apontarem a divergência molecular entre linhagens, os agentes evolutivos, como a seleção natural, não atuam diretamente sobre a diversidade genética, mas sim sobre os fenótipos (Shorrocks 1980). Por isso, linhagens que não podem ser reconhecidas como espécies distintas a partir da morfologia representam espécies crípticas, como é o caso dos subclados leste A, leste B e linhagem central. A definição mais recente do conceito de espécie unificada sugere que, para serem consideradas espécies, as linhagens não necessitam ser distinguíveis ou diagnosticáveis morfologicamente, monofiléticas, isolados reprodutivamente, ecologicamente divergentes ou outras definições (de Queiroz 2007). Segundo o autor, basta as linhagens evoluírem separadamente de outras linhagens. Entretanto, estas definições podem servir como critérios para avaliar se as espécies estão evoluindo separadamente (de Queiroz 2007).

Levando em consideração o conjunto de análises apresentados, nossos resultados apontam os subclados A e B da linhagem leste como possíveis linhagens alopátricas que, junto com as linhagens nordeste e central, representam um grupo biológico com indícios de especiação, dada a divergência evolutiva apontada pelas hipóteses filogenéticas. Já as linhagens extremo oeste e norte, apesar da ausência de caracteres diagnósticos (Saldanha & Rossi, no prelo) e leve sobreposição morfométrica, representam linhagens evolutivas distintas. O reconhecimento da linhagem norte como espécie distinta é corroborado por caracteres citogenéticos, com os representantes desta linhagem apresentando cariótipo com $2n = 62$, distinto das demais linhagens, $2n = 60$ (Suárez-Villota et al. 2018; Malcher et al. 2017; Saldanha & Rossi, no prelo).

Neste estudo, apresentamos a primeira abordagem para a inferência filogenética e diversificação do complexo *O. catherinae* com mtDNA, ddRADseq e morfometria combinados. Devido às semelhanças morfológicas entre as linhagens e variação individual de caracteres dentro das linhagens, as análises integrativas são essenciais para

auxiliar o entendimento da diversidade oculta deste complexo. Com nossos resultados, confirmamos *Oecomys* sp. nov. como espécie distinta do complexo, e a existência de três espécies no complexo *O. catherinae* que correspondem as linhagens extremo oeste (espécie 1), linhagem norte (espécie 2) e as linhagens leste A e B, nordeste e central (espécie 3 = *Oecomys catherinae*). Não pudemos confirmar se a evolução das linhagens da Mata atlântica e Cerrado possuem histórias evolutivas distintas, o que nos leva a considerar estas linhagens como uma única espécie. Para elucidar as relações evolutivas entre os subclados da Mata Atlântica, sugerimos um estudo mais amplo com amostras provenientes do estado da Bahia e demais pontos da porção mais norte da Mata Atlântica.

5. REFERÊNCIAS BIBLIOGRÁFICAS

Aljanabi, S. M. & Martinez, I. (1997). Universal and rapid salt-extraction of high quality genomic DNA for PCR-based techniques. *Nucleic Acids Research*, 25, 4692–4693.

Asfora, P.H., Palma, A.R.T., Astúa, D. & Geise, L. (2011). Distribution of *Oecomys catherinae* Thomas, 1909 (Rodentia: Cricetidae) in northeastern Brazil with karyotypical and morphometrical notes. *Biota Neotropical*, 11(2), 415–424.

Bandelt, H.J., Forster, P. & Röhl, A. (1999). Median-joining networks for inferring intraspecific phylogenies. *Molecular Biology Evolution*, 16(1), 37–48.

Bouckaert, R., Heled, J., Kühnert, D., Vaughan, T., Wu, C-H., Xie, D., Suchard, M.A., Rambaut, A., & Drummond, A. J. (2014). BEAST 2: A Software Platform for Bayesian Evolutionary Analysis. *PLoS Computational Biology*, 10(4), e1003537.

Carleton, M.D. & Musser, G.G. (1995). Systematic studies of oryzomyine rodents (Muridae: Sigmodontinae): definition and distribution of *Olygoryzomys vegetus* (Bangs, 1902). *Proceedings of the biological society of Washington*, 108(2), 338–369.

Carleton, M.D. & Musser, G.G. (2015). Genus *Oecomys* Thomas, 1906. In: *Mammals of South America, vol.2, Rodents* (Eds Patton, J., Pardiñas, U.F.J. & D’Elia, G.). University of Chicago Press, Chicago, Illinois. pp. 393–417.

Colombi, V.H., Lopes, S.R. & Fagundes, V. (2010). Testing the rio Doce as a riverine barrier in shaping the Atlantic rainforest population divergence in the rodent *Akodon cursor*. *Genetics and Molecular Biology*, 33(4), 785–789. doi.org/10.1590/S1415-47572010000400029

Costa, L.P. (2003). The historical bridge between the Amazon and the Atlantic Forest of Brazil: a study of molecular phylogeography with small mammals. *Journal of Biogeography*, 30, 71–86.

Costa, L.P., Leite, Y.L.R., Fonseca, G.A.B. & Fonseca, M.T. (2000). Biogeography of South American Forest Mammals: Endemism and Diversity in the Atlantic Forest. *Biotropica*, 32(4b), 872–881.

Costa, L.P. & Leite, Y.L. (2012). Historical Fragmentation Shaping Vertebrate Diversification in the Atlantic Forest Biodiversity Hotspot. In: *Bones, Clones, and Biomes: The History and Geography of Recent Neotropical Mammals*. (Editores: Patterson, B. D. & Costa, L. P.) University of Chicago Press. pp. 283–306.

Cunha, H.A. & Solé-Cava, A.M. (2012). Análise filogeográfica. In *Biologia Molecular e Evolução*. 2ª edição (Editores: Matioli, S.R. & Fernandes, F.M.C). Holos Editora, Ribeirão Preto, Brasil. pp 197–215.

- Darriba, D., Taboada, G.L., Doallo, R. & Posada, D. (2012). jModelTest 2: more models, new heuristics and parallel computing. *Nature Methods*, 9(8), 772.
- De Queiroz, K. (2007). Species Concepts and Species Delimitation. *Systematic Biology*, 56(6), 879–886.
- Doyle, J.J. & Doyle, J.L. (1987). A rapid DNA isolation procedure for small quantities of fresh leaf tissue. *Phytochemical Bulletin*, 19, 11–15.
- Drummond, A.J., Suchard M.A., Xie D. & Rambaut A. (2012). Bayesian Phylogenetics with BEAUti and the BEAST 1.7. *Molecular Biology and Evolution*, 29(8), 1969–1973.
- Eaton, D. A. R. (2014). PyRAD: Assembly of de novo RADseq loci for phylogenetic analyses. *Bioinformatics*, 30(13), 1844–1849.
- Galtier, N., Nabholz, B., Glémin, S. & Hurst, G.D.D. (2009). Mitochondrial DNA as a marker of molecular diversity: a reappraisal. *Molecular Ecology*, 18(22), 4541–4550.
- Haffer, J. & Prance, G.T. (2002). Impulsos climáticos da evolução na Amazônia durante o Cenozóico: sobre a teoria dos Refúgios da diferenciação biótica. *Estudos Avançados*, 16(46), 175–208.
- Haffer, J. (1969). Speciation in Amazonian Forest Birds. *Science*, 165, 131–137.
- Haffer, J. (2008). Hypotheses to explain the origin of species in Amazonia. *Brazilian Journal of Biology*, 68, 917–947.
- Hall, T.A. (1999). BioEdit: A user-friendly biological sequence alignment editor and analysis program for Windows 85/98/NT. *Nucleic Acids Symposium Series*, 41, 95–98.
- Kass, R.E. & Raftery, A.E. (1995). Bayes Factors. *Journal of the American Statistical Association*, 90(430), 773–795.
- Kimura, M. (1980). A Simple Method for Estimating Evolutionary Rates of Base Substitutions Through Comparative Studies of Nucleotide Sequences. *Journal of Molecular Evolution*, 16, 111–120.
- Kocher, T.D., Thomas, W.K., Meyer, A., Edwards, S.V., Pääbo, S., Villablanca, F.X. & Wilson, A.C. (1989) Dynamics of mitochondrial DNA evolution in animals: amplification and sequencing with conserved primers. *Proceedings of the National Academy of Sciences of the United States of America*, 86, 6196–200.
- Leaché, A.D. & Bouckaert, R.R. (2018). Species trees and species delimitation with SNAPP: a tutorial and worked example.
- Leite, R.N., Kolokotronis, S., Almeida, F., Werneck, F.P., Rogers, D.S. & Weksler, M. (2014). In the Wake of Invasion: Tracing the Historical Biogeography of the South American Cricetid Radiation (Rodentia, Sigmodontinae). *PLoS ONE*, 9(6), 100687.
- Malcher, M.S., Pieczarka, J.C., Geise, L., Rossi, R.V., Pereira, A.L., O'Brien, P.C.M., Asfora, P.H., Silva, V.F., Sampaio, M.I., Ferguson-Smith, M.A. & Nagamachi, C.Y. (2017). *Oecomys catherinae* (Sigmodontinae, Cricetidae): Evidence for chromosomal speciation? *PLoS ONE*, 12(7), e0181434.
- Musser, G.G., & Carleton, M.D. (2005). Superfamily Muroidea. In *Mammal Species of the World: a taxonomic and geographic reference*. 3^o edição (Editores: Wilson, D.E. & Reeder, D.M.). Johns Hopkins University Press, Baltimore, Maryland. pp. 894–1531.
- Nascimento, F.F., Lazar, A., Menezes, A.N., Durans, A.M., Moreira, J.C., Salazar-Bravo, J., D'Andrea, P.S. & Bonvicino, C.B. (2013). The Role of Historical Barriers in the Diversification Processes in Open Vegetation Formations during the Miocene/Pliocene Using an Ancient Rodent Lineage as a Model. *PLoS ONE*, 8(4), e61924.
- Parada, A., Pardiñas, U.F.J., Salazar-Bravo, J. D'Elía G. & Palma R.E. (2013). Dating an impressive Neotropical radiation: Molecular time estimates for the Sigmodontinae (Rodentia) provide insights into its historical biogeography. *Molecular Phylogenetics and Evolution*, 66, 960–968.

Peterson, B.K., Weber, J.N., Kay, E.H., Fisher, H.S. & Hoekstra, H.E. (2012). Double digest RADseq: An inexpensive method for de novo SNP discovery and genotyping in model and non-model species. *PLoS ONE*, 7(5), e37135.

Raj, A., Stephens, M. & Pritchard, J.K. (2014). FastSTRUCTURE: Variational Inference of Population Structure in Large SNP Data Sets. *Genetics*, 197(2) 573–589.

Rambaut, A. (2016). FigTree v1.4.3 2006-2016. <http://tree.bio.ed.ac.uk/software/figtree/>

Rambaut, A., Suchard M.A., Xie D. & Drummond A.J. (2014). Tracer v1.6. <http://tree.bio.ed.ac.uk/software/tracer/>.

Reig, O.A. (1977). A proposed unified nomenclature for the enamelled components of the molar teeth of the Cricetidae (Rodentia). *Journal of Zoology (London)*, 181, 227–241.

Rocha, R.G., Duda, R., Flores, T., Rossi, R.V., Sampaio, I., Mendes–Oliveira, A.C., Leite, Y.L.R. & Costa, L.P. (2018). Cryptic diversity in the *Oecomys roberti* complex: revalidation of *Oecomys tapajinus* (Rodentia, Cricetidae). *Journal of Mammalogy*, 99, 174–186.

Rognes, T., Flouri, T., Nichols, B., Quince, C. & Mahé, F. (2016). VSEARCH: a versatile open source tool for metagenomics. *PeerJ*, 4, e2584.

Ronquist F., Teslenko M., van der Mark P., Ayres, D.L., Darling, A., Höhna, S., Larget, B., Liu, L., Suchard, M.A. & Huelsenbeck, J. P. (2012). MrBayes 3.2: efficient Bayesian phylogenetic inference and model choice across a large model space. *Systematic Biology*, 61 (3), 539–542.

Saldanha, J. & Rossi, R.V. (no prelo). Integrative analysis supports a new species of the *Oecomys catherinae* complex (Rodentia, Cricetidae) from Amazonia. *Journal of Mammalogy*.

Saldanha, J., Ferreira, D.C., Silva, V.F., Santos–Filho, M., Mendes–Oliveira, A.C., & Rossi, R.V. (2019). Genetic diversity of *Oecomys* (Rodentia, Sigmodontinae) from the Tapajós River basin and the role of rivers as barriers for the genus in the region. *Mammalian Biology*, 97, 41–49.

Shorrocks, B. (1980). A origem da diversidade - as bases genéticas da evolução. Queiroz, São Paulo. pp. 1–181.

Silva, J.M.C. & Straube, F.C. (1996). Systematics and Biogeography of Scaled Woodcreepers (Aves: Dendrocolaptidae). *Studies on Neotropical Fauna and Environment*, 31(1), 3–10. doi.org/10.1076/snfe.31.1.3.133217

Smith, M.F. & Patton, J.L. (1993). The diversification of South American murid rodents: Evidence from mitochondrial DNA sequence data for Akodontine tribe. *Biological Journal of the Linnean Society*, 50, 149–177.

Stamatakis, A. (2014). RAxML Version 8: A tool for Phylogenetic Analysis and Post-Analysis of Large Phylogenies. *Bioinformatics*, 30(9), 1312–1313.

Suárez-Villota, E.Y., Carmignotto, A.P., Brandão, M.V., Percequillo, A.R. & Silva, M.J.J. (2018). Systematics of the genus *Oecomys* (Sigmodontinae: Oryzomyini): molecular phylogenetic, cytogenetic and morphological approaches reveal cryptic species. *Zoological Journal of the Linnean Society*, 184, 182–210.

Thomas, O. (1909). Notes on some South-American Mammals, with descriptions of new species. *Annals and Magazine of Natural History*, 8(4), 230–242.

Villamil, J., Avila, L.J., Morando, M., Sites Jr., J.W., Leaché, A.D., Maneyro, R. & Camargo, A. (2019). Coalescent-based species delimitation in the sand lizards of the *Liolaemus wiegmanni* complex (Squamata: Liolaemidae). *Molecular Phylogenetics and Evolution*, 138, 89–101.

Voss, R.S. (1988). Systematics and ecology of Ichthyomyine rodents (muroidea): patterns of morphological evolution in a small adaptive radiation. *Bulletin of the American Museum of Natural History*, 188(2), 259–493.

ANEXO 01

Tabela 1. Número de campo, tombo, acesso do Genbank (Citocromo b), exemplares incluídos nas análises genômicas (ddRADseq) e localidades dos exemplares utilizados neste estudo. Linhagens do complexo *Oecomys catherinae*: central, extremo oeste, leste A, leste B, nordeste e norte.

Linhagem / espécie	Campo	Tombo	ddRAD	GenBank	Localidade
Central	MRT3875	MZUSP35549	ok	MG323761	Brasil: Tocantins, Paranã
Central	MRT3897	MZUSP35550	ok	MG323762	Brasil: Tocantins, Paranã
Central	PCH3998	-	ok	MG323764	Brasil: São Paulo, São Joaquim da Barra
Central	PCH4077	-	ok	MG323763	Brasil: São Paulo, São Joaquim da Barra
Central	-	MN37763	-	FJ361051	Brasil: Goiás, Caldas Novas
Central	-	MN37764	-	FJ361052	Brasil: Goiás, Caldas Novas
Central	-	MN37765	-	FJ361053	Brasil: Goiás, Caldas Novas
Central	-	MN37766	-	FJ361054	Brasil: Goiás, Caldas Novas
Central	-	MN37767	-	FJ361055	Brasil: Goiás, Caldas Novas
Central	-	MN37768	-	FJ361056	Brasil: Goiás, Caldas Novas
Central	-	MN37769	-	FJ361057	Brasil: Goiás, Caldas Novas
Central	OT7446	-	-	FJ361058	-
Central	OT7447	-	-	FJ361059	-
Central	-	MN36231	-	FJ361060	Brasil: Goiás, Colinas do Sul
Central	-	MN36273	-	FJ361061	Brasil: Goiás, Colinas do Sul
Central	-	MN36301	-	FJ361062	Brasil: Goiás, Colinas do Sul
Central	-	MN36330	-	FJ361063	-
Central	-	MN36336	-	FJ361064	-
Central	-	MN36350	-	FJ361065	Brasil: Goiás, Colinas do Sul
Central	-	MN36747	-	FJ361068	Brasil: Goiás, Minaçu

Linhagem / espécie	Campo	Tombo	ddRAD	GenBank	Localidade
Central	-	MN36791	-	FJ361069	Brasil: Goiás, Minaçu
Central	-	LBCE8791	-	MG323760	Brasil: Mato Grosso do Sul, Dois Irmãos de Buriti
Extremo Oeste	APC243	MZUSP35535	ok	MG323759	Brasil: Mato Grosso, Aripuanã
Extremo Oeste	APC249	MZUSP29532	ok	MG323758	Brasil: Mato Grosso, Aripuanã
Extremo Oeste	-	MN37776	-	FJ361050	Brasil: Rondônia, Guajará-Mirim
Extremo Oeste	-	AVG594	-	MG988098	Peru: Cusco, Laconvencio, Echarate, Camisea, Lote 88
Leste A	FS6-14	MN74364	ok	-	Brasil: Rio de Janeiro, Cachoeiras de Macacu, Fazenda "sem
Leste A	FS13-16	MN74370	ok	-	Brasil: Rio de Janeiro, Cachoeiras de Macacu, Fazendas Pica
Leste A	FS14-20	MN74371	ok	KY605393	Brasil: Rio de Janeiro, Cachoeiras de Macacu, Sítio
Leste A	FS14-35	NM74372	ok	KY605394	Brasil: Rio de Janeiro, Cachoeiras de Macacu, Sítio
Leste A	MFD 01	MN79852	ok	-	Brasil: Rio de Janeiro, Cachoeiras de Macacu, Estação
Leste A	MFD 06	MN79857	ok	-	Brasil: Rio de Janeiro, Cachoeiras de Macacu
Leste A	SQM80	-	ok	-	Brasil: Rio de Janeiro, Cachoeiras de Macacu
Leste A	FU16	-	ok	KY605396	Brasil: Rio de Janeiro, Casseiro de Abreu, Reserva
Leste A	FU17	-	ok	KY605397	Brasil: Rio de Janeiro, Casseiro de Abreu, Reserva
Leste A	FS4-1	MN74359	ok	KY605388	Brasil: Rio de Janeiro, Guapimirim, Fazenda Chorona
Leste A	FS4-38	MN74361	ok	KY605390	Brasil: Rio de Janeiro, Guapimirim, Fazenda Chorona
Leste A	FS8-21	MN74366	ok	KY605391	Brasil: Rio de Janeiro, Guapimirim, Fazenda Iguaçú
Leste A	FS8-55	MN74368	ok	KY605392	Brasil: Rio de Janeiro, Guapimirim, Fazendas Consorciadas
Leste A	ITA30	MN72737	ok	KY605398	Brasil: Minas Gerais, Pirapetinga
Leste A	ITA31	MN72738	ok	KY605399	Brasil: Minas Gerais, Pirapetinga
Leste A	SU63	-	ok	KY605403	Brasil: Rio de Janeiro, Sumidouro
Leste A	PSP01	MN74375	ok	-	Brasil: São Paulo, Ubatuba, Parque Estadual da Serra do Mar
Leste A	PSP19	MN74378	ok	KY605401	Brasil: São Paulo, Ubatuba, Parque Estadual da Serra do Mar

Linhagem / espécie	Campo	Tombo	ddRAD	GenBank	Localidade
Leste A	PSP38	MN74379	ok	KY605402	Brasil: São Paulo, Ubatuba, Parque Estadual da Serra do Mar
Leste A	-	MVZ200982	-	HM594616	Brasil: São Paulo, Capão Bonito
Leste A	FS4-35	MN74360	-	KY605389	Brasil: Rio de Janeiro, Guapimirim
Leste A	FS14-40	MN74373	-	KY605395	Brasil: Rio de Janeiro, Cachoeiras de Macacu
Leste A	PSP12	MN74377	-	KY605400	Brasil: São Paulo, Ubatuba
Leste A	SU86	-	-	KY605404	Brasil: Rio de Janeiro, Sumidouro
Leste A	-	LBCE10774	-	MG323771	Brasil: Rio de Janeiro, Paraty
Leste A	PSP42	MN74380	-	-	Brasil: São Paulo, Ubatuba, Parque Estadual da Serra do Mar
Leste B	MF29	-	-	EU579507	-
Leste B	-	UFES247	-	JQ966233	Brasil: Espírito Santo, Águia Branca
Leste B	MF29	-	-	GU126525	Brasil: Espírito Santo, rio Doce
Leste B	CIT2096	CIT2096	ok	MG323772	Brasil: Minas Gerais, Parque Estadual do rio Doce
Leste B	CIT2097	CIT2097	ok	MG323773	Brasil: Minas Gerais, Parque Estadual do rio Doce
Nordeste	PHA466	UFPE1891	ok	-	Brasil: Pernambuco, Jaqueira, Usina Colônia, RPPN Frei
Norte	PSA128	MPEG39899	ok	KY605384	Brasil: Pará, Parauapebas
Norte	PSA139	MPEG39900	ok	KY605385	Brasil: Pará, Parauapebas
Norte	PSA176	MPEG39903	ok	KY605387	Brasil: Pará, Parauapebas
Norte	APC289	MZUSP35539	ok	MG323766	Brasil: Mato Grosso, Vila Rica
Norte	APC304	MZUSP29533	ok	MG323767	Brasil: Mato Grosso, Vila Rica
Norte	APC310	MZUSP35542	ok	MG323770	Brasil: Mato Grosso, Vila Rica
Norte	CS26	-	-	KT737237	Brasil: Pará, Floresta Nacional Tapirape-Aquiri
Norte	-	USNM549530	-	KT737238	Brasil: Pará, East bank rio Xingu, 52 km SSW Altamira
Norte	-	MZUSP29533	-	KY605382	Brasil: Mato Grosso, Vila Rica
Norte	I AVR D330	MPEG38898	-	KY605383	Brasil: Pará, Marabá

Linhagem / espécie	Campo	Tombo	ddRAD	GenBank	Localidade
Norte	PSA164	MPEG39901	-	KY605386	Brasil: Pará, Parauapebas
Norte	APC288	MZUSP35538	-	MG323765	Brasil: Mato Grosso, Vila Rica
Norte	APC292	-	-	MG323768	Brasil: Mato Grosso, Vila Rica
Norte	APC297	-	-	MG323769	Brasil: Mato Grosso, Vila Rica
<i>Oecomys</i> sp. nov.	RVR 89	UFMT4118	ok	MK874365	Brasil: Mato Grosso, Alta Floresta
<i>Oecomys</i> sp. nov.	UTP177	UFMT1776	ok	MK874372	Brasil: Pará, Jacareacanga, margem direita rio Teles Pires
<i>Oecomys</i> sp. nov.	UTP158	UFMT1772	ok	MK874368	Brasil: Mato Grosso, Paranaíta, margem esquerda rio Teles
<i>Oecomys</i> sp. nov.	APC244	MZUSP29531	ok	MG323756	Brasil: Mato Grosso, Aripuanã
<i>Oecomys</i> sp. nov.	PEU960006	-	ok	MG323755	Brasil: Mato Grosso, Aripuanã
<i>Oecomys</i> sp. nov.	M97055	MZUSP35543	ok	MG323754	Brasil: Mato Grosso, Cláudia
<i>Oecomys</i> sp. nov.	M000029	MZUSP29516	ok	MG323753	Brasil: Mato Grosso, Gaúcha do Norte
<i>Oecomys</i> sp. nov.	BRM-060	-	ok	-	Brasil: Mato Grosso, Nova Ubiratã
<i>Oecomys</i> sp. nov.	LGS-01	-	ok	-	Brasil: Mato Grosso, Sapezal
<i>Oecomys</i> sp. nov.	APC145	MZUSP35537	-	MG323757	Brasil: Mato Grosso, Juruena
<i>Oecomys</i> sp. nov.	UTP02	UFMT1680	-	MK874366	Brasil: Mato Grosso, Paranaíta
<i>Oecomys</i> sp. nov.	UTP132	UFMT1686	-	MK874367	Brasil: Pará, Jacareacanga
<i>Oecomys</i> sp. nov.	UTP159	UFMT1773	-	MK874369	Brasil: Mato Grosso, Paranaíta
<i>Oecomys</i> sp. nov.	UTP162	UFMT1774	-	MK874370	Brasil: Mato Grosso, Paranaíta
<i>Oecomys</i> sp. nov.	UTP176	UFMT1775	-	MK874371	Brasil: Pará, Jacareacanga
<i>Oecomys</i> sp. nov.	UTP181	UFMT1806	-	MK874373	Brasil: Mato Grosso, Paranaíta
<i>O. auyantepui</i>	-	-	-	AJ496304	-
<i>O. bicolor</i>	RVR146	UFMT4333	ok	MK874356	Brazil: Mato Grosso, Sinop
<i>O. concolor</i>	JLP16806	-	-	HM594615	Brail: Amazonas, rio Jau
<i>O. franciscorum</i>	roe_224	-	-	KF207846	Argentina: Pampa del Indio, Chaco

Linhagem / espécie	Campo	Tombo	ddRAD	GenBank	Localidade
<i>O. mamorae</i>	PZ316	-	-	KT737225	Bolivia: La Paz, Buena Vista
<i>O. paricola</i>	UTP669	UFMT1848	ok	MK874426	Brazil: Mato Grosso, Paranaita
<i>O. rex</i>	CSA22	-	-	MK874428	Brazil: Para
<i>O. roberti</i>	-	UFES1370	-	HM594603	Para, Santana do Araguaia
<i>O. rutilus</i>	T-1896	MNHN1995.3236	-	AJ496309	French Guiana:Saint-Eugene
<i>O. superans</i>	-	MVZ155006	-	AY275123	-
<i>O. sydandersoni</i>	LHE1407	USNM:588189	-	KT737235	Bolivia: Santa Cruz, El Refugio
<i>O. tapajinus</i>	LPC710	MVZ197511	-	HM594595	Tocantins, Peixe
<i>O. trinitatis</i>	-	MUSM13320	-	GU126527	Peru: Loreto, rio Galvez
<i>Oligoryzomys destructor</i>	-	-	-	EU258544	-
<i>Oligoryzomys flavescens</i>	-	-	-	GU185919	-
<i>Oligoryzomys fulvescens</i>	-	-	-	DQ227457	-
<i>Oligoryzomys microtis</i>	-	-	-	AY439000	-
<i>Oligoryzomys nigripes</i>	-	-	-	GU185910	-
<i>Holochilus brasiliensis</i>	-	-	-	EU579496	-
<i>Holochilus chacarius</i>	-	-	-	DQ227455	-
<i>Holochilus sciureus</i>	-	-	-	EU579497	-
<i>Hylaeamys megacephalus</i>	-	-	-	MG323696	-
<i>Hylaeamys megacephalus</i>	-	-	-	AY275124	-

ANEXO 02

Os espécimes utilizados nas análises morfométricas estão depositados nas seguintes instituições: Museu Nacional (MN), Rio de Janeiro; Museu de Zoologia da Universidade de São Paulo (MZUSP), São Paulo; Museu Paraense Emílio Goeldi (MPEG), Belém; Universidade do Estado de Mato Grosso (Unemat), Cáceres; Universidade Federal de Mato Grosso (UFMT), Cuiabá. Universidade de Brasília (UnB), Brasília; e Universidade Federal do Espírito Santo (UFES), Vitória. O material examinado também inclui espécimes não catalogados, coletados por: A. Casagrande (AC), que serão depositados na Unemat. Coletados por Ana Paula Carmignoto (APC) e coletados na Pequena central Hidrelétrica de São Joaquim da Barra (PCH), serão depositados no MZUSP.

Oecomys sp. nov. (n = 14): Brasil: Mato Grosso: Alta Floresta (1): UFMT 4118 (10°00'25"S, 56°02'17"W); Aripuanã: MZUSP 29531 (10°10'01"S, 59°27'W); Cláudia: MZUSP 35543 (11°34'58"S, 55°10'01"W); Juruena: MZUSP 35537 (10°19'01"S, 58°28'58"W); Paranaíta: UFMT 1772, 1773, 1774 (9°29'06"S, 56°28'19"W); Rosário Oeste: Unemat-AC 207, 230, 266 (15°04'45.9"S, 56°33'15.7"W); Pará: Jacareacanga: UFMT 1680 (9°29'06"S, 56°28'19"W), UFMT 1776, 1686 (9°18'40"S, 56°46'05"W). Rondônia: Vilhena: MPEG 34224 (12°43'S, 60°7'W).

Complexo *Oecomys catherinae* (n = 77)

linhagem central (n = 9): Brasil: Distrito Federal: Brasília: MN 21996, 22013 (15°45'21"S, 48°06'28"W), UnB 3319, 3320 (15°56'55"S, 47°56'02"W); Goiás: Anápolis: MN 4348 (16°20'37"S 48°53'08"W); São Domingos: MPEG 10901 (13°23'36"S 46°18'55"W); São Paulo: São Joaquim da Barra (34): MZUSP-PCH 3998 (20°28'58"S, 47°51'W); Tocantins: Paranã: MZUSP 35549, 35550 (12°37'01"S, 47°52'58"W).

Linhagem extremo oeste (n = 6): Brasil: Amazonas: Humaitá: MPEG 13171 (7°41'53"S, 62°33'11"W); Mato Grosso: Aripuanã: MZUSP 29532, 35535 (10°10'01"S, 59°27'W); Colniza: MPEG 12654, 12691, 13173 (9°10'S, 60°38'W).

Linhagem leste A (n = 13): Brasil: Minas Gerais: Pirapitinga: MN 72373 (21°41'28"S, 42°22'05"W); Rio de Janeiro: Cachoeira de Macacu: MN 74364, MN 74367 (22°31'S, 42°48'W), MN 74370, 74374 (22°30'S, 42°45'W), MN 74371 (22°28'58"S, 42°51'W); Casimiro de Abreu: MN 44805 (22°29'32"S, 42°12'43"W); Guapimirim: MN 74359 (22°34'58"S, 42°57'W), MN 74360 (22°33'00"S 42°57'00"W, ,), MN 74369 (22°34'S,

42°54'W); Paraty: MN 75261 (23°01'30"S, 44°38'13"W); Silva Jardim: MN 66137 (22°38'09"S, 42°23'13"W); São Paulo: Ubatuba: MN 74375 (23°19'58"S, 44°49'58"W).

Linhagem leste B (n = 23): Brasil: Espírito Santo: Águia Branca: UFES 160, 272, 273, 274 (18°58'24"S, 40°45'46"W); UFES 275 (18°58'47"S, 40°43'11"W); UFES 276, 277 (18°52'29"S, 40°47'10"W); UFES 278 (18°53'23"S, 40°48'24"W); Aracruz: UFES-MF29 (19°48'46"S, 40°10'28"W); Cariacica: UFES 569, 570 (20°16'52"S, 40°30'41"W); Pancas: UFES 279 (19°12'16"S, 40°46'17"W); Santa Tereza: UFES 902, 903, 904 (19°57'10"S, 40°30'30"W); São José do Calçado: UFES 2312, 2313, 2314, 2315, 2316 (21°02'33"S, 41°43'09"W); Viana: UFES 810, 811, 812 (20°23'20"S, 40°26'19"W).

Linhagem norte (n = 26): Brasil: Mato Grosso: Vila Rica: MZUSP-APC 292, MZUSP 29533, 35538, 35539, 35542 (10°01'01"S, 51°07'01"W); Pará: Altamira: MPEG 10913 (3°22'01"S, 52°22'58"W), MPEG 10251, 10911, 10912 (3°41'S, 53°45'W); Belterra: MPEG 15293, 15294 (2°38'S, 54°57'W); Canaã dos Carajás: UFES 1567 (6°23'14"S, 50°21'37"W); Marabá: MPEG 38898, 38976 (6°S, 51°19'58"W), UFMT 1294 (5°47'51.8"S 50°46'15.3"W), MPEG 39899, 39900 (5°49'01"S, 50°28'58"W), MPEG 39903, 39909 (5°46'58"S, 50°31'58"W); Novo Repartimento: MPEG 10924 (4°41'S, 49°32'W); Santarém: MPEG 8229, 15094, 15099, 15120, 15121 (2°29'34"S, 54°44'06"W); Vitória do Xingu: UFES 2924 (3°16'19"S, 51°45'26"W).

3. CONCLUSÃO FINAL

- Evidenciamos a existência de complexos de espécies com alta diversidade na bacia do rio Tapajós, algumas destas em simpatia e com distribuição moldada pelos rios Amazônicos;
- Uma das linhagens do complexo *O. catherinae* corresponde à uma nova espécie válida, a qual descrevemos com base em dados moleculares e morfológicos;
- As diversificações entre as linhagens do complexo *O. catherinae* ocorreram no pleistoceno, possivelmente moldada durante as mudanças climáticas do Pleistoceno e mudanças vegetacionais e refúgios a elas associadas durante os períodos de glaciação na Amazônia e Mata Atlântica.
- O complexo *O. catherinae* é composto por três espécies distintas.
- Duas das linhagens do complexo *O. catherinae*, extremo oeste e norte, correspondem a espécies distintas (espécie 1= extremo oeste, espécie 2= norte);
- As linhagens do complexo *O. catherinae* com ocorrência na Mata atlântica e cerrado constituem um único grupo biológico, a qual consideramos como uma única espécie (espécie 3) com históricos de evolução ainda obscuro.